Universidade do Minho
Escola de Ciências

Pedro Miguel Bento Ferreira

Designing RNA based biopesticides for the control of cork oak phytopathogens

October 2022

Designing RNA based biopesticides for the control of cork oak phytopathogens

Pedro Ferreira

UMinho | 2022

Universidade do Minho
Escola de Ciências

Pedro Miguel Bento Ferreira

Designing RNA based biopesticides for the control of cork oak phytopathogens

Master Thesis

Master's Degree in Molecular Biology, Biotechnology and Bioentrepreneurship in Plants

Work developed under supervision of

Doctor Francisca Rodrigues dos Reis

Professor Doctor Maria Teresa Correia Guedes Lino Neto

October 2022

Copyrights and Terms of Use of Work by Third Parties

This is an academic work that can be used by others as long as the internationally accepted rules and good practices are respected, regarding copyright and related rights.

Thus, this work can be used under the terms set out in the license below.

If the user needs permission to be able to use the work under conditions not provided for in the indicated licensing, he must contact the author, through the RepositóriUM of the University of Minho.

Atribuição-NãoComercial-SemDerivações

CC BY-NC-ND

https://creativecommons.org/licenses/by-nc-nd/4.0/

Acknowledgments

This thesis was only possible with the support of many people.

To Professor Doctor Teresa Lino-Neto, few are the words that can describe how grateful I am for you to be always available, for transmitting your knowledge the best you could, for trusting in my work and for all the opportunities that you had offer. Thank you so much!

To Doctor Athanasios Dalakouras thank you for your help in this process and for being always available, when necessary, your knowledge within the area was a key component for a better work. For this I am grateful!

To Doctor Francisca Reis I am sincerely grateful for the introduction of such a unique and fascinating theme as is RNAi. For your trust in me to continue the work that you have been developed in the past years. Thank you so much!

To Doctor Daniela Costa, thank you for all the support in the lab and the support during the bioinformatic analysis. Thank you!

To all the lab team in *Centro de Biologia Funcional de Plantas*, with a special thanks to Ana Teresa for the help in the lab and for the excellent reading recommendations. Thank you!!

To my friends, in special the ones that have accompanied me in this all process. Thank you so much Rui Manta for your friendship and for all the support that you had given to me during this process. To Miguel Rodrigues for been always available and for always being there when he is needed. To both thank you!

To my girlfriend Eunice Pereira that has been an enormous support in my life that without a doubt this thesis would be possible without her. Thank you!

For las but not least, to my Family. In special to my mother that have always support me in my decisions, to my father for the right words in the right time. To the both of you thank you this thesis would be possible without your support.

Statement of integrity

I hereby declare having conducted this academic work with integrity. I confirm that I have not used plagiarism or any form of undue use of information or falsification of results along the process leading to its elaboration.

I further declare that I have fully acknowledged the Code of Ethical Conduct of the University of Minho.

Assinado por: **Pedro Miguel Bento Ferreira**
Num. de Identificação: 14842120
Data: 2022.10.28 21:42:59+01'00'

CHAVE MÓVEL

_____

(Signature)

Designing RNA based biopesticides for the control of cork oak phytopathogens

Abstract

Cork oak (*Quercus suber* L.) is an evergreen tree species with a great ecological and economic impact along the Mediterranean basin. Although being widely distributed, *Q. suber* forest has been declining for the past 80 years, being further enhanced by the climate changes. An example is severe drought, which is exposing cork oaks to an extra layer of stress allowing opportunistic pathogenic attacks. An example is the charcoal diseases caused by *Biscogniauxia mediterranea*, and bot canker caused by *Diplodia corticola.* The lack of a specific treatment for both diseases and the progressive ban of chemical fungicides in the EU, calls for new and innovative alternatives. In this context, RNA interference (RNAi) based fungicides are a promising strategy. Spray-induced gene silencing (SIGS) is a state-of-the-art RNAi silencing approach that targets specific pathogen genes, following the spraying of the host plant with a solution containing double stranded RNA (dsRNA). In this work, the possibility of using such approach for controlling both cork oak pathogens was explored. For the success of this biotechnological solution, the pathogen needs to uptake dsRNA molecules and process them for silencing targeted genes. *In silico* results revealed that both *B. mediterranea* and *D. corticola* contained the required protein machinery to uptake and process exogenous dsRNA. This result was corroborated by testing the capacity of both fungi in uptaking a labelled *sGFT*-dsRNA and by using an *in vitro* assay with sGFP transformants for testing silencing machinery. After testing the designed dsRNAs for fungal growth impairment, differences were detected in both cork oak pathogens. *B. mediterranea* appears to be more recalcitrant to the use of a SIGS approach than *D. corticola*. This work provided evidences of the potential of SIGS in controlling cork oak pathogens, particularly *D. corticola.*

Keywords: Cork oak; RNA interference; Spray-induced gene silencing (SIGS); *Biscogniauxia mediterranea*; *Diplodia corticola*

Desenvolver biofungicidas baseados em RNA para controlar fitopatógenos de sobreiro

Resumo

O sobreiro (*Quercus suber L.*) é uma espécie arbórea perene com grande impacto ecológico e económico presente na bacia mediterrânica. Apesar de amplamente distribuída, a floresta *Q. suber* tem vindo nos últimos 80 anos a apresentar indícios de declínio, potencializado pelas alterações climáticas. Um exemplo destas condições é a seca severa, que expõe os sobreiros a uma camada extra de stress o que permite ataques por patógenos oportunistas. Exemplos de doenças causadas por estes ataques são a doença do carvão do entrecasco causada pelo fungo *Biscogniauxia mediterranea* e o cancro do sobreiro causada pelo fungo *Diplodia corticola*. A falta de tratamento específico para ambas as doenças e a proibição progressiva de fungicidas químicos na UE exigem novas e inovadoras alternativas. Neste contexto, fungicidas baseados em RNA de interferência (RNAi) são uma estratégia promissora. A técnica *Spray-induce gene silencing* (SIGS) é uma abordagem de silenciamento por RNAi de última geração que tem como alvo, genes específicos do patógeno, após a pulverização da planta hospedeira com uma solução que contém RNA de cadeia dupla (dsRNA). Neste trabalho, foi explorada a possibilidade de utilização desta abordagem para o controlo de ambos os agentes patógenos do sobreiro. Para o sucesso desta solução biotecnológica, o agente patogénico precisa captar moléculas de dsRNA e processá-las para que possa silenciar os genes alvo. Os resultados *in silico* revelaram que tanto *B. mediterranea* quanto *D. corticola* contêm a maquinaria proteica necessária para captar e processar dsRNA exógeno. Este resultado foi corroborado testando a capacidade de ambos os fungos em captar um sGFT-dsRNA marcado com fluorescência. Assim como um ensaio *in vitro* com transformantes sGFP dos fungos em estudo para testar a maquinaria de silenciamento. As moléculas de dsRNAs foram desenvolvidas e testadas para a sua capacidade de provocar uma deficiência no crescimento fúngico. Os resultados demonstraram efeito das moléculas em ambos os patógenos do sobreiro. Contudo, *B. mediterranea* parece ser mais recalcitrante ao uso de uma abordagem SIGS do que *D. corticola*. Este trabalho forneceu evidências do potencial do SIGS no controlo de agentes patogénicos do sobreiro, particularmente *D. corticola*.

Palavras-chave: Sobreiro; RNA de interferência; Spray-induced gene silencing (SIGS); *Biscogniauxia mediterranea*; *Diplodia corticola*

Index

Abbreviations list

°C – Degree Celsius

ANOVA - Analysis of Variance

APCOR - Associação Patronal do Setor Corticeiro

BLAST – Basic Local Alignment Search

DNA – Deoxyribonucleic Acid

h – Hours

min. – minutes

l – Litre

ha – hectare

m – Mettre

Da –Dalton

M – Molar

g – gram

LB - Luria-Bertani

PDA - Potato dextrose Agar

PDB – Potato dextrose broth

RNA - Ribonucleic acid

UV - Ultraviolet

v/v – Volume/volume

w/v – Weight/volume

°C – Degree Celsius

ANOVA - Analysis of variance

BLAST – Basic Local Alignment Search

DNA – Deoxyribonucleic acid

h - Hour

UV - Ultraviolet

v/v – Volume/volume

w/v – Weight/volume

RNAi – RNA interference

dsRNA – double stranded ribonucleic acid

siRNA – small interfering RNA

HIGS – Host induced gene silencing

SIGS – Spray induced gene silencing

BF – Bright-field

GFP – Green fluorescent protein

Figure Index

Index table

1. Chapter I: General introduction

Cork oak (*Quercus suber* L.) is an evergreen tree species from the Fagaceae family, considered as a long-lived tree (200-250 years) and presenting slow grow rates. The optimal climate conditions for this species are characterized by a relatively humid climate. Annual precipitation values must be higher than 450 mm, being the optimal levels between 600 and 1000 mm and annual medium temperatures between 13-18°C (Gil, 2008). These conditions are found in the Mediterranean basin, where cork oaks are distributed along 1 million hectares on the north of Africa and 1.5 million hectares on the south of Europe (Figure 1.1 a). However, it is on the Iberian Peninsula that cork oak forests assumes a special importance (Lionello *et al.*, 2014).

In Portugal, cork oak is distributed in an area of 736,775 hectares (APCOR, 2022), being this area 34% of the worldwide cork oak area. Two different forest agrosystems can be recognized (Costa and Pereira, 2007). The cork oak forests at the north of Portugal (*sobreirais*) are defined by a denser distribution (around 400 trees/ha, Figure 1b) and a shrub layer, without any agro-pastoral activity. *Montados* (or *dehesas* in Spanish) are typical for southern regions, representing about 70 % of the total area of Portuguese cork oak forests. These stands comprise an agro-forestry-pastoral ecosystem, which is characterized by scattered trees (60-100 trees/ha, Figure 1c), dominated by evergreen oaks and agriculture fields, normally composed by wheat, barley, and oats.

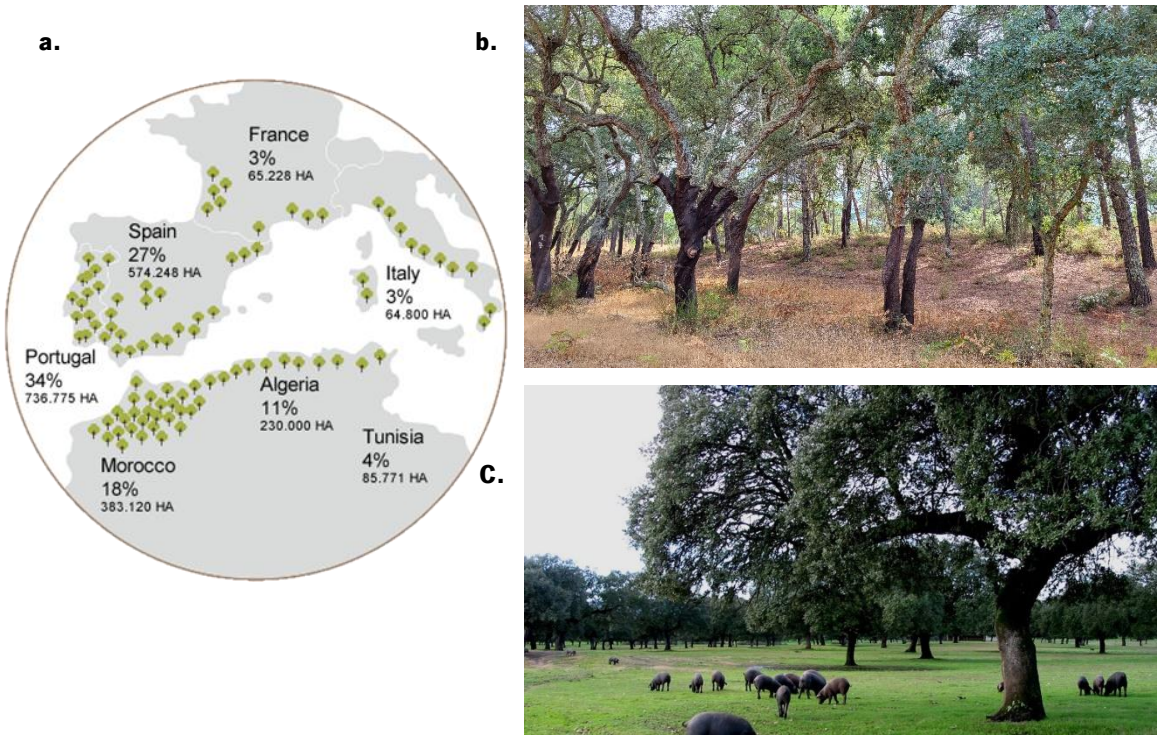

Figure 1. 1: Cork oak distribution in the Mediterranean basin (a), in which two agrosystems can be recognized - *sobreiral* (b) and *montado* (c) (a. Adapted from: APCOR, 2022) [Photo: Pedro Ferreira, 2022].

1.1. Ecological and economic importance of cork oak forests

The unique distribution of *montados* vegetation offers the shelter for a vast variety of species, in particular to predators, where the open areas are ideal to hunt and the denser ones offers them shelter. An example of two predators is the black vulture (*Aegypius monachus*) and the Iberian lynx (*Lynx pardinus*), two species that are considered critically endangered in Portugal (Simonson *et al.*, 2018). The conjunction of these factors reveals the ecological importance of *montados*, which have been recognized through their protection status, described in the Annex I 'Habitats of Community importance' under the European Community Habitats Directive (Council Directive 92/43/EC).

Despite their important ecological role, cork oak forests are greatly recognized by their high economic value (APCOR, 2022). Indeed, *Q. suber* is mostly known by the production of a thick layer of bark – the cork (Leite and Pereira, 2017). The cork oak suber is recognized by its lower density and lower permeability to gases and liquids. These characteristics are the reason for cork to be such an interesting product, for example for the manufacture of bottle stoppers, sealants, agglomerates, composites, and clothing. In Portugal, the cork processing industry is responsible for the creation of 640 companies that together employ more than 8,000 people (APCOR, 2022). Furthermore, Portugal is responsible for 63% of the global cork exportations, which are translated into 161 million euros each year. Adding the value of processed goods, like bottle stoppers or construction materials, the Portuguese cork industry reveals an intern commercial balance of 831 million euros (APCOR, 2022). Besides the cork industry, other products obtained from cork oak forests are associated with other incomes, including livestock farming, hunting, honey and mushroom production.

1.2. Cork oak forest decline

The cork oak distribution is mostly related to drought severity and soil-water availability (Oliveira and Costa, 2012; Costa, 2021). In the past 80 years, the cork oak populations have been suffering a decline (Kim *et al.*, 2017). This is a complex phenomenon, which has been described as being triggered by an increase in plant stress. The weakened stressed trees are then infected by pathogens (Costa *et al.*, 2010; Vilà-Cabrera *et al.*, 2018). In the last years, the main cause of plant stress has been attributed to climate changes, even though cork oak species are well adapted to the Mediterranean climate (hot and dry summers, associated with mild and wet winters). However,

the physiological and morphological adaptations of cork oak, which could support small periods of drought, may not be enough (Costa *et al.*, 2009). Climate modulation reveal that the Mediterranean basin will suffer an increase in temperature and decrease in precipitation levels in the forthcoming years (Goubanova and Li, 2007; Ozturk *et al.*, 2015). These new climate conditions will directly affect *Q. suber* populations. Besides influencing plant physiology, the new conditions will potentiate an outbreak of tree pests and pathogens (Kim *et al.*, 2017).

Several pests are already affecting cork oak population (Tiberi *et al.*, 2016). The bark- and wood- boring insects play a major role in oak decline in Europe. They are able to dig galleries under the bark and into the wood, playing a major role in pathogens spread within cork oak tissues. One of the most notorious is *Platypus cylindus*.(Tiberi *et al.*, 2016).This Coleoptera is able to attack not only stressed trees, but also apparently healthy trees, causing their death into 1-3 years. Some soil-borne pathogens are considered specially devastating, in particular those belonging to the genus *Phytophthora* (Homet *et al.*, 2019). Indeed, *Phytophthora cinnamomi* has been considered one of the most aggressive pathogens for woody species (Hardham and Blackman, 2018). This oomycete destroys host roots, blocking nutrient and water uptake, leading to tree dieback. Other two important pathogens in cork oak trees are *Biscogniauxia mediterranea* and *Diplodia* corticola, which are endophytic opportunistic fungi. These fungi live within the host tissues, without generating symptoms, only becoming pathogenic when conditions are proper for disease development.

B. mediterranea is a fungal species from the Sordariomycetes class (Ascomycota) that causes the cork oak disease known as “charcoal canker”. The life cycle of *B. mediterranea* is partially spent as an endophyte in different organs and tissues including twigs, bark, buds and leaves (Mazzaglia *et al.*, 2001). This behaviour changes to pathogenic, when host stress levels are increased. The severe drought plays an essential role to induce the pathogen attack, being recognized as the main condition for pathogenic change (Nugent *et al.*, 2005). Charcoal disease promoted by *B. mediterranea* is characterized by the development of bark lesions, exhibiting the blackish stroma formed by the fungus (Figure 1.2). The charcoal canker is induced by the development of a large number of black stromata harbouring perithecia (Henriques, 2015).

The same behaviour change occurs in *Diplodia corticola*, a fungal species from the Dothideomycetes class (Ascomycota). Like reported for *B. mediterranea*, this fungus life-cycle includes an endophytic stage, but this strategy changes when cork oaks are weakened by stresses

and *D. corticola* starts acting as a pathogen (Campanile *et al.*, 2007). Indeed, *D. corticola* is one of the causing agents for dieback and bot canker disease of oaks (Figure 1.2) (Campanile *et al.*, 2007). Actually, *D. corticola* has been recognized as the most widely distributed and aggressive pathogen linked to the cork oak decline (Smahi *et al.*, 2017).

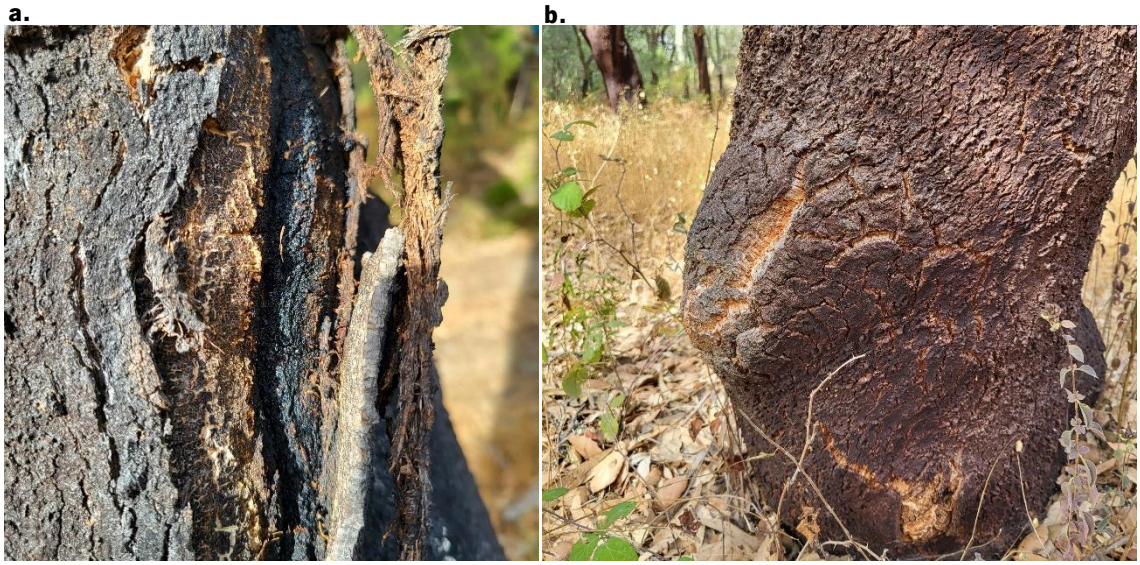

Figure 1. 2: Symptoms of charcoal disease caused by *B. mediterranea* (a) and bot canker caused by *D. corticola* (b). A charcoal like texture and black colour is visible beneath the cork (a), which is related to the necrosis caused by the development black stromata with perithecia of *B. mediterranea*. The symptoms of *D. corticola* includes branch and stem bot cankers (b). [Photo: Pedro Ferreira, 2022].

1.3. Control of cork oak diseases

Among the opportunistic pathogens, *B. mediterranea* and *D. corticola* have being described as prominent in declining cork oak forests and their incident rate has been rising in the last years. There is no specific treatment for these pathogens. For this reason, good phytosanitary measures are essential to prevent disease spread from tree wounds, derived from pruning or cork extraction (Moricca *et al.*, 2011). Application of chemical fungicides, as thiophanate-methyl or carbendazim have shown effective results as a preventative control measure (Luque *et al.*, 2008; Henriques, 2015). However, the use of chemical fungicides is being restricted, due to their environmental impacts. For example, the use of thiophanate-methyl has been banned from the European Union, since April 2021 (European Commission directive 2011/540/EC). The eradication of such chemical fungicides will be a trend in the European Union, due to the "Farm-to-Fork programme" that predicts the reduction in 50% of all hazardous pesticides by 2030 (European commission

directive 1107/2009/EC). For this reason, more sustainable methods must be developed to fight plant diseases.

New strategies for plant disease control have been emerging. For example, biocontrol strategies make use of beneficial microorganisms that are able to compete or be direct antagonists of plant pathogens (Syed Ab Rahman *et al.*, 2018). The use of *Simplicillium aogashimaense* revealed an inhibition effect on both *B. mediterranea* and *D. corticola* growth and promote mycelial/hyphal deformations (Costa *et al.*, 2020). Further, *Trichoderma harzianum* has revealed some success in controlling *B. mediterranea* disease in *Q. suber* (Yangui *et al.*, 2020). Other example of biotechnological solutions for controlling plant diseases is HIGS (*Host induced gene silencing*) and SIGS (*Spray induced gene silencing*) strategies. Both are based on the eukaryotic cellular process of RNA interference (RNAi) and have been recently implemented as a new sustainable way to control different types of plant pathologies (Filho *et al.*, 2021).

1.4. RNA interference

New technological advances were achieved after discovery of the RNA interference process (Fletcher *et al.*, 2020). This has been recognized as a conserved eukaryotic mechanism of post-transcriptional gene silencing, which evolved as a defence strategy against mobile genetic elements, such as transposons or viruses (Dang *et al.*, 2011). The first insights on the RNAi mechanism were through the transformation of petunia plants to change the colour of flowers (Napoli *et al.*, 1990). In an attempt of overexpressing the chalcone synthase (*CHS*), in order to obtain more prominent purple flowers, the result was the abolition of the anthocyanin biosynthesis, resulting in white or patterned flowers. The authors suggested the co-suppression of homologous genes, explaining that the hight levels of transcripts caused by the transgene was responsible for silencing both, the endogenous gene and the transgene itself. Fire and co-authors (1998), started to reveal the essential pieces of this mechanism, by injecting a double-strand RNA (dsRNA) molecule, complementary to a 742-nucleotide segment of *unc22* gene, into the body cavity or gonads of *Caenorhabditis elegans*. The resulting phenotype was an increase of twitching, which had been associated to a decrease production of *unc22* transcript, thus providing evidences for the capacity of this dsRNA molecule to initiate a gene silencing mechanism. These results gave new insights on petunia gene suppression. The transcript of *CHS* transgene produced a hairpin structure that initiated the RNAi mechanism, resulting in the post-transcriptional silencing of *CHS* genes (Agrawal *et al.*, 2003).

Many other advances to understand RNAi mechanism were perform (reviewed by Rosa *et al.*, 2018; Cooper *et al.*, 2019), including the biochemical analysis of *Drosophila* cell extracts and embryos (Geley and Müller, 2004). These studies identified the protein complex responsible for the mRNA silencing process, the so-called RISC (RNA-induced silencing complex), and the enzyme responsible for dsRNA processing (Dicer, DCL). The combination of the acquired knowledge created a model that explains the RNAi mechanism.

1.4.1. RNAi mechanism, an overview

The proposed model explaining RNAi mechanism comprise two different phases: an initiation and an effector phase (Hannon, 2002). In the initiation phase, a long double-strand RNA is recognized and processed into smaller fragments of 20-25 nucleotides (Paturi and Deshmukh, 2021). This step is performed by a Dicer enzyme that belongs to the ribonuclease III (RNase III) family, a highly conserved family of dsRNA specific endoribonucleases. Dicer composition and architecture is highly variable through eukaryotes (Paturi and Deshmukh, 2021). For example, DCL-2 from *Neurospora crassa* (the model organism for RNAi silencing in filamentous fungi) contains six domains: a Helicase-ATP-binding domain, a Helicase C domain, a Dicer dimerization domain, two tandem RNase III domains, and a C-terminal dsRNA-binding domain (Figure 1.3).

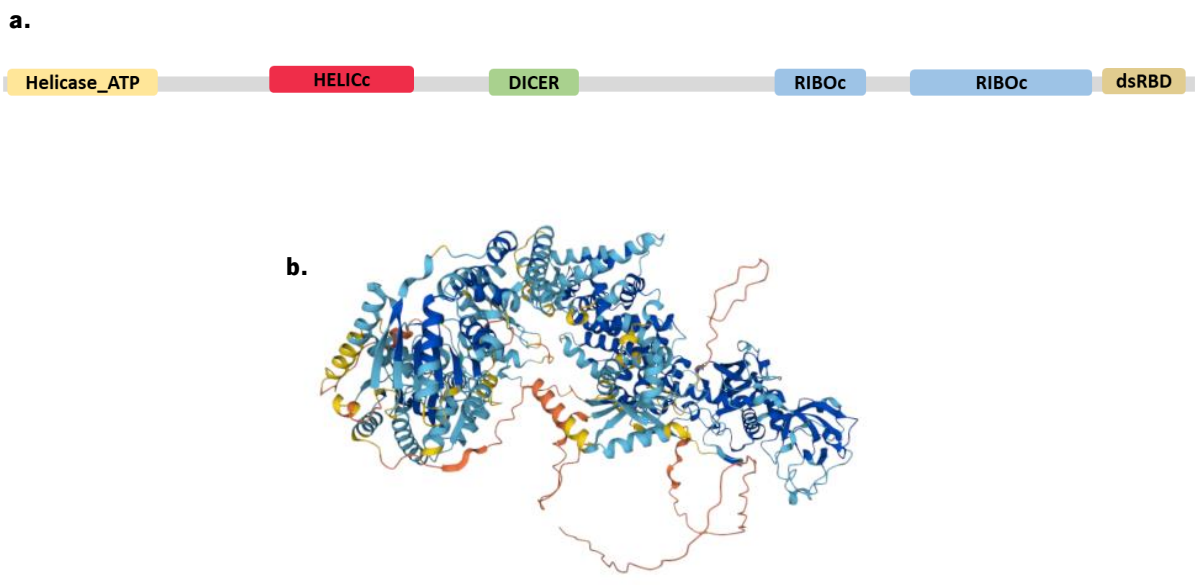

Figure 1. 3: Composition of *Neurospora crassa* DCL-2 (a) and respective three-dimensional structure (b). DCL-2 contains six domains: a Helicase-ATP-bind domain (in yellow), a Helicase C domain (HELICc, in red), a Dicer dimerization domain (DICER, in green), two tandem RNase III domains (RIBOc, in blue), and a C-terminal dsRNA-binding (DSRBD, in beige).

Due to the presence of this last domain, it has been hypothesised that Dicer is capable of recognizing dsRNA. After this recognition, two cleavage events performed by both RNase III domains, one in each RNA strand, results into small RNAs. This cleavage leaves two 3'nucleotide overhangs at each RNA strand, comprising a unique molecular signature, essential for downstream events (Court *et al.*, 2013).

In the process of RNAi silencing is possible to distinguish two main categories of small RNAs produced by double-stranded precursors: microRNAs (miRNA) and short interfering RNAs (siRNA) (Wang *et al.*, 2021). While miRNAs are important gene regulation tools, originated from endogenous MIR genes, siRNAs are derived from exogenous dsRNA and play defensive purposes (Figure 1.4). The endogenous dsRNA is mostly derived from miRNA activity, which produces a single strand RNA molecule that is then converted to dsRNA. The exogenous dsRNA could be linked to different sources as viral or transgene (Tiwari and Rajam, 2022).

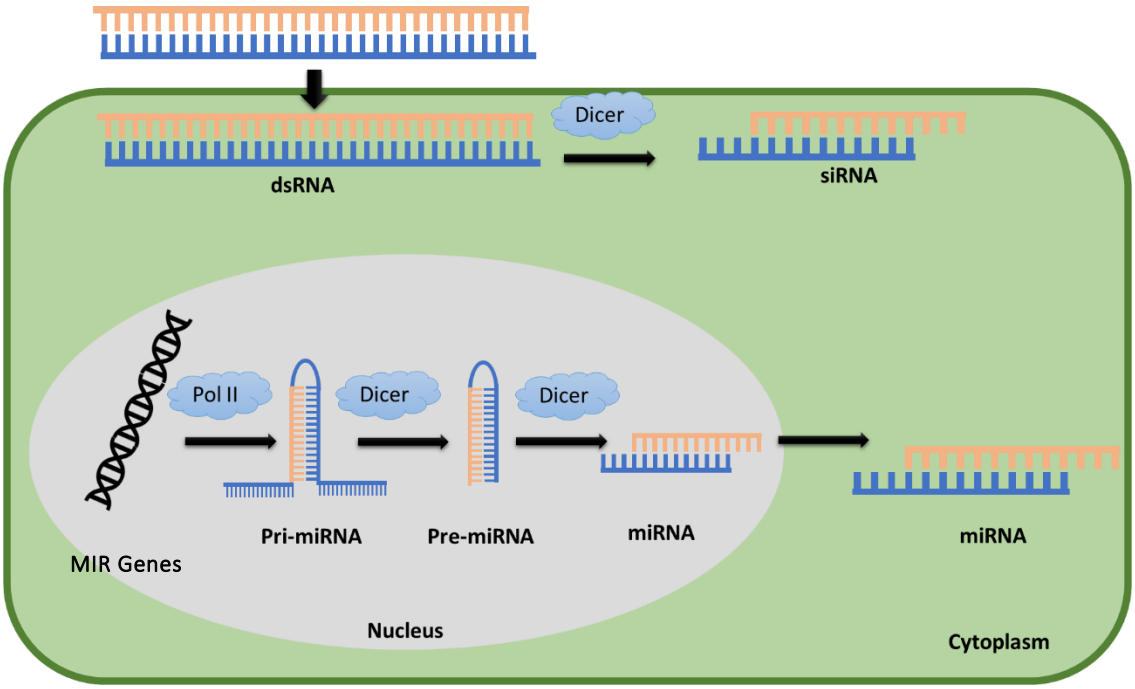

Figure 1. 4: Categories of small RNAs produced in the initiation phase of RNAi mechanism. The short interfering RNA (siRNA) is produced from an exogenous double-stranded RNA uptake by cells, which is further processed by a Dicer in the cytosol. In contrast, microRNA (miRNA) is originated by the transcription of an endogenous non-coding MIR gene, through the action of DNA Polymerase II, resulting in the creation of a pri-miRNA with a typical internal stem-loop structure. The produced dsRNA region is processed by Dicer enzymes inside the nucleus and exported to the cytoplasm as a miRNA.

After the production of miRNA or siRNAs, the next phase (execution) will result in the silencing of corresponding genes. A large multiple protein complex (RNA induced silencing complex; RISC), containing in its core the Argonaute (AGO) protein, is firstly activated (Hung and Slotkin, 2021). The Argonaute protein presents four conserved domains: a N-terminal ArgoN domain (with dsRNA unwinding activity), a PAZ domain (capable of recognizing and binding the 3´nucleotide overhangs), a MID domain (able to bind to 5´phosphates of a single strand of siRNA) and a C-terminal PIWI domain (able to cleave the target mRNA, slicer activity) (Figure 1.5).

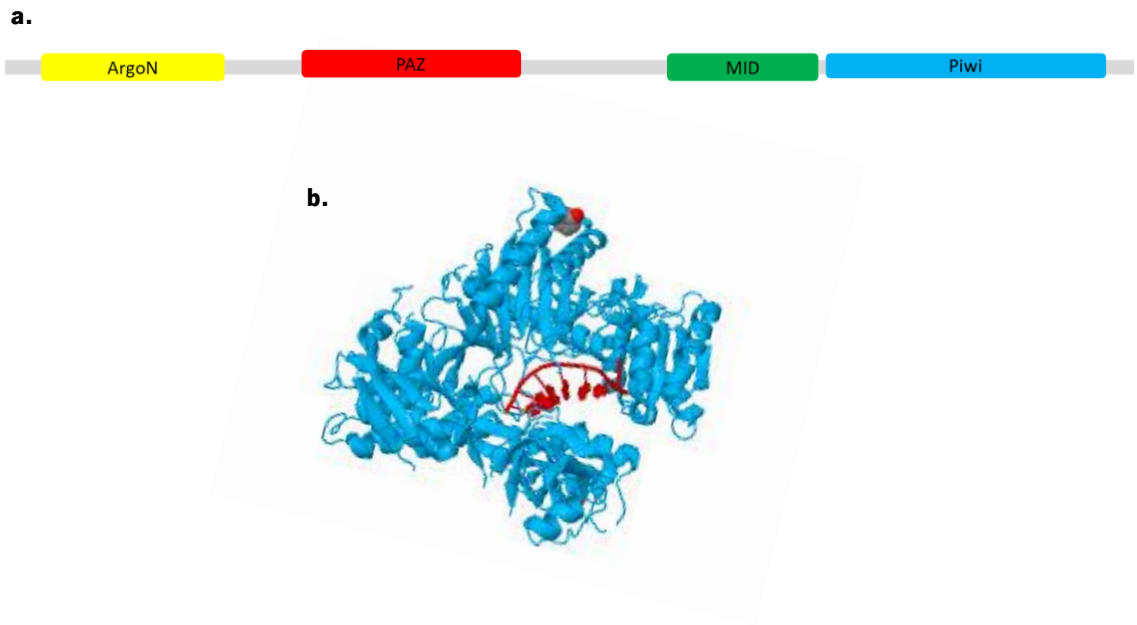

Figure 1. 5: Composition of *Neurospora crassa* AGO1 (a) and respective three-dimensional structure (b). AGO proteins contains typically four domains: a N-terminal ArgoN domain (in yellow), a PAZ domain (in red), a MID domain (in green), and a PIWI domain (in blue). The red molecule in the 3D model represents a single strand RNA, in an attempt to reveal its interaction with the AGO protein**.**

The unwinding event, occurring during AGO processing, is necessary for separating both siRNA strands, resulting in the formation of a *passenger strand* and a *guide strand* (Figure 1.6). The *passenger strand* is degraded, but the 5' nucleotide of the *guide strand* is incorporated into the binding pocket created by the MID and PIWI domains, while the 3' end is enclosed within a cavity of the PAZ domain (Medley *et al.*, 2021). The strand selection is based on a thermodynamic asymmetry rule, following the cleavage and ejection of the *passenger strand* (Wu *et al.*, 2020).

The RISC complex starts to search actively for mRNA to *guide strand* (Hung and Slotkin, 2021). In a scenario of a full complementarity between both RNAs, the PIWI domain will cleave the target mRNA on the 10-11 nucleotide of the *guide* molecule. Two fragments are produced from this event, that will be degraded causing the gene silencing.

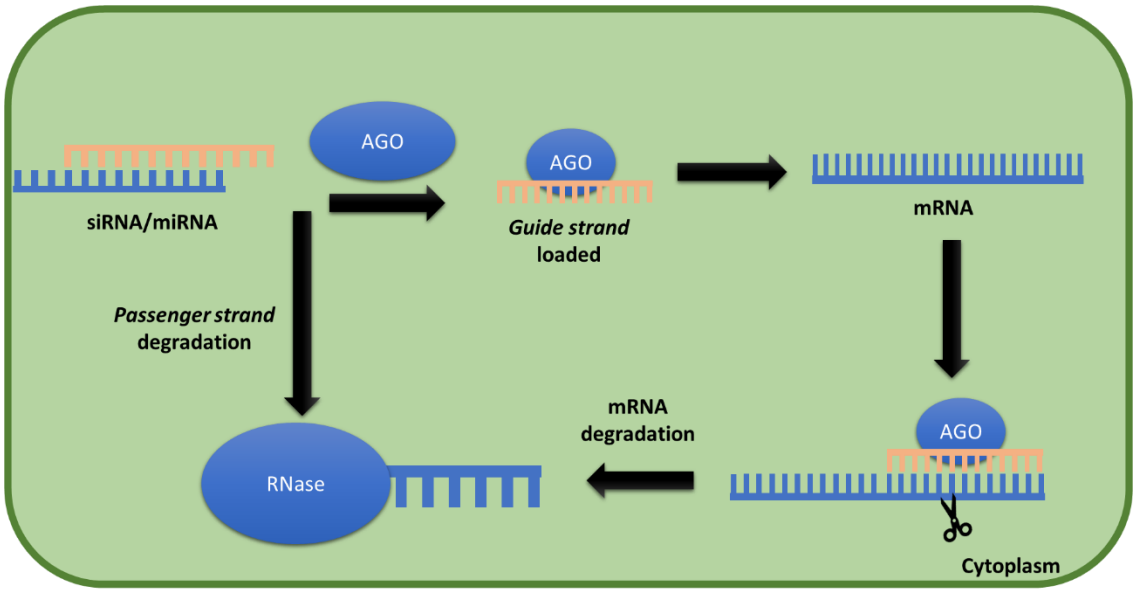

Figure 1. 6: The execution of RNAi silencing. During the execution phase, siRNA/miRNA molecules are loaded into the Argonaute protein, activating the RISC complex. In this process, the *passenger strand* is degraded by RNase, while the *guide strand* leads the Argonaute to complementary mRNAs, thus promoting the RNA silencing process.

Although RNAi mechanism is conserved among eukaryotes, each kingdom contains a distinct number of protein paralogs and different RNAi silencing approaches (Cerutti *et al.*, 2006). For example, in the plant model *Arabidopsis thaliana* there are four different Dicer-like (DCL) paralogs. Each DCL is capable of producing different siRNA/miRNA lengths (Figure 1.7). Specifically, DCL-2 generates siRNA fragments with 22-nucleotides, DCL-3 with 24-nucleotides and DCL-4 produces fragments with 21-nucleotides. DCL-1 is capable of recognizing the pre-miRNAs hairpin structures, generating fragments with 21/22 nucleotides from miRNAs. The siRNAs of 21-nucleotides produced by DCL-4 are loaded into the RISC complex, in which the *guide strand* scans for complementary mRNA. The target transcripts are then cleaved and degraded, resulting in a *post-transcriptional gene silencing* (Dalakouras *et al.*, 2021). The siRNAs of 22-nucleotides produced by DCL-2 also bind to an AGO1 domain from RISC, although the additional nucleotide is able to change the AGO1 configuration, resulting in the binding of the *Suppressor of Gene Silencing 3* protein (SGS3) (Hung *et al.*, 2021). In this case, once the mRNA cleavage event is

ended, the RNA-directed RNA polymerase 6 (RDR6) will bind to the recently cleaved transcript, protecting it from degradation. The protection and stabilization of these non-polyadenylated RNAs, results in the amplification of the initial trigger by the biosynthesis of new dsRNA molecules. The produced siRNA fragments of 24-nucleotide by DCL-3 are incorporated into the AGO4. This protein has the capability to recognize the cognate DNA (or nascent transcript) and recruits methyltransferases to methylate cytosine residues of both DNA strands and causing a *transcriptional gene silencing*. The activity of DCL4 thus results in the RNA-directed DNA methylation (Dalakouras and Vlachostergios, 2021).

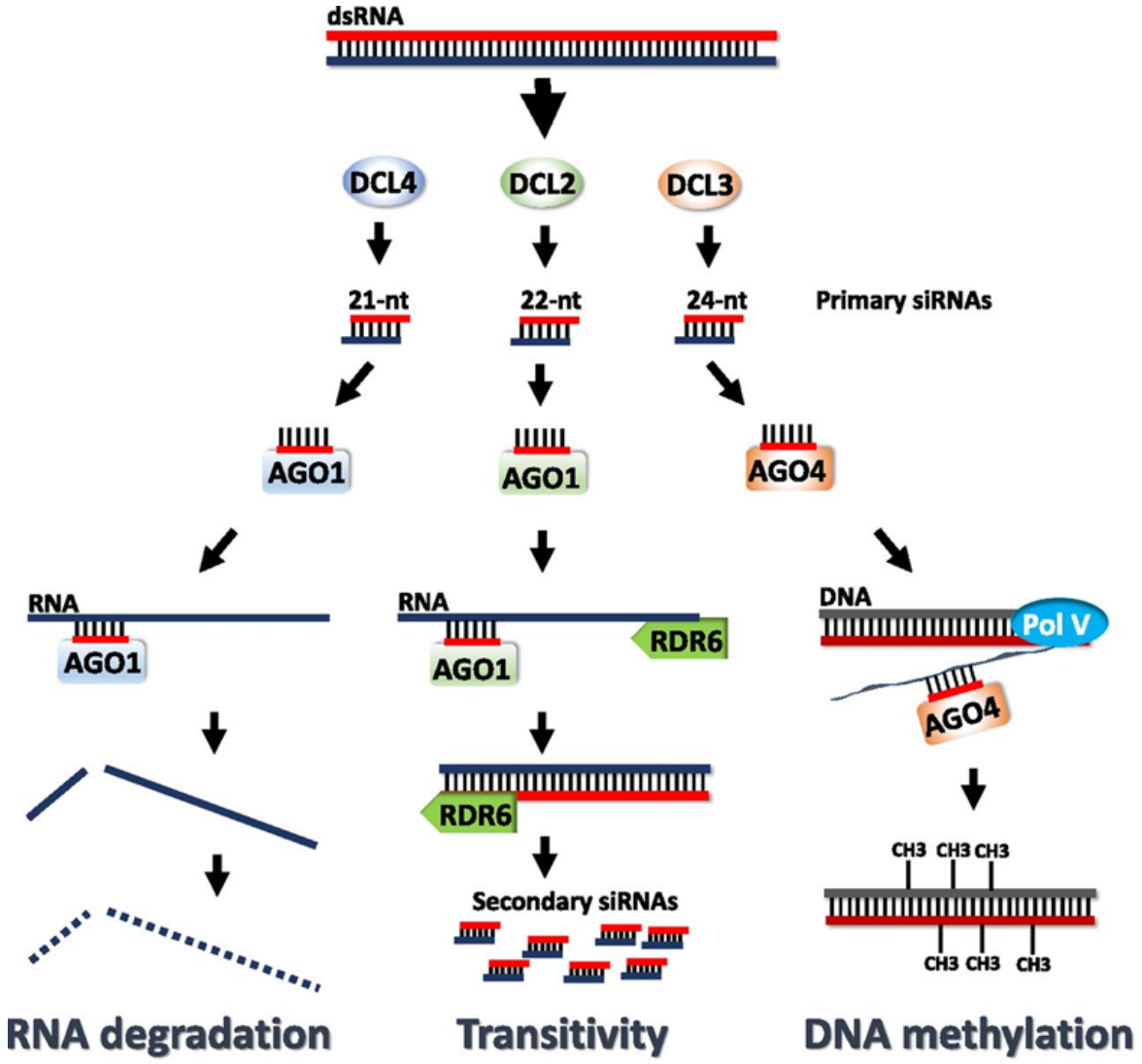

Figure 1. 7: The production of siRNA by different DCLs and corresponding downstream events. DCL4 generates 21-nt siRNAs that are loaded onto AGO1 and target complementary transcripts for cleavage. DCL2 generates 22-nt siRNAs that are also loaded onto AGO1 and recruit RDR6 to the 3′ ends of target transcripts for the generation of secondary siRNAs. Finally, DCL3 generates 24-nt siRNAs that are loaded onto AGO4 and trigger DNA methylation (Adapted from: Dalakouras *et al.*, 2020).

1.4.2. RNAi silencing in fungi

Fungi have been exploiting RNAi mechanisms to regulate a large variety of cellular activities, from defence against exogenous and potentially harmful DNA to drug tolerance (Lax *et al.*, 2020). Two different mechanisms related to RNAi can be distinguished on the model organism *Neurospora crassa*: the meiotic silencing unpaired DNA (MSUD) and the quelling (Figure 1.8).

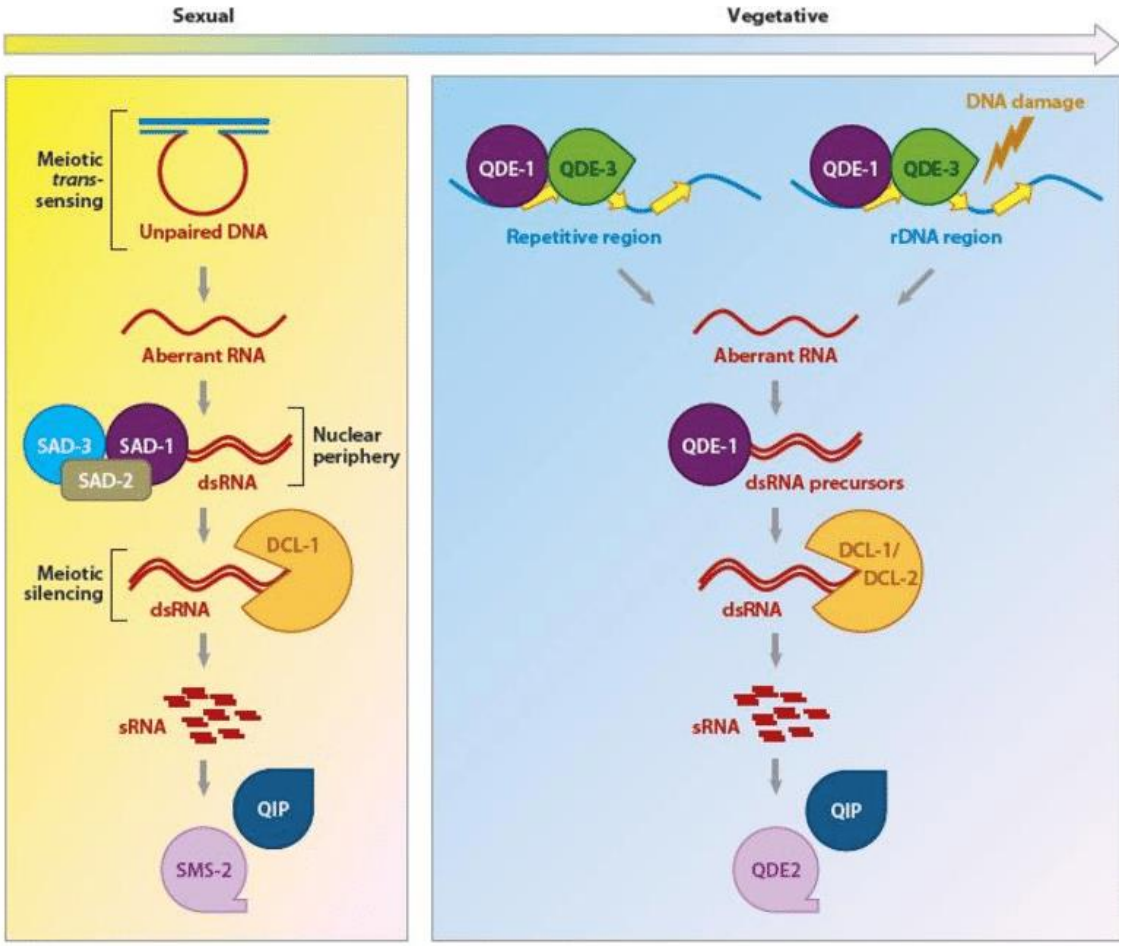

Figure 1. 8: RNAi-related pathways in *Neurospora crassa*. During meiosis, the meiotic silencing by unpaired DNA (MSUD) mechanism is able to sense unpaired DNA and promote the production of aberrant RNAs (aRNA). These aRNAs are converted to dsRNAs by SAD1 (RdRP), SAD2, and SAD3 (helicase) in the nuclear periphery. The produced dsRNAs are further processed by nuclear DCL-1 into sRNAs, which are then loaded onto the Argonaute protein SMS-2. During the vegetative stage, a defensive strategy (quelling) could take place. Repetitive transgene DNA loci lead to the production of aRNAs by QDE-1 (DdRp/RdRp) and QDE-3 (RecQ helicase). Single-stranded aRNAs are then converted to dsRNA precursors by QDE-1. The dsRNAs are further processed by cytosolic DCL-1 and DCL-2, producing siRNAs. From these, a *guide strand* is loaded on the Argonaute protein QDE2, directing the silencing events (Adapted from: Chang *et al.*, 2012).

The MSUD mechanism is only found during fungal meiosis, being used for silencing unpaired DNA and transposons. This process has been well-described in the haplontic *Neurospora crassa* (Chang *et al.*, 2012). All the structures of this fungus are haploid, but the fusion of two haploid nucleus from opposite matting types results in a diploid cell (zygote). In the subsequent meiosis, MSUD process occurs during the prophase of the first meiotic division (Chang *et al.*, 2012). Unpaired DNA regions are recognized and aRNAs are created by the transcription of the unpaired regions (reviewed by Hammond, 2017). Such aRNAs are then converted into dsRNAs by SAD-1 (with RNA-dependent RNA polymerase domains) with the help of SAD-2 (with any known conserved domain) and SAD-3 (with RNA/DNA helicase domains). The processed dsRNAs are cleaved by DCL-1 into siRNAs, which are loaded into SMS-2 (Argonaute homologous). After the cleavage and degradation of the *passenger strand* by QIP (an exonuclease), an active RISC complex is created through the incorporation of the *guide strand* (Chen *et al.*, 2021).

In contrast to MSUD, quelling has been described as a defence mechanism (reviewed by Bhattacharjee *et al.*, 2019). This process occurs in the vegetative stage of fungi and is responsible for silencing specific transgenes. With this process, the fungi are able to protect themselves against virus or mobile elements, such as transposons. Fungi are able to recognize a repetitive or a damaged DNA region, through the Replication Protein A (RPA) that binds to single stranded DNA and recruits QDE-3 (RecQ helicase). The complex DNA-RPA-QDE-3 recruits QDE-1, which is both a RNA-dependent RNA-polymerase (RdRP) and a DNA-dependent RNA polymerase (DdRP). These enzymes are firstly responsible for the synthesis of an aberrant RNA (aRNA), based on the interaction of a single-stranded DNA-binding protein (RPA) that targets the DNA region. Using as template a single strand DNA, QDE-1 first converts the single-stranded DNA to aRNA. The aRNA produced is then converted into dsRNA, by the RdRP activity of QDE-1. The resulting dsRNA is then processed by cytosolic DCL-1 and DCL-2 into siRNAs, in an ATP dependent process. The newly siRNAs bind to QDE-2 protein (homologous to Argonaute). While the *passenger strand* is cleaved and degraded by the QIP exonuclease, the *guide strand* is integrated into the RISC complex, promoting the gene silencing (Li *et al.*, 2010).

1.4.3. RNA uptake for defence

Despite much has been elucidated, the RNAi mechanism still possesses mysteries to be solved. One of them is how dsRNA uptake occurs, which is an essential step for the RNAi mechanism to function. In the last years, some clues have been unveiled, which lead to the hypothesis that endocytosis plays an essential role for the uptake of this molecule (Vélez and Fishilevich, 2018).

Endocytosis is an eukaryotic cellular process where small membrane vesicles are formed (60-120 nm) and used to transport molecules from the plasma membrane into the cytoplasm. Indeed, the molecules uptake could be linked to a vast number of physiological processes, like nutrients uptake, cell signalling, cell adhesion and others. For this reason, a multitude of endocytosis pathways have been described, being the major endocytic route for molecules the clathrin-mediated endocytosis (CME) (Bitsikas *et al.*, 2014). This process is responsible for the transport of a vast array of molecules into the cell cytoplasm, assuming an important role in a multitude of physiological events, such as in cellular homeostasis or intercellular signalling. The CME process was also suggested to transport dsRNA into the cells, following the observation of dsRNA uptake in S2 *Drosophila* cells (Saleh *et al.*, 2006). Later, the enrolment of this pathway was also observed on red flour beetle (*Tribolium castaneum*) (Xiao *et al.*, 2015a) and Colorado potato beetle (*Leptinotarsa decemlineata*) (Cappelle *et al.*, 2016). Only recently, Wytinck and co-authors (2020) suggested the relation of the CME pathway to the dsRNA uptake in filamentous fungi. By using labelled RNA molecules, the authors detected dsRNA uptake as early as two hours after molecule treatment, in the filamentous fungus *Sclerotinia sclerotiorum*. These results suggested that CME components were related to dsRNA uptake. Furthermore, after knocking-out the CME-related genes *ADP-ribosylation factor* (*ARF72A*), *clathrin heavy chain* (*CHC*), *clathrin light chain* (*CLC*), *adaptor protein 2* (*AP2*), *F-bar domain only protein 1* (FCHO1), *amphiphysin* (*Amph*), and *vacuolar H+ ATPase* (*V-ATPase*), the RNAi capacity was lost.

The model of CME process is summarized in Figure 1.9. The endosome formation results from the self-assembly of the triskelion-shaped clathrin proteins into a polyhedral lattice that will organize the recruitment of proteins to coated pits, promoting the concentration of cargo vesicles (Wilbur *et al.*, 2010). The assembly unit of this coat, known as triskelion, is formed from three clathrin heavy chain (CHC) subunits, in association with three clathrin light chain (CLC) proteins in an extended three-legged structure (Haar *et al.*, 1998).

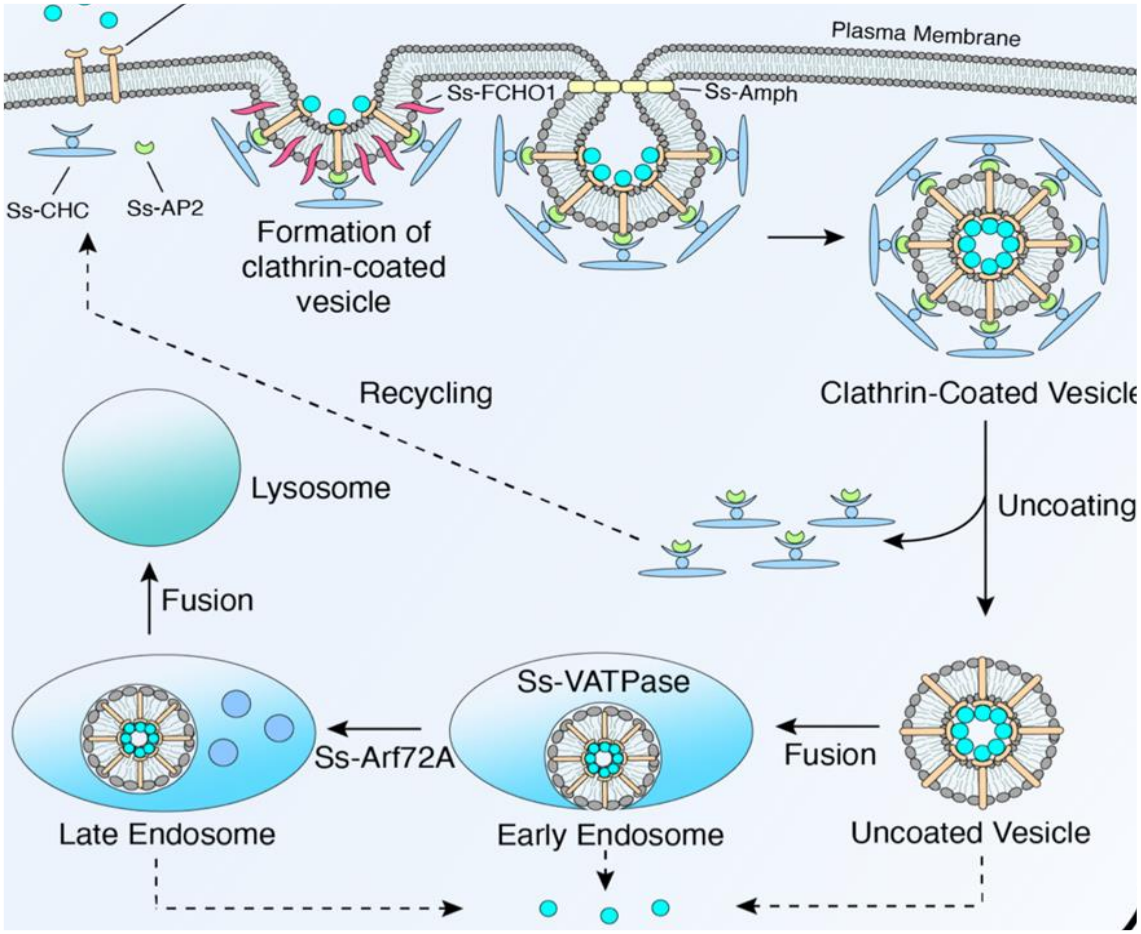

Figure 1. 9: Clathrin-mediated endocytosis pathway. The binding of exogenous dsRNA (represented by light blue circles) to its receptor induces the localization of clathrin and its adaptor to the membrane. FCHO1 contributes to the invagination of the vesicle and amphiphysin to its release from the membrane. Arf72A aids in the transition from early to late endosome, and vesicle acidification via VH + ATPase induces cytoplasmic dsRNA release. (Adapted from: Wytinck *et al.*, 2020)

The clathrin coated endosomes appears not to be able to bind the cargo, unless in the presence of certain "assembling factors". The two known polypeptides with this function are adaptor factor 1 (AP1) and adaptor factor 2 (AP2). Despite playing homologous function, both factors act on different membranes (Beacham *et al.*, 2019). AP1 is responsible for trafficking molecules from Golgi complex to endosomes, while transport from plasma membranes into the cytoplasm is more related to AP2. For this reason, the understanding of dsRNA uptake through CME pathway requires the characterization of AP2 protein. This factor is a protein complex formed by two large subunits of 100–130 kDa (α and β2), a medium subunit of ~50 kDa (μ2), and a small subunit of 17–20 kDa (σ2) (reviewed by Collins *et al.*, 2002). The trunk domain of AP2 α subunit is able to bind phosphatidyl inositol-4,5-bisphosphate (PIP2) or phosphatidyl inositol-3,4,5-

trisphosphate headgroups (PIP3), targeting AP2 to the plasma membrane and playing a central role on vesicle trafficking (Mandal, 2020). The strong binding ability of AP2 to PIP3 and PIP2 in plasma membrane is due to the large number of basic side amino acidic chains present in the N-terminus of α subunit that promotes a general electrostatic effect. However, for being functional, the AP2 complex should present an active conformation, where the binding pockets for both cargo and membrane are coplanar, thus allowing their interaction (Kovtun *et al.*, 2020). The AP2 complex activation results from the interaction with other clathrin- associated proteins, such as the F-bar domain only protein 1 (FCHO1).

As the vesicle coat expands, the curvature of the membrane becomes more pronounced until it undergoes a constriction and fission, which is another essential process for CME (Kaksonen and Roux, 2018). Amphiphysin (Amph) is an important member of the N-BAR (Bin/Amphiphysin/Ryvs) domain-containing proteins (Aryal *et al.*, 2022). During the endocytic process two funtions are associated to Amph: the interaction with multiple endocytic proteins and the promotion of a membrane curvature. Clathrin and AP2 are able to bind amphiphysin through the CLAP (Clathrin/AP2-binding) domain in the central region of the protein. In addition, Amph is able to bind dynamin (a GTPase-like protein) through the C-terminus SH3 domain, which is essential for the fission process and ultimately forms the endocytic vesicles (Takeda *et al.*, 2018). Through the BAR domain, Amph is also able to bind the phospholipid membrane, promoting an increase in the membrane curvature (Aryal *et al.*, 2022).

Proteins associated with assembling and functioning of late endosomes, including an ADP ribosylation factor-like 1 protein (ARF72A) and a Vacuolar H^+ ATPase (V-ATPase), have been also confirmed to be essential for effective RNAi (Wytnick *et. al,* 2020). ARFs can be found in an inactive state when bound to a GDP, becoming active when bound to a GTP. Such active ARFs are able to associate with membranes, interacting with proteins related to the CME an assisting the endosome formation. For the release facilitation of endocytosed contents, a proton pump responsible for the acidification of endosomal vesicles is crucial for CME (Farsi *et al.*, 2018). When luminal pH is lowered through the activity of a V-ATPase, the release of the cargo into the cytoplasm is facilitated. V-ATPases are large proton pumps, composed by several subunits, containing an ATP-hydrolytic domain (V1) and a proton-translocation domain (Vo) (Mazhab-Jafari and Rubinstein, 2016).

1.4.4. HIGS and SIGS, two biotechnological approaches

The RNAi mechanisms are recently being applied for designing new plant disease control strategies to be used as alternatives to synthetic fungicides. Two main techniques have been suggested: the Host-induced gene silencing (HIGS) and the Spray-induced gene silencing (SIGS) (Figure 1.10).

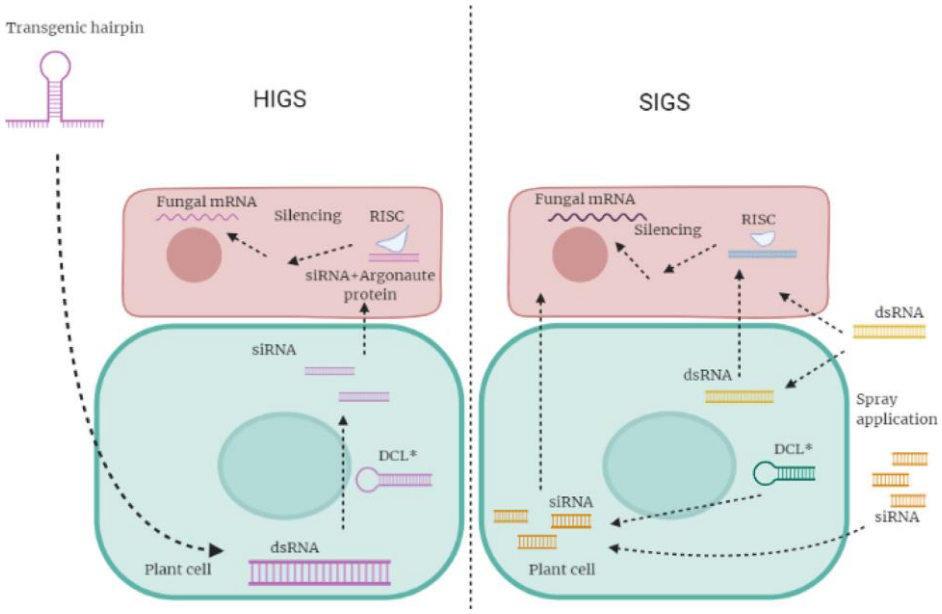

Figure 1. 10: Host-induced gene silencing (HIGS) and Spray Induced gene silencing (SIGS) strategies. Difference in the action of both techniques are represented. In HIGS, the plant is genetically modified to produce RNA hairpins that will generate the dsRNA to silence the fungal target gene. As for SIGS, the dsRNA is exogenously applied and uptaked by both plant and pathogen, with which the pathogen target gene will be silenced (Adapted from: Filho *et al.*, 2021)**.**

Both strategies can provide sustainable, effective and environmental-friendly strategies for the control of fungal diseases (Sang and Kim, 2020).

The HIGS technique is based on the creation of genetic modified plants that will produce dsRNA (or hairpin-structured dsRNA) that targets a specific pathogen gene. The transgenic plants are capable of using the produced dsRNA to induce RNAi mechanisms, acquiring protection against the pathogen attack (Tetorya and Rajam, 2021). This innovative technique has been also proved to be effective for controlling pests. An example is the *SmartStax PRO* maize, which was the first commercial genetically engineered RNAi plant to receive approval in Canada and USA, in 2021. This transgenic maize proved to effectively control the western corn rootworm, *Diabrotica virgifera*, a devasting Coleoptera corn pest (Moar *et al.*, 2017). Several pathogenic diseases have been also controlled by applying the HIGS technique. For example, engineered rice is able to silence a fungal

component of histidine kinase (*MoAP1*), required for cell wall integrity and pathogenicity, improving the plant resistance against 11 strains of *Magnaporthe oryzae* (H. Zhang *et al.*, 2010).

In contrast with HIGS, the SIGS strategy do not require the host transformation. The targeting dsRNA is delivered through a spray onto the plant surface. In this process, the plant protection is ensured through two different pathways (Koch *et al.*, 2016b). The dsRNA is directly uptaked by the fungal pathogen, which will then induce its own RNAi mechanism, silencing essential genes. But, the host plant could also uptake the dsRNA, inducing the plant RNAi machinery and magnifying the siRNA signal. Later, the processed dsRNA will target the fungal cells, during plant-pathogen/pest interactions. This strategy was successfully applied for controlling *Fusarium graminearum*, one of the causing agents of head blight diseases in cereal crops (Werner *et al.*, 2020). When dsRNA molecules were created from *F. graminearum* DCL genes, the resistance to head blight diseases was enhanced, showing the effectiveness of this technique in fungi.

However, both techniques possess their limitations (Niu *et al.*, 2021). By using genetically modified plants that express dsRNAs targeting the essential genes of pathogen/pests, HIGS revealed to be a successful approach to control plant diseases (Tetorya and Rajam, 2021). However, HIGS is strongly limited by the lack of transformation techniques in many plants. Furthermore, current public opinion is still resistant to the use of genetically modified organisms (GMO) and most of them have been banned from the European agricultural production (San-Epifanio, 2022). Therefore, plant protection measures that does not involve GMO are highly preferred. Another breakthrough started since the work of Kock and co-authors (2016), where *F. graminearum* was found to uptake environmental dsRNA and promote the silencing of pathogen genes. From these discoveries, the SIGS approach emerged. This new technique has been regarded as a GMO-free solution that could be used as a tailored high specific control measure to an unlimited range of pathogens and pests. However, even SIGS approach display some limitations (Das and Sherif, 2020). Indeed, several factors could affect the efficiency of SIGS, such as concentration and length size of dsRNA, the application method and molecule stability under environmental conditions.

1.5. Aims and thesis outline

Biscogniauxia mediterranea and *Diplodia corticola* incidence have been arising in the last years, leading to a more pronounced decline of *Quercus suber* population. The development of a specific treatment against these pathogens could reverse this decline. The main objective of this work is to develop an effective new generation biofungicide, based on RNAi mechanism to be applied through SIGS. Due to the lack of research in RNAi field involving both *B. mediterranea* and *D. corticola*, this thesis presents the following specific aims: (1) understand the feasibility of pathogen RNAi machineries for pursuing with a RNA-based approach, and (2) design dsRNA molecules able to inhibit *B. mediterranea* and *D. corticola* growth.

For understanding if the studied pathogens possess all the necessary protein machinery for dsRNA uptake and RNAi silencing, an *in silico* screening will be performed on the **chapter III**. On **chapter IV**, both pathogens will be tested for their capacity to uptake and process dsRNA. If *B. mediterranea* and *D. corticola* present the capacity to use RNAi mechanisms, the design of possible target genes will be performed on **chapter V**, which will also test them against the pathogens and off-target species. The capacity to affect fungal development will be tested through *in vitro* assays and will be described in **chapter VI**, where different conditions will be used to understand the possible outcomes on the use of SIGS technique.

2. Chapter II: Methodology

2.1. Methods for testing *in silico* CME and RNAI machinery

2.1.1. Identification and characterization of components for dsRNA uptake and RNAi silencing

Nucleotide sequences of genes that code proteins related with dsRNA uptake [*clathrin heavy chain* (*CHC*, ID 7417), *clathrin light chain* (*CLC*, ID 8186), *adaptor protein 2 subunit* α (*AP2-α*, ID 13037, *F-bar domain only protein 1* (*FCHO1*, ID 1114), *amphiphysin* (*Amph*, ID 10432), *ARF2A* (ID 13701), and *V-ATPase* (ID 13729)] from *Sclerotinia sclerotiorum* were downloaded from *Joint Genome Institute* (JGI). Similarly, the nucleotide sequences of genes coding RNAi components [*Dicer* (*DCL-1*, ID XP_961898.1; *DCL-2*, ID XP_963538.3), *Argonaute* (*SMS-2*, ID XP_958586.1; *QD-2*, ID XP_011394903.1), RNA-dependent RNA polymerase (*SAD-1*, ID XP_964248.3; *QDE-1*, ID XP_959047.1; RRP -3, ID XP_963405.1)] of the fungal model *Neurospora crassa* were obtained from *NCBI GenBank*. The retrieved sequences were used as references for BLASTn comparations against the annotated *B. mediterranea* (performed on JGI database) and *D. corticola* genomes (performed on NCBI database). Hits with the highest e-values were selected for further analysis The functional domains and other structural aspects of complete encoded proteins were identified using *InterPro* (https://www.ebi.ac.uk/interpro), *Pfam 35.0* (http://pfam.xfam.org/) and *Simple Modular Architecture Research Tool* (SMART) (http://smart.embl-heidelberg.de/).

2.1.2. Phylogenetic analysis

Homologous proteins from 28 fungi were searched for studying the evolution and diversification of DCL, AGO, and RdRP proteins (for accession numbers, see Supplementary Tables S.1 to S.3), including those from *B. mediterranea* and *D. corticola*. Multiple sequence alignments were performed using *MUSCLE* algorithm, implemented in *MEGA version x software*. Maximum likelihood trees were created based on JTT method, using *MEGA version 11 X software*, and the tree nodes was tested with 1000 bootstrap replicates.

2.2. Methods for testing dsRNA uptake and RNAi silencing

2.2.1. Agrobacterium competent cells preparation

An *Agrobacterium tumefaciens* strain GV3101 was grown in solid LB medium (10 g l^{-1} of tryptone, 5 g l^{-1} of yeast extract, 10 g l^{-1} of NaCl, 35 g l^{-1} of agar). A single colony was used to inoculate 5 ml of LB liquid medium (same as solid LB medium, without agar) and growth was promoted overnight, at 30° C, with a constant shacking at 200 rpm. This culture (50 µl) was used to inoculate 50 ml of LB medium that was incubated in the same conditions. The resultant culture was transferred to two 50 ml tubes (previously cooled in ice for 10 min), which were centrifuged at 3,000 *g*, at 4° C for 6 min. The resulting pellet was briefly washed with 1 ml $CaCl_2$ (20 mM, cooled at –20°C) and suspended in 10 ml of $CaCl_2$ (20mM, cooled at – 20°C) and divided into aliquots of 100 µl, using microtubes previously cooled in ice. Cells were immediately frozen in liquid nitrogen and stored at -80°C.

2.2.2. Agrobacterium transformation

For the transformation of Agrobacterium cells a pCAMBgfp vector was gently provided by Athanasios Dalakouras (Dalakouras *et al.*, 2022). The construct contains a *GFP* gene variant (*sGFP*) under control of a PToxA promoter, based on the promoter from *Pyrenophora tritici - repentis ToxA* gene (Figure 2.1). This *sGFP* variant is known to promote a serine-to-threonine substitution at the amino acid 65 of GFP, resulting into a highest concentration and fluoresce levels (Lorang *et al.*, 2001), and have been thoroughly used in RNAi studies (Dalakouras *et al.*, 2022). The expression construct also displays a TNOS (terminator for the nopaline synthase gene), as well as a kanamycin and hygromycin resistance gene for selection.

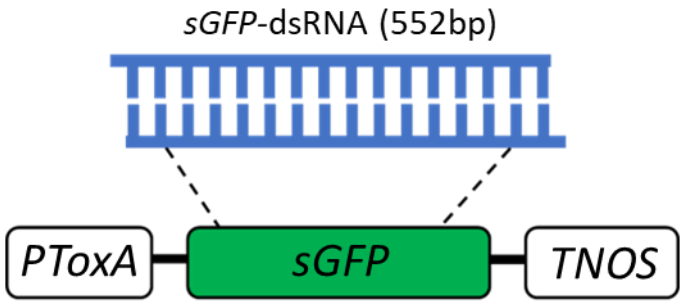

Figure 2. 1: Representation of the used *sGFP* transgene. *PToxA*: promoter from *Pyrenophora tritici - repentis ToxA* gene; *sGFP*: *GFP* variant that contains a serine-to-threonine substitution at amino acid 65; *TNOS*: terminator for the nopaline synthase gene. The 552 bp fragment chosen for in vitro transcription of dsRNA is depicted

For bacterial transformation, 1 µg of pCAMBgfp vector was added to 100 µl of Agrobacterium competent cells. After mixing by inversion, cells were immediately frozen in liquid nitrogen, for 5 min. Following an incubation for 10 min, at room temperature, 1 ml of LB liquid medium was added and cells were incubated for 3 h, at 30° C, with a constant shaking at 200 rpm. The resultant culture was centrifuged at 4,000*g*, for 1min, at room temperature. After discarding 1 ml of the supernatant, the pellet was suspended in the remaining solution. The obtained culture was plated onto LB solid medium, supplemented with 20 µg ml^{-1} rifampicin and 100 µg ml^{-1} kanamycin for transformants selection.

2.2.3. Fungal cultures

Biscogniauxia mediterranea and *Diplodia corticola* isolates were kindly provided by Daniela Costa (Costa, 2021). Both fungi had been isolated from *Quercus suber* twigs, in which they were growing as endophytes (Costa *et al.*, 2020). Spore suspensions of both fungi were prepared in glycerol (50%, v/v) and have been kept in -80 °C. The fungi have been also maintained by subculturing them on PDA medium and keeping them at room temperature (21-23 °C), under dark conditions.

2.2.4. Fungal conidia preparation

Spore suspensions of *Biscogniauxia mediterranea* and *Diplodia corticola* (glycerol; 50%, v/v) were spread onto PDA plates and incubated for 10-15 days, in the dark, at 25 °C, to allow sporulation. The produced spores were harvested by adding 5 ml of 0.9% (w/v) NaCl to each plate and gently scraping the surface of mycelia with a glass spreader. The resulting suspension was filtered through *Miracloth* into a 15 ml tube. The conidia were centrifuged for 10 min at 1,000 *g* at room temperature, the supernatant was discarded and spores were suspended into 1 ml of 0.9% (w/v) NaCl. Spore concentration was determined using a hemacytometer and diluted to a final concentration of 1 x 10^7 conidiospores ml^{-1} (Michielse *et al.*, 2008).

2.2.5. Fungal transformation

Fungi were transformed by using an *Agrobacterium tumefaciens* - mediated transformation method. Transformed Agrobacteria with pCAMBgfp vector (section 2.2.2) were grown in LB liquid medium, supplemented with 20 µg ml^{-1} rifampicin and 100 µg ml^{-1} kanamycin for selective pressure. Growth was promoted at 30° C, with constant shaking at 250 rpm, for 24 h. Bacterial cells (1,5 ml) were harvested and centrifuged for 10 min, at 2,400 *g*, at room temperature. After discarding the supernatant, the cells were washed and suspended using 250 µl of Induced Medium

(IM) [0.8 ml of phosphate buffer (1.25 M, pH 4.8), 20 ml of MN buffer (30 g l^{-1} $MgSO_4.7H_2O$, 15 g l^{-1} NaCl), 1 ml of 0.1 g l^{-1} $CaCl_2.2H_2O$, 10 ml of 0.001 g l^{-1} $FeSO_4$, 5 ml of trace elements (0.21 g l^{-1} $ZnSO_4.7H_2O$, 0.11 g l^{-1} H_3BO_3, 0.05 g l^{-1} $MnCl_2.4H_2O$, 0.05 g l^{-1} $FeSO_4.7H_2O$, 0.017 g l^{-1} $CoCl_2.6H_2O$, 0.016 g l^{-1} $CuSO_4.5H_2O$, 0.015 g l^{-1} $Na_2MoO_4.2H_2O$, 0.51 g l^{-1} EDTA), 2.5 ml of 20% (w/v) NH_4NO_3, 10 ml of 50% (v/v) glycerol, 40 ml of 1 M MES (pH 5.5), and 10 ml of 20% (w/v) glucose to 900.7 ml of sterilized water]. The cell suspension was centrifuged again for 5 min, at 2,400 *g* at room temperature, and the resulting pellet was suspended in 5 ml of IM, containing 5 µl of 0.2 M acetosyringone (AS). The cells were further incubated for 4-5 h, at 28° C at 100 rpm. The culture was then diluted in IM, up to an OD_{600nm} near 0.8 (4-5 x 10^8 bacterial cells/ml).

Induced Agrobacterium cells (100 µl) and fungal conidiospores (100 µl, section 2.2.4) were mixed, being the resultant suspension evenly spread onto a *Hybond-N+ membrane* (Amersham Biosciences, Amersham, United Kingdom), previously placed on solid IM (liquid IM with 35 g l^{-1} of agar), supplemented with 200 µM of AS. Following an incubation at 25° C for 72 h, the *Hybond-N+ membrane* was transferred to a new PDA plate, supplemented with 200 µM hygromycin and 200 µM cefotaxime. This medium would select the putative hygromycin positive (Hyg+) fungal transformants, while cefotaxime would kill *A. tumefaciens* cells. Following a new incubation for 72 h at 30° C in the dark, the resulting transformants were transferred to a fresh selection medium (PDA, supplemented with 200 µM hygromycin) for single conidiospore isolation (Michielse et all, 2008). The production of sGFP by transformed fungi was confirmed by observation using a fluorescence microscope *Olympus BX63F2*, equipped with an *Olympus DP74* camera.

2.2.6. Production of *sGFP*-dsRNA and labelled *sGFP*-dsRNA

For assaying the ability of *sGFP* gene silencing and dsRNA uptake, *sGFP*-dsRNA and labelled *sGFP*-dsRNA were respectively synthesized. The cloned *sGFP* sequence, included in pCAMBgfp vector, was used as template for both dsRNAs. For this, DNA was extracted from both transformed fungi, using the *Quick-DNA Fungal/Bacterial Miniprep* kit (Zymo Research, California-USA). PCR reactions were prepared in 20 µl volume using 2 µl of DNA (previously extracted), 2 µM of each primer containing T7 adapter (forward primer-TAATACGACTCACTATAGGGAGAGCGACGTAAACGGCCACAAG; reverse primer TAATACGACTCACTATAGGGAGATACAGCTCGTCCATGCCGTG; T7 adapter underlined) and 0.4 U μl^{-1} of NZYTaq II 2× Green Master Mix (NZYTech, Portugal). The amplifications were performed using the following PCR program: i) initial denaturation at 94 °C, for 3 min; ii) 35 cycles

of 30 s at 94 °C, 30 s at 58.5 °C and 35 s at 72 °C; and iii) final elongation at 72 °C for 10 min. PCR products were evaluated after a gel electrophoresis on a 1% (w/v) agarose gel, stained with *Green Safe Premium* (NZYTech, Portugal). DNA samples that resulted in amplification were quantified using a fluorescent DNA quantification assay with *Qubit dsDNA HS Assay kit* (ThermoFisher Scientific, USA) and detected with a *Qubit 3.0 Fluorometer* (ThermoFisher Scientific, USA). For *sGFP*-dsRNA synthesis, the resulting amplicon (200 ng) was used as template for *MEGAscript RNAi* kit (Ambion™, ThermoFisher), following the protocol provided by the manufacturer. Labelled *sGFP*-dsRNA was obtained by using the same amplicon (200 ng) as template for the *Fluorescein RNA Labelling Mix* (Sigma-Aldrich, Oakville, ON, CA), following the manufacturer instruction.

2.2.7. Uptake dsRNA assay

PDA medium (1 ml) was evenly distributed on sterile microscope slides. A mycelium-colonized agar plug (5 mm) was placed on the border of the slide to create space for fungal growth. The slides were incubated in dark conditions, at 25° C for 24 hours, in a sterile petri dish. After this period, 150 ng of labelled sGFP-dsRNA (section 2.2.6.) was added and fluorescent signals were observed after an incubation at 25 °C, during 8 h. An *Olympus BX63F2* fluorescence microscope, equipped with an *Olympus DP74* camera, was used for observation.

2.2.8. Assay for *in vitro* RNAi silencing

The conidia of transformed fungi (comprising the *sGFP* transgene) were obtained as described in section 2.2.5 and suspended in potato dextrose broth (PDB). The conidia of each sGFP transformed fungus were quantified using a hemacytometer and diluted to a final concentration of 60 conidia ml^{-1} (in PDB). Conidia suspension (100 µl) was added to 24 wells of a 96-well plate. While 100 µl of *in vitro* transcribed sGFP dsRNA (1 ng μl^{-1}, produced in section 2.2.6) were added in 12 wells, 100 µl of water was added to the remaining 12 wells (control samples) (Figure 2.2). Blanks were performed by adding 200 µl of PDB to other 12 wells. The 96-well plate was covered and incubated at 25°C. Immediately before incubation (0 h), 24 h and 48h of incubation, the fluorescence was determined using the *Tecan infinite 200 Pro* microplate reader. Specifically, the sGFP fluorescence (excitation 488 nm, emission 515 nm) was measured, as well as the growth-

indicative absorbance (wavelength 595 nm). At the end, the relative fluorescence units (RFU) were determined, as the ratio of both measures.

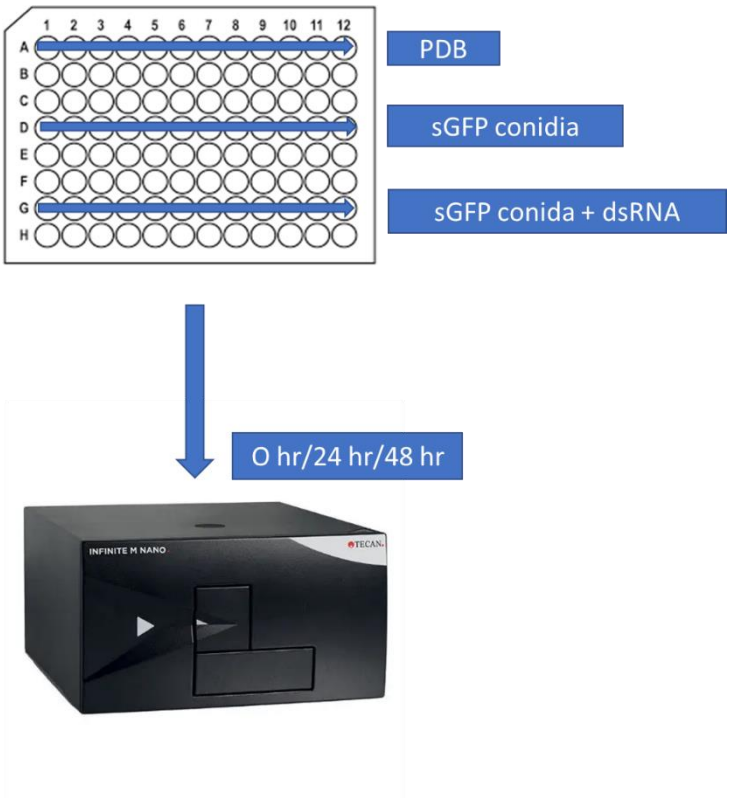

Figure 2. 2: Experimental design for evaluating in vitro RNAi silencing assay. The distribution on the 96-well plate was as follow: i) 12 wells included PDB medium and serves as blanks (PDB); ii) 12 wells contained transformed *B. mediterranea* or *D. corticola* conidia and serve as controls (BmsGFP/DCsGFP), iii) 12 wells contained transformed cork oak pathogens conidia and dsRNA targeting *sGFP.* The plate was read for fluorescence (excitation 488 nm, emission 515 nm) and for growth-indicative absorbance (wavelength 595 nm), immediately before incubation, 24 and 48hr post dsRNA application (BmsGFP/DCsGFP).

2.3. Methods for designing and synthetizing dsRNA molecules

2.3.1. dsRNA design and synthesis

Two different methods were used for designing dsRNA molecules (Figure 2.3). In the first method (non-conserved domain approach), the sequence of target protein and corresponding homologs were analysed and the conserved domains in cork oak pathogens were identified. Primers for the most variable regions were designed, reducing the probability of an off-target effect. In the second

method (gene fragmentation approach), the entire gene was fragmented into pieces of 450-500 bp, and primers were designed to amplify these fragments.

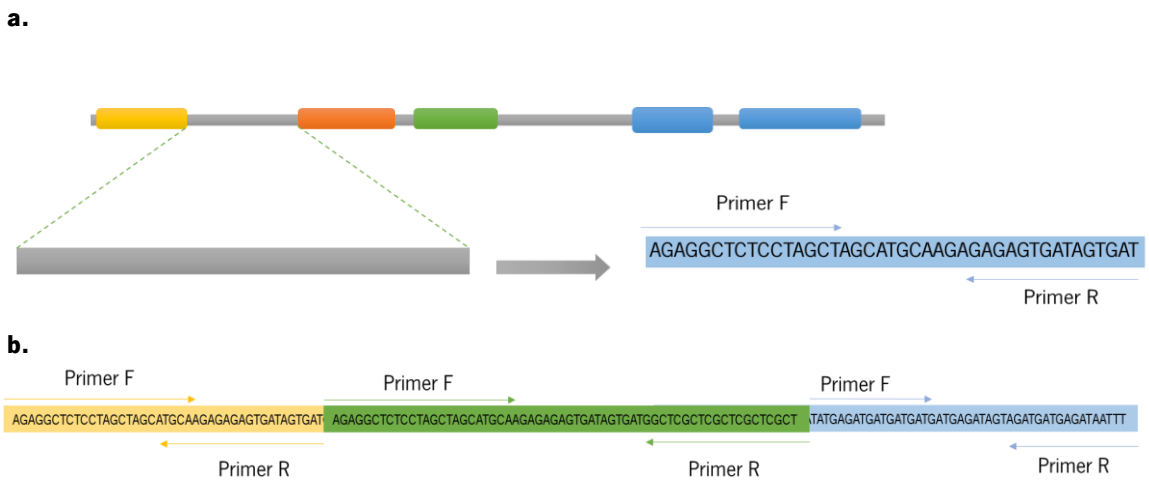

Figure 2. 3: Representation of the used dsRNA design methods, a non-conserved domain (a) and a gene fragmentation (b) approach. The use of regions with non-conserved domains results in more specific dsRNA targets, avoiding possible off-targets. The use of gene fragmentation method results in many dsRNAs able to target these regions.

To obtain the designed gene region, genomic DNA extraction from both cork oak pathogens was performed using the *Quick-DNA Fungal/Bacterial Miniprep* kit (Zymo Research, California-USA). PCR reactions were prepared in 20 µl volume using 2 µl of DNA (previously extracted), 2 µM of each primer containing the T7 adapter and 0.4 U μl^{-1} of *NZYTaq II 2× Green Master Mix* (NZYTech, Portugal). DNA target amplifications were performed using the following PCR program: i) initial denaturation at 94 °C, for 3 min; ii) 35 cycles of 30 s at 94 °C, 30 s 54-58 °C (depending on the specific primers) and 35 s at 72 °C; and iii) final elongation at 72 °C for 10 min. PCR products were analysed using a 1% (w/v) agarose gel, stained with *Green Safe Premium* (NZYTech, Portugal). Amplicons within the expected size were quantified by using a fluorescent DNA quantification assay with *Qubit dsDNA HS Assay kit* (ThermoFisher Scientific, USA) and detection with a *Qubit 3.0 Fluorometer* (ThermoFisher Scientific, USA). For the dsRNA synthesis, the resulting amplicon (200 ng) was used as template for *MEGAscript RNAi kit* (AmbionTM, ThermoFisher), following the protocol provided by the manufacturer. RNA concentration was determined using a fluorescent RNA quantification assay with *Qubit™ RNA High Sensitivity* assay kit (ThermoFisher

Scientific), followed by detection with a *Qubit 3.0 Fluorometer* (ThermoFisher Scientific). Additionally, the quality of the produced dsRNA was evaluated through an electrophoretic analysis of the produced dsRNA (diluted (1/10), using a 1% (w/v) agarose gel stained with *Green Safe Premium* (NZYTech, Portugal).

2.3.2. Prediction of off-targets and number of siRNA produced

For off-targets prediction, every sequence selected for dsRNA synthesis was *in silico* compared against available *Quercus suber* transcriptome and their known fungal endophytes, using the *si-Fi v21 software* (default parameters). By combining the BOWTIE-based sequence similarity search for siRNA targets with probability calculation of local target-site and thermodynamics, this software provides a high sensitivity output that allows to understand if the designed dsRNA is an off-target (Lück *et al.*, 2019). The same software was used for to predict the number of possible effective siRNA for each of the designed molecules.

2.4. Methods for testing produced dsRNA in *B. mediterranea* and *D. corticola*

2.4.1. *In vitro* assays for determining dsRNA effects on cork oak pathogens growth

To test the effect of all designed dsRNAs in both cork oak pathogens, a mycelium-colonized agar plug (5 mm) was taken from the margins of a freshly PDA-medium-grown colonies (3 days old) (Figure 2.4). The plug was placed in the center of a PDA plate (9 cm in diameter), in direct contact with an aliquot (10 µl) of a specific dsRNA solution (directly obtained from the *in vitro* transcription kit, section 2.3.1). As control, a similar mycelium-plug was placed in the center of a PDA plate, in order to follow fungal growth with no further interference (no-dsRNA control). Additionally, to discard possible effects caused by high humidity, a similar mycelium-plug was placed in the center of a PDA plate in direct contact with ultrapure sterilized water (10 µl, control H_2O). The cultures were grown in the dark at 25° C for five days, during which the area occupied by the fungus was measured each day. The corresponding area was calculated using the software *ImageJ*. Using these conditions, dsRNA molecules were tested in different concentrations (5 - 100 ng/µl, dilutions in sterile ultrapure water). Each treatment contained three replicates and the entire experiment

was repeated three times. Statistical analysis was performed using ANOVA in *GraphPad Prism 9.00* software (La Jolla, CA, USA) to understand the impact of dsRNA on pathogen growth.

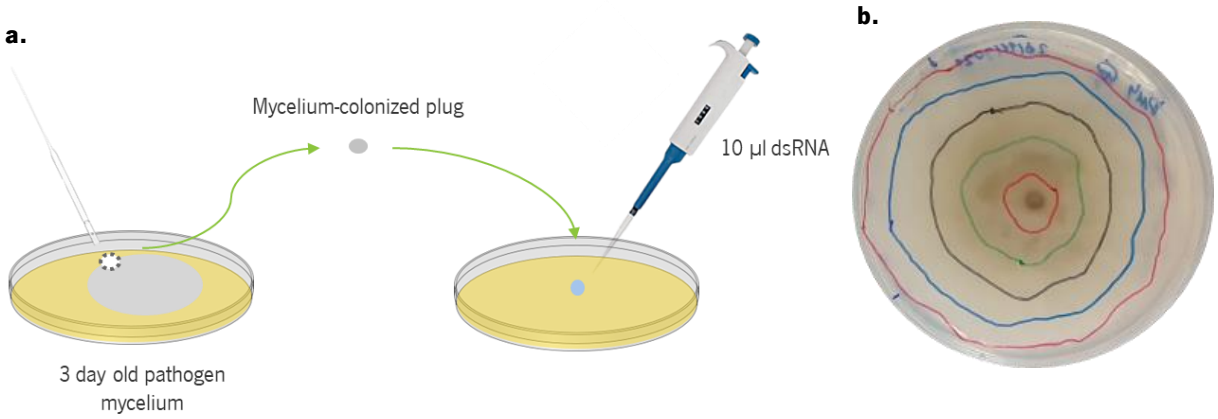

Figure 2. 4: Assay for determining dsRNA efficiency to impair cork oak pathogens growth (a) and corresponding result (b). Example of the daily area measures performed (b). A plug taken from actively growing pathogen was placed in the center of a PDA plate, in direct contact with the dsRNA solution. During five days, the area occupied by the fungus was daily measured, as displayed is figure where each coloured circle corresponds to 24 h of fungal growth.

2.4.2. *In vitro* assays under the constant presence of dsRNA

To test the effect of sustained presence of dsRNA, a mycelium-colonized agar plug (5 mm) was taken from the margins of freshly PDA-medium-grown colonies (3 days old). The plug was placed in the center of PDA plate (9 cm in diameter), supplemented with dsRNA (2 µg 10 ml^{-1} PDA) immediately before plated. As control, a similar mycelium-contain plug was placed in the center of a PDA plate (without dsRNA supplementation) to grown with no further interference. Additionally, a *sGFP*-dsRNA control was used as a non-target gene (*sGFP* control). The assayed conditions, growth measurements and data analysis were identical to those described before.

2.4.3. *In vitro* assays under stress conditions

To examine the influence of stress conditions (oxidative and osmotic stress) on dsRNA effects, the same assays as described in section 2.4.2 were performed in PDA plates, supplemented with designed dsRNA and stress agents, both added immediately before plating. For testing the effects

of oxidative stress, PDA was supplemented with hydrogen peroxide (H_2O_2) up to a final concentration of 3 mM, whereas for studying osmotic stress effects a supplementation with sorbitol up to a final concentration of 1.2 mM was used. Non-target gene controls (*sGFP* control) were prepared by adding 2 μg of *sGFP*-dsRNA, instead of targeted dsRNA. Fungal growth controls were prepared by placing similar mycelium plugs in the center of PDA plates, only supplemented with stress agents and not with dsRNA. The assayed conditions, growth measurements and data analysis were identical to those described before.

2.4.4. *In vivo* assay for determining the effects of dsRNAs on hyphae morphology

For determining the effects of dsRNA application on the morphology of cork oak pathogen hyphae, a live imaging assay was performed. PDA medium (1 ml) was evenly distributed on the sterile surface of sterile microscope slides. A mycelium-colonized agar plug (5 mm) was placed on the border of the slide to create space for fungal growth. Slides were incubated in dark conditions, at 25° C, for 24 hours in a sterile petri dish. After incubation, 2 μl of dsRNA (100 ng μl^{-1}, prepared in sterile ultrapure water) was added near the grown mycelium. Microscopy observation under bright-field on a *Olympus BX63F2*, equipped with an *Olympus DP74* camera, was performed 24 hr after dsRNA application.

3. Chapter III: RNAi machinery in cork oak pathogens and phylogenetic analysis

Before designing any RNAi silencing approach for controlling the development of fungal pathogens, the critical RNAi components should be investigated in the pathogenic species under study. In this chapter, *Biscogniauxia mediterranea* and *Diplodia corticola* genomes will be analysed to understand if they display the necessary genes encoding the protein machinery for SIGS to work. In addition, and due to their focal importance on RNAi silencing mechanism, a phylogenetic analysis of DCL, AGO and RdRP will be performed, mainly considering ascomycetes. The diversification of such RNAi-related proteins could give new insights on RNAi silencing evolution in fungi. When searching for protein homologs of clathrin-mediated endocytosis (CME) and RNAi components in *D. corticola* and *B. mediterranea*, both cork oak pathogens displayed all these genes (Table 3.1).

3.1. Components of clathrin-mediated endocytosis in cork oak pathogens

Many CME components were detected *in silico* in both cork oak pathogens (*B. mediterranea* and *D. corticola*), although some variations were detected. In yeast, the CHC protein is composed by three main conserved domains: a N-terminus Propeller domain (CLP), a H linker (CLH), and eight Clathrin Heavy Chain Repeats (CLH) (Brodsky, 2012). The fungal model for CME pathway, *S. sclerotiorum*, contains two CLP domain in the N-terminus. As for, *B. mediterranea* and *D. corticola* both fungi contain three CLP domains (Figure 3.1). Using the *Interpro database*, both compositions (with three or two CLP domains) are commonly found in Ascomycota phylum. For this reason, besides presenting structural differences, the results suggest that both pathogen CHC proteins could be functional.

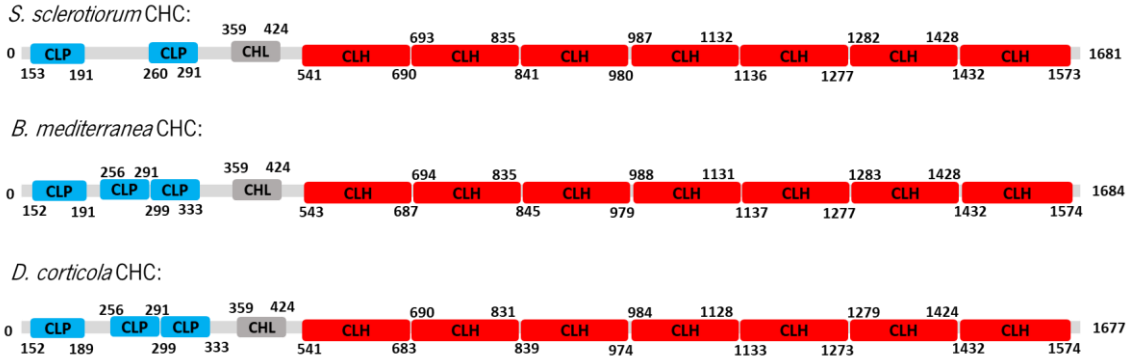

Figure 3. 1: Structure of clathrin heavy chain (CHC) proteins from the model species *S. sclerotiorum* and cork oak pathogens (*B. mediterranea* and *D. corticola*). The three main domains of CHCs are highlighted in colour: Propeller domain (CLP, in blue), H linker (CLH, in grey), and Clathrin Heavy Chain Repeats (CLH, in red).

Table 3. 1: *B. mediterranea* and *D. corticola* genes, homologous to those used for coding dsRNA uptake components in *Sclerotinia sclerotiorum*. Information about the accession number, gene length and structure, as well as corresponding protein length and domains are given. The platform used for accessing genomic information from *B. mediterranea* was JGI, while NCBI was used to access genomic information from *D. corticola.*

Protein name	Species	Gene accession number	Gene length (bp)	Exons	Protein length (aa)	Domains
Clathrin heavy chain (CHC)	*B. mediterranea*	188933 (JGI)	5570	4	1684	Clathrin-propel (IPR02236) Clathrin-H-Link (PF13838) Clathrin Heavy (IPR00054)
	D. corticola	BKCO1_520003 (NCBI)	5363	7	1677	
Clathrin light chain (CLC)	*B. mediterranea*	287350 (JGI)	1541	3	235	Coiled region
	D. corticola	BKCO1_490002 8 (NCBI)	945	3	256	
Adaptor protein2 (AP2-α)	*B. mediterranea*	501414 (JGI)	4171	7	983	Clathrin-adaptor (IPR00255) α2adaptine (IPR00815) α adaptine (IPR00316)
	D. corticola	BKCO1_200090 (NCBI)	2932	2	936	
F-bar domain only protein 1 (FCHO1)	*B. mediterranea*	621480 (JGI)	4052	5	868	FCH (IPR18808) MuHD (IPR02856)
	D. corticola	BKCO1_800011 0 (NCBI)	3064	7	905	
Amphiphysin (Amph)	*B. mediterranea*	623027 (JGI)	2458	3	508	BAR (IPR004148) SH3 (IPR001452)
	D. corticola	BKCO1_130001 55 (NCBI)	1699	3	522	
ADP-ribosylation factor (Arf72A)	*B. mediterranea*	671337 (JGI)	794	4	181	Small_GTP (IPR005225)
	D. corticola	BKCO1_400017 5 (NCBI)	734	4	183	
Vacuolar H + ATPase (V-ATPase V1)	*B. mediterranea*	354652 (JGI)	2359	4	478	V-ATPase_v1 (IPR004908)
	D. corticola	BKCO1_400081 (NCBI)	1579	3	481	

Regarding the CLC proteins, only a coiled region followed by a 70 amino acid sequence in the C-terminus is considered as essential for a functional CHC protein (Wang *et al.*, 2006). For this reason, no specific conserved domain was identified in the *in silico* analysis. Nevertheless, both the coiled region and the tandem 70 amino acid were identified in all three proteins (Figure 3.2).

Figure 3. 2: Structure of clathrin light chain (CLC) proteins from the model species *S. sclerotiorum* and cork oak pathogens (*B. mediterranea and D. corticola*). No conserved domains were identified in the CLC proteins.

The α subunit of the assembling factor AP2 for vesicle trafficking do not reveal structural differences among the studied fungi. Besides the basic domain for promoting phospholipid components of cell membranes (clathrin adaptin-like domain), AP2-α comprise two smaller domains in the C-terminus, which allow the linkage to AP2-σ2 subunit (Collins *et al.*, 2002). The AP2-α components of *S. sclerotiorum*, described to be essential for dsRNA uptake, contain the described domains that were similarly found in the homologous proteins from both pathogen (Figure 3.3).

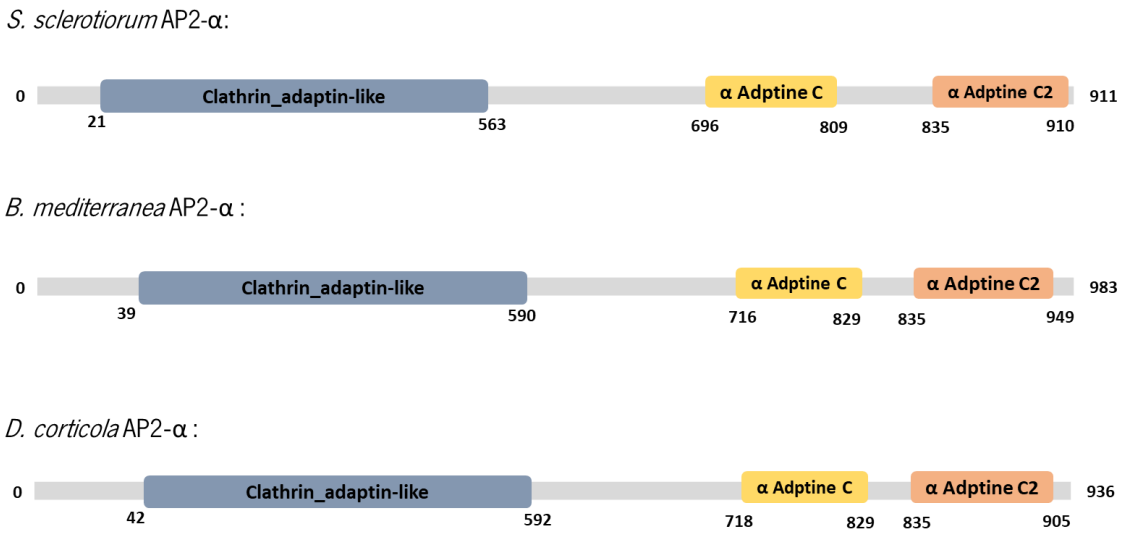

Figure 3. 3: Structure of adaptor protein 2 (AP2-α) proteins from the model species *S. sclerotiorum* and cork oak pathogens (*B. mediterranea* and *D. corticola*). The three main domains of AP2-α are highlighted in colour: Clathrin adaptin-like (in blue), α Adaptine C (in yellow), and α Adaptine C2 (in orange).

The AP2 interacts with FCHO1, which comprises an F-bar domain (FCH), a linker region and a C-terminal μ-homology domain (muHD) (Hollopeter *et al.*, 2014). The FCHO1 proteins from cork oak pathogens comprise all these domains, as detected in *S. sclerotiorum* (Figure 3.4).

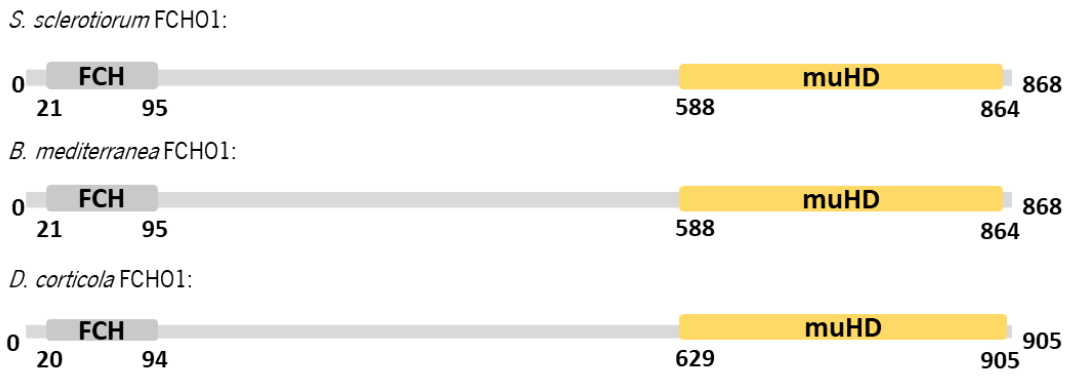

Figure 3. 4: Structure of F-bar domain only protein 1 (FCHO1) proteins from the model species *S. sclerotiorum* and cork oak pathogens (*B. mediterranea* and *D. corticola*). The two main domains of FCHO1 are highlighted in colour: F-bar domain (FCH in grey) and μ-homology domain (muHD in yellow).

The main domains of amphiphysin were similarly detected in the studied fungi, in particular the N-BAR domain that promotes the increase in the membrane curvature and C-SH3 domain, both essential for vesicle constriction and fission (Figure 3.5). However, the CLAP domain, commonly found in most animal amphiphysins, was not detected in any studied fungi (*S. sclerotiorum* or cork oak pathogens), suggesting possible limitations in protein interaction with AP2 and clathrin proteins.

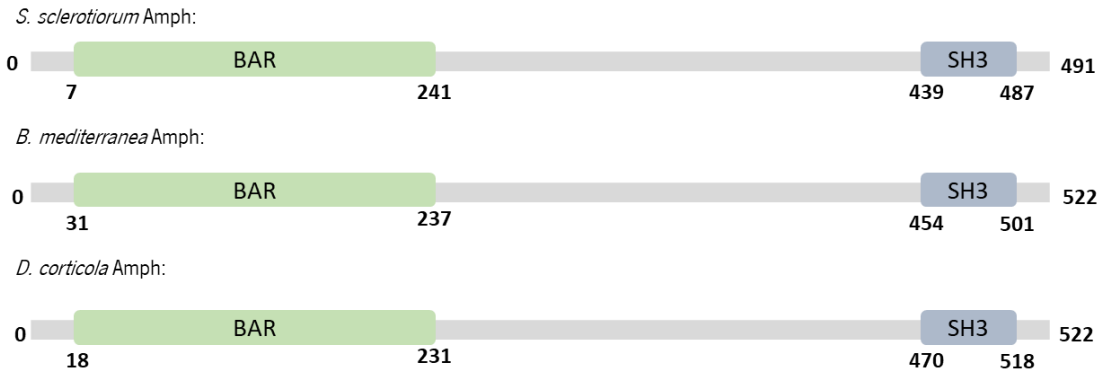

Figure 3. 5: Structure of Amphiphysin (Amph) proteins from the model species *S. sclerotiorum* and cork oak pathogens (*B. mediterranea* and *D. corticola*). The two main domains of Amph are highlighted in colour: Bin/Amphiphysin/Ryvs domain (BAR in green), SH3 domain (in blue).

The proteins associated with late endosomes, ARF72A and V-ATPase subunit V1 were also found in studied fungi. Homologous protein to the *S. sclerotiorum* ARF72A and V-ATPase V1 were found in both cork oak pathogens (Figures 3.6 and 3.7). The structure of all proteins is very similar, being ARF72A characterized by a GTP/GDP interaction domain related with its activation.

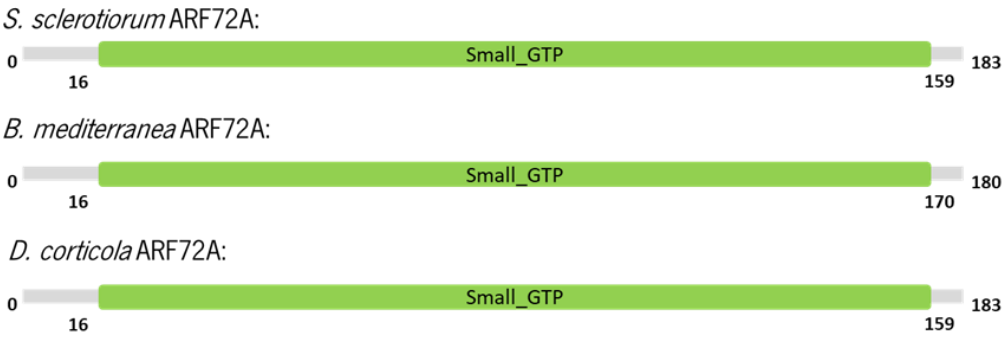

Figure 3. 6: Structure of ARF72 proteins from the model species *S. sclerotiorum* and cork oak pathogens (*B. mediterranea* and *D. corticola*). The GTP/GDP interaction domain (Small_GTP) is highlighted in green.

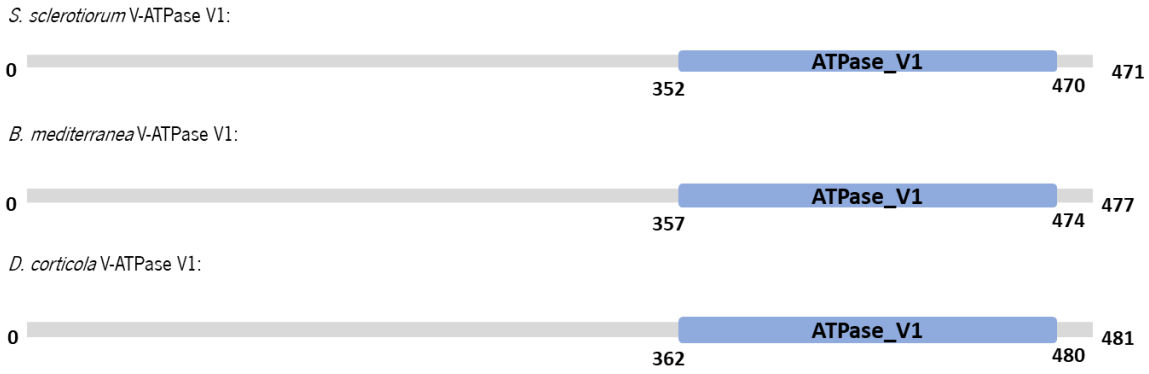

Figure 3. 7: Structure of V-ATPase subunit V1 proteins from the model species *S. sclerotiorum* and cork oak pathogens (*B. mediterranea* and *D. corticola*). The ATP-hydrolytic domain (V1) (ATPase_V1) is highlighted in blue.

In conclusion, both cork oak pathogens present all the components for an effective clathrin-mediated endocytosis, as revealed for the model species *S. sclerotiorum*. The CME pathway is the major endocytic route for the uptake of a vast array of macromolecules (Bitsikas *et al.*, 2014). In particular, this special form of vesicle budding has been recognized as playing a key function in dsRNA uptake. The main building blocks of the clathrin coats, including clathrin (CHC and CLC proteins) and adaptor protein AP2-α subunit, were all detected in both cork oak pathogens. These proteins display a similar structure to the protein from the model species *S. sclerotiorum*. The only

difference was related with the number of CLP domains in CHC proteins, in which the cork oak pathogen revealed one additional CLP domain when compared to *S. sclerotiorum*. The CLP domain, also called TD domain, is able to interact to proteins that contain an adaptor motif called clathrin-box, an example of which is Amph (Von Kleist *et al.*, 2011). The additional CLP domain on both *B. mediterranea* and *D. corticola* could result on a better recruitment of these essential proteins, facilitating vesicle formation and fission, in comparison to *S. sclerotiorum*.

The vesicle coat assembling starts with the activation and oligomerization of AP2 (promoted by FCHO1), followed by the recruitment of clathrin. The action of several other proteins assist the formation of clathrin-coated vesicles and regulate their dynamics. For example, Amph appears to function as a multifunctional adaptor that contributes to the recruitment of several coat proteins, including dynamin that promotes the fission event. Both ARF72A and ATPase_V1 are also essential for the assembling and functioning of late endosomes. All these proteins were found in both cork oak pathogens and do not reveal major structural differences in relation to the model species *S. sclerotiorum*. Only the Amph proteins composition of studied fungal species differs from what was previously described (Takeda *et al.*, 2018). The lack of a CLAP domain in Amph structure, even in the model fungus *S. sclerotiorum*, suggests differences in the interaction of this protein with clathrin and AP2. This could compromise one of Amph functions, namely the interaction with other endocytic proteins (clathrin and AP2). Still, the presence of a BAR domain may sustain the capacity of phospholipid binding and promotion of membrane curvature, as previously described (Aryal *et al.*, 2022). As clathrin is highly attracted to sites of high membrane curvature, the formed clathrin complex could still extend and stabilize membrane curvature (Zeno *et al.*, 2021). For this reason, in the studied fungi lacking the CLAP domain in Amph, an assumption is that the BAR domain is promoting the curvature of the membrane, which will be indirectly responsible for recruiting clathrin proteins.

Altogether, these results revealed that *B. mediterranea* and *D. corticola* seem to have an effective CME pathway for uptaking dsRNA. Previous studies confirm that CME pathway plays an essential role in dsRNA uptake in both pathogens and pests. In *Tribolium castaneum* (red flour beetle), when TcChc (an CHC homolog), TcAP50 (an AP2 homolog), TcVhaSFD (an V-ATPase homolog) or TcRab7 (ARF72A homolog) were supressed, the insect displayed a decrease in RNAi silencing, due to the lack of dsRNA to initiate the RNAi pathway (Xiao et al., 2015b). Furthermore, when silencing *CHC*, *CLC*, *AP-2-α*, *FCHO1*, *Amph*, *ARF72A*, *V-ATPase* genes in *S. sclerotiorum* (Ascomycota), the ability to use the RNAi machinery was also decreased (Wytinck *et al.*, 2020). In

any case, another essential step in CME pathway is the successful dsRNA recognition by plasma membrane receptors. In *Drosophila* S2 cells, this recognition is made through scavengers receptors, such as SR-CL or Eater that together are responsible for 90% of dsRNA uptake (Ulvila *et al.*, 2006). Fungi lack homologs to these insect scavengers receptors (Wytinck *et al.*, 2020). For example, even though *Zymoseptoria tritici* (Ascomycota) exhibits all the previously described CME components, is not able to uptake exogenous dsRNA (Kettles *et al.,* 2019). A possible explanation is that *Z. tritici* may lack a scavenger receptor required to uptake dsRNA. For this reason, although the described CME machinery could be present in the studied cork oak pathogens, further testing with labelled dsRNA should be performed to truly prove the uptake capacity of these fungi.

3.2. Components of RNAi silencing in cork oak pathogens

The silencing RNAi mechanism occurs in two different phases, each involving specific protein components (Dang *et al.*, 2011). After searching for homologous RNAi components of the fungal model *Neurospora crassa* in *B. mediterranea* and *D. corticola*, both cork oak pathogens revealed the presence of all genes related to core RNAi proteins (Table 2.2).

The recognition of dsRNA and production of siRNA is achieved during the initiator phase through the Dicer-like proteins (DCL). The number of Dicer homologs in each species can vary (Paturi and Deshmukh, 2021). Two Dicers (DCL-1 and DCL-2) are present in the model species of RNAi mechanism in fungi (*Neurospora crassa*). The same number was detected in each cork oak pathogen (Figure 2.8). Both DCL-1 and DCL-2 proteins, from each fungus, share no significant homology among them [*D. corticola* proteins (25.32%); *B. mediterranea proteins* (24.89%)].

Neurospora crassa DCL-2 is composed by five different domains: a Helicase-ATP-binding domain (Helicase_ATP), a Helicase C domain (HELLICc), a Dicer dimerization domain (DICER), two tandem Ribonuclease III domains (RIBOc), and a C-terminal dsRNA-binding domain (dsRBD). When compared to *N. crassa* proteins, the DCLs structure of cork oak pathogens are very similar (Figure 3.8). However, the presence of dsRBD domains is highly variable, being only present in *N. crassa* DLC-2 and *D. corticola* DCL-1

Table 3. 2: *B. mediterranea* and *D. corticola* genes, homologous to those used for coding RNAi components in *Neurospora crassa*.

Protein name	Species	Gene accession number	Gene length (bp)	Exons	Protein length (aa)	Domains
DCL-1	*B. mediterranea*	695637	5078	6	1550	Helicase-ATP binding (IPR014001)
	D. corticola	BKCO1_11000117	4665	1	1554	Helicase C (IPR001650)
DCL-2	*B. mediterranea*	673614	4717	6	1448	Dicer dimerization (IPR005034)
	D. corticola	BKCO1_3100013	5192	5	1689	Ribonuclease III (IPR000999) dsRNA-binding (IPR014720)
AGO-1	*B. mediterranea*	685559	3809	8	1037	The N-terminal ArgoN (IPR032474)
	D. corticola	BKCO1_21000109	4089	6	1019	Linker 1 (IPR014811)
AGO-2	*B. mediterranea*	644019	3809	4	1038	Paz (IPR003100)
	D. corticola	BKCO1_18000151	3111	4	1036	Linker 2 (IPR032472)
AGO-3	*B. mediterranea*	675297	3340	3	1068	MID (IPR032473)
	D. corticola	BKCO1_1000249	3000	1	999	PIWI (IPR003165)
RdRP1	*B. mediterranea*	677750	4493	7	1278	
	D. corticola	XP_020126451.1	3849	4	12221	
RdRP2	*B. mediterranea*	85913	5030	1	1449	RNA-dependent RNA polymerase (IPR007855)
	D. corticola	XP_020130197.1	4089	2	1562	
RdRP3	*B. mediterranea*	675978	4242	3	1382	
	D. corticola	XP_020134021.1	4946	3	1065	

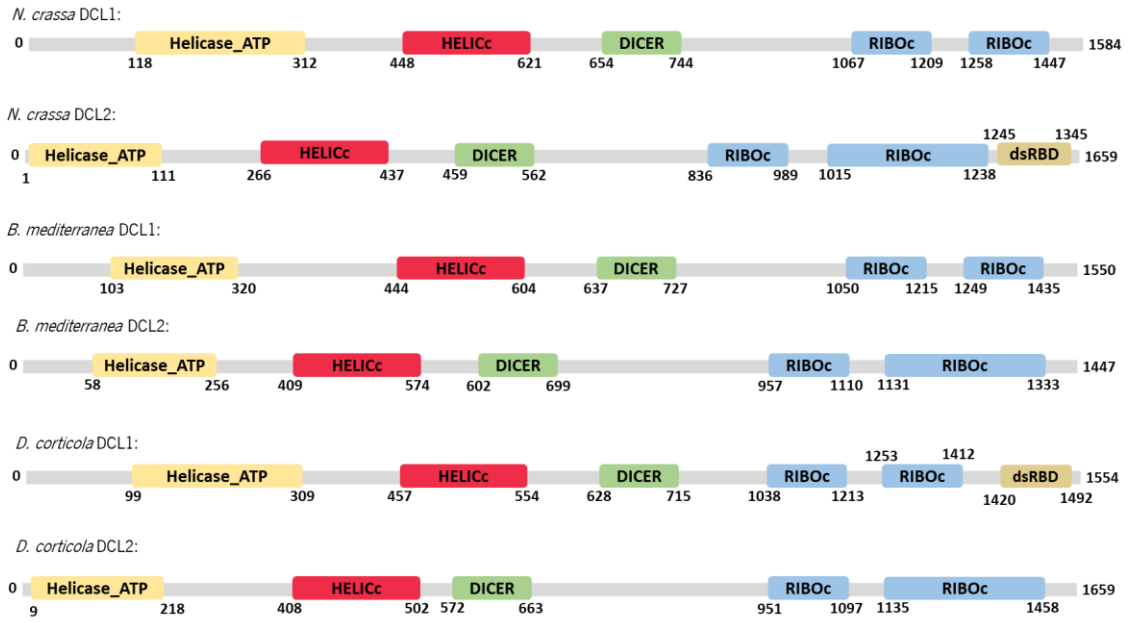

Figure 3. 8: Structure of DCL proteins from the model species *N. crassa* and cork oak pathogens (*B. mediterranea* and *D. corticola*). The five main domains are highlighted in colour: Helicase-ATP-binding domain (Helicase_ATP, in yellow), Helicase C domain (HELLICc, in red), Dicer dimerization domain (DICER, in green), Ribonuclease III domains (RIBOc, in blue) and dsRNA-binding domain (dsRBD, in brown).

During the execution phase, the silencing of homologous mRNA by the target dsRNAs is achieved by the multiprotein complex RISC, in which Argonaute (AGO) protein plays a crucial role (S. M. Hammond, 2005). *N. crassa* contains two AGO proteins: one related with meiotic silencing unpaired DNA (MSUD), the silencing meiotic suppressor 2 (sms-2), and the other related with the quelling process, the quelling deficient 2 (qd-2) protein (Dang *et al.,* 2011). When searching *B. mediterranea* and *D. corticola* for AGO homologs, three AGO proteins were detected in each (Figure 2.10). Furthermore, the three AGO proteins from each fungal pathogen do not share significant homology [in *D. corticola* (DicAGO1xDicAGO2 28.03%, DicAGO1xDicAGO3 25.16%, DicAGO2xDcaAGO3 38.11%); in *B. mediterranea* (BimAgo1xBimAgo2 25.92%, BimAgo1 BimAgo3 22.88% and BimAgo2xBimAgo3 37.09%)].

Argonaute proteins usually contain four main conserved domains: a N-terminal ArgoN domain, a PAZ domain, a MID domain and a C-terminal PIWI domain (Hung and Slotkin, 2021). In *N. crassa*, all described domains are present in sms-2, but the MID domain is missing on qd-2 protein. When compared to *N. crassa*, cork oak pathogen AGO proteins present differences in their structure. Indeed, the presence of the MID domain appears to be highly variable in the studied proteins. Like in qd-2, the *N. crassa* AGO related with quelling, MID domain is lacking in all *D. corticola* AGO proteins and *B. mediterranea* AGO2 and AGO3 (Figure 3.9).

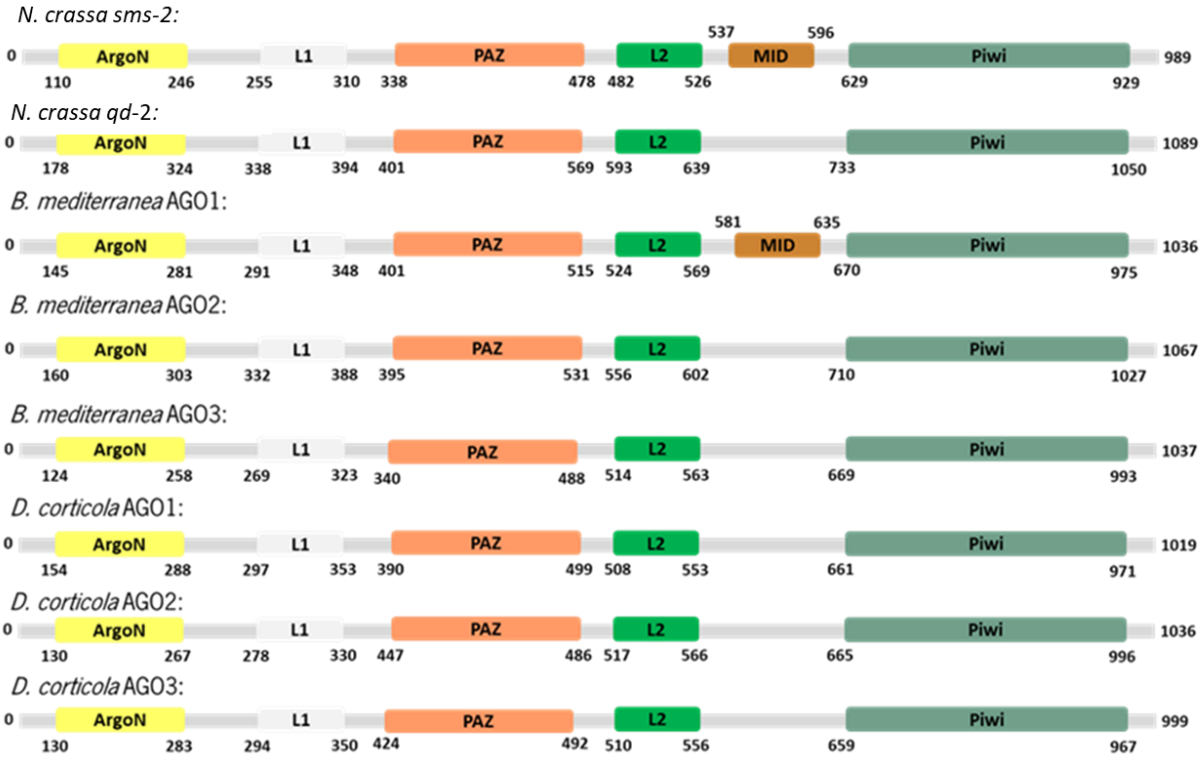

Figure 3. 9: Structure of AGO proteins from the model species *N. crassa* and cork oak pathogens (*B. mediterranea* and *D. corticola*). The AGO main domains are highlighted in colour: N-terminal ArgoN domain (ArgoN in yellow), Linker 1 (L1 in grey), Piwi/Argonaute/Zwille domain (PAZ in orange), Linker 2 (in green), MID domain (in brown), PIWI domain (in greenish).

For execution of RNAi silencing mechanism, an RNA-dependent RNA polymerase (RdRP) is required for producing dsRNA from aRNA and to amplify the initial exogenous RNAi trigger (Tsai *et al.,* 2015). The three RdRP proteins from *N. crassa* display a single RdRP domain (Figure 3.10). Both cork oak pathogens also possess three different RdRP that do not share significant homology between them [(DicRdRP1xDicRdRP2 19.89%, DicRdRP1xDicRdRP3 20.14%, DicRdRP2x DcaRdRP3 28.28%)], but all display a similar RdRP domain to *N. crassa* RdRPs.

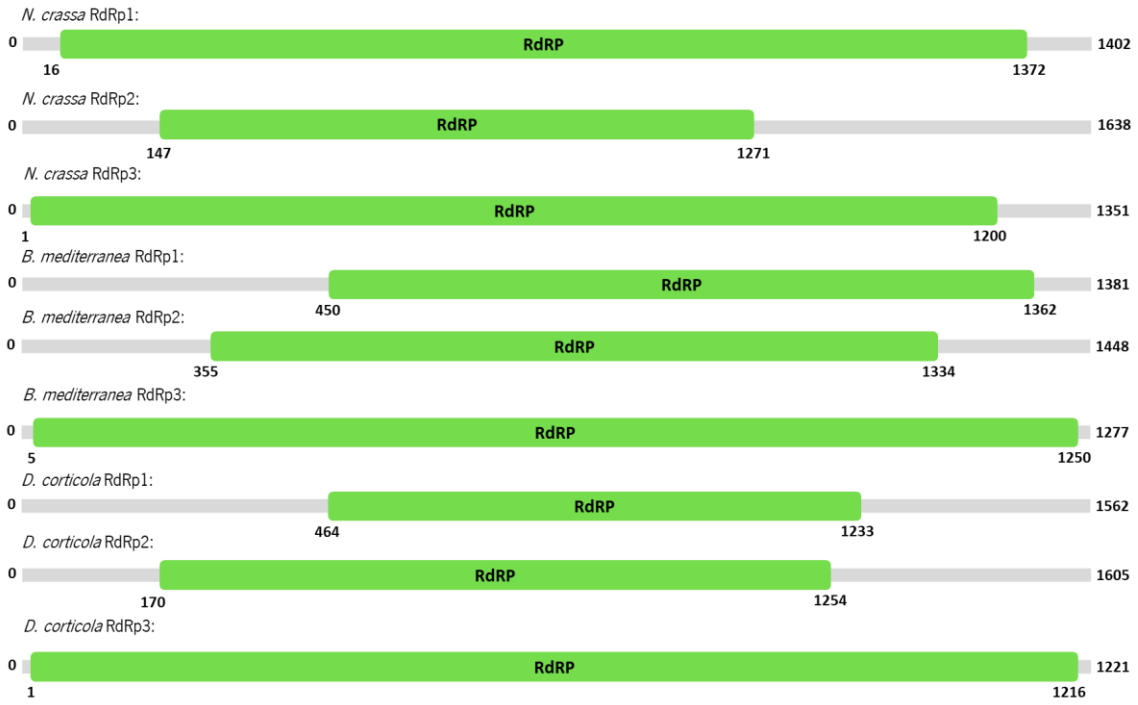

Figure 3. 10: Structure of AGO proteins from the model species *N. crassa* and cork oak pathogens (*B. mediterranea* and *D. corticola*). The RNA-dependent RNA polymerase domain (RdRP) is highlighted in a green colour.

In conclusion, both cork oak pathogens contain all the three core components (DCL, AGO, and RdRP) of RNAi silencing. Through the recognition of dsRNA, DCL can produce small interference RNAs that will bind to the AGO proteins, which will promote the silencing of complementary RNA. The RdRP protein is capable of producing dsRNA from aberrant RNA (aRNA), but also to amplify an initial dsRNA molecule (Chang *et al.*, 2012). Some differences in the structure of these core components were detected, specifically in the presence/absence of dsRBD domains (in DCL) or MID domains (in AGO).

The protein composition of DCL family is known to be diversified in different species, including the presence or absence of dsRBD (a dsRNA binding domain) and/or PAZ domains (Cerutti and Casas-Mollano, 2006). In any case, two tandem RNaseIII domains are almost always present (Mukherjee *et al.*, 2013), as was the case in DCL proteins from cork oak pathogens. The absence of dsRBD domain in certain fungal proteins may suggest differences in substrate specificities and/or interaction with proteins for directing processed siRNAs to the appropriated effector complex, as suggested for plant DCLs (Margis *et al.*, 2006). This could suggest differences in dsRNA processing in DCLs displaying or not the dsRBD domain.

Most AGO proteins from both cork pathogens lack the MID domain, being the only exception *B. mediterranea* AGO1. The MID domain is described to interact with the 5' end of the siRNA *guide strand*, helping to determine which siRNAs are loaded into each AGO protein (Wang *et al.*, 2019). Therefore, the loss of the MID domain could change the interaction of AGO with the 5' *guide strand* of siRNA, leading to differences in siRNA recognition by AGO and gene silencing variation. In any case, the binding of siRNA *guide strand* 5' could be also performed by the PIWI domain, as many amino acid residues from this domain are capable to interact with the 5'-phosphate (Kuhn and Joshua-Tor, 2013). *N. crassa*, *Botrytis cinerea* and *Fusarium graminearum*, fungi with known RNAi activity (Li *et al.*, 2010; Koch *et al.*, 2016b; Wang *et al.*, 2016b) also miss the MID domain in one of their AGO proteins.

Altogether, the results reveal the presence/absence of certain domains from core RNAi silencing components of studied fungi (*N. crassa*, *B. mediterranea* and *D. corticola*), suggesting an evolution and fungal adaptation of RNAi silencing-related genes. For this reason, a more detailed analysis should be performed to understand the differences on RNAi silencing components and their specific protein function.

3.3. Phylogenetic analysis of RNAi silencing components

The number of detected RNAi silencing components (DCL, AGO, RdRP) in *B. mediterranea* and *D. corticola* (two ascomycetes) was distinct from the model *N. crassa* (also an ascomycete), being also detected differences in the presence/absence of specific protein domains. For understanding the protein evolution and shedding some light to the pathways in which specific proteins could be involved, a phylogenetic analysis of RNAi silencing components was performed.

The core components of RNAi mechanism have been considered as evolutionarily conserved, suggesting that this process is present since the last eukaryotic common ancestor (Shabalina and Koonin, 2008) (Figure 3.11 to 3.12). Furthermore, even though a prokaryotic RNAi silencing mechanism is not functional, homologs of the three main core proteins (DCL, AGO, RdRP) have been identified (Shabalina and Koonin, 2008). Indeed, the functional building blocks of DCL proteins are encoded in archaea and bacteria, despite no multi-domain DCL was found on those linages (Mukherjee *et al.*, 2013). The Argonaute evolution is also suggested to occur from prokaryotes, after the fusion of a PIWI-like RNase H domain with a MID domain, resulting in the first guide-dependent prokaryotic AGO (Swarts *et al.*, 2014). Further domain associations then occurred for AGO evolution, in special with the ArgoN and PAZ domain. Different domain associations possibly dictated if the resulting AGO-like protein would be functional or inactive. Lastly, RdRP proteins are assumed to be an evolution from viral RdRPs (Shabalina and Koonin, 2008). These evidences could reveal that RNAi machinery could have evolved in eukaryotes by joining different building blocks of prokaryotic origin, which substantially changed each component function (Shabalina and Koonin, 2008).

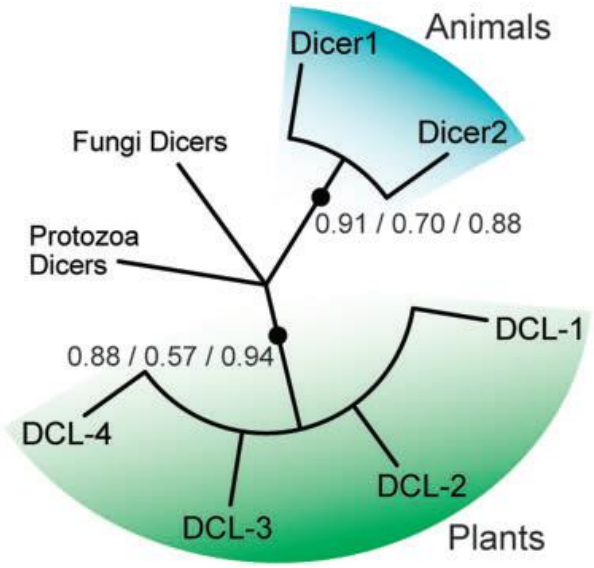

Figure 3. 11: Evolution of Dicer: DCL phylogenetic analysis supports the independent diversification of an ancient eukaryotic Dicer protein in plants, animals, fungi and protozoa (adapted from Mukherjee *et al.*, 2013)

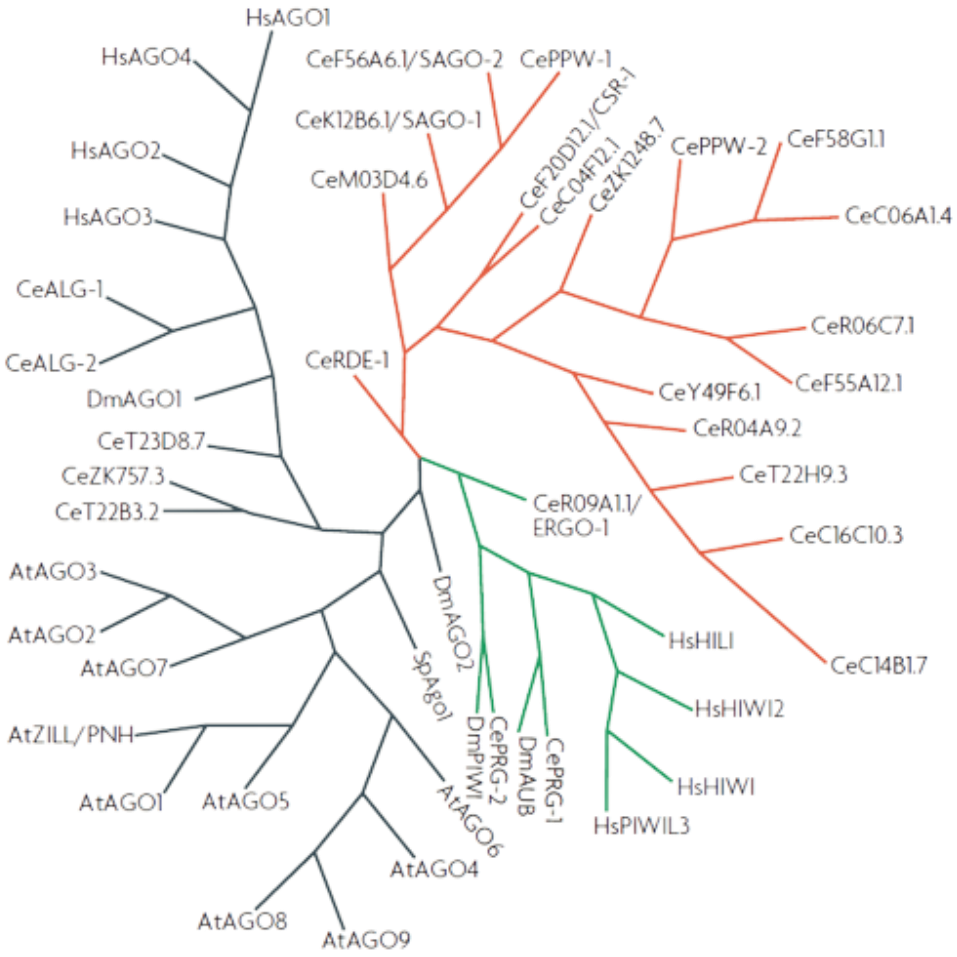

Figure 3. 12: Evolution Argonaute. i) Argonaute-like proteins, which interact with miRNA or siRNAs and are involved in cytoplasmic post-transcriptional gene-silencing processes; ii) PIWI-like proteins, which are mainly expressed in germlines, interact with PIWI-interacting RNAs (piRNA), and function in silencing transposable genetic elements; iii) WAGO proteins, which are exclusive to worms, like *Caenorhabditis elegans,* and amplify the RNAi signal mediated by siRNAs. The Argonaute-like group found in plants, animals and fungi is indicated in black. The Argonaute clade in green represents the Piwi-like group. WAGO proteins clade is indicated in red (adapted from Hutvagner and Simard, 2008).

In the present work, the search of homologous DCL, AGO and RdRP from *N. crassa* in 28 fungal genomes resulted in the identification of 57 DCL, 74 AGO-, and 109 RdRP-like proteins (Tables 3.3; Tables S.1 to S.3). The number of copies of each protein differs among species. The number of DCL copies ranged from one in *Schizosaccharomyces pombe* and *Melampsora lini* to three in *Puccinia triticina*, *Heterobasidion annosum* and *Stereum hirsutum.* Similarly, the number of AGO copies ranged from one in *Schizosaccharomyces pombe* and seven in *Heterobasidion annosum*, while the number of RdRP copies was the most diverse in different species, ranging from one in *Schizosaccharomyces pombe* to eleven in *Stereum hirsutum*.

Table 3. 3: Number of RNAi proteins for each species under study and corresponding taxonomic classification. The number of proteins for each RNAi component is represent for each described species. Different classes of fungi are highlighted in different colours: Sordariomycetes (in blue), Dothideomycetes (in yellow), Eurotiomycetes (in green), Leotiomycetes (in orange), Schizosaccharomycetes (in pink), Pucciniomycetes (in red) and Agaricomycetes (in grey).

Phylum	Class	Species	Nº DCL	Nº AGO	Nº RdRp
Ascomycota	Sordariomycetes	*Biscogniauxia mediterranea*	2	3	3
		Fusarium graminearum	2	2	5
		Fusarium oxysporum	2	2	5
		Fusarium solani	2	2	4
		Fusarium verticillioides	2	2	4
		Fusarium culmorum	2	3	5
		Colletotrichum gloeosporioides	2	2	3
		Pyricularia oryzea	2	3	3
		Neurospora crassa	2	2	3
		Verticillium dahliae	2	2	3
		Verticillium longisporum	2	3	5
	Dothideomycetes	*Alternaria alternata*	2	3	3
		Bipolaris oryzae	2	2	3
		Bipolaris sorokiniana	2	2	3
		Diplodia corticola	2	3	3
		Fulvia fulva	2	3	3
		Venturia inaequalis	2	2	5
	Eurotiomycetes	*Aspergillus flavus*	2	3	3
		Aspergillus parasiticus	2	2	3
	Leotiomycetes	*Blumeria graminis*	2	3	2
		Botrytis cinerea	2	2	4
		Sclerotinia sclerotiorum	2	2	3
	Schizosaccharomycetes	*Schizosaccharomyces pombe*	1	1	1
Basidiomycota	Pucciniomycetes	*Melampsora lini*	1	2	4
		Puccinia striiformis	2	3	5
		Puccinia triticina	3	2	3
	Agaricomycetes	*Heterobasidion annosum*	3	7	7
		Stereum hirsutum	3	6	11

3.3.1. Dicer protein evolution

The number of DCL proteins seems to be more homogenous in the Ascomycota phylum, in which all studied species display two DCL homologs, with the exception of *Schizosaccharomyces pombe* (Table 3.3). In the Basidiomycota phylum, the number is more variable, ranging from one to three DCL proteins. The phylogenetic analysis revealed that the *DCL* gene present in the ancestral fungi suffered a duplication event, leading to two major DCL protein paralogs found in Ascomycota and Basidiomycota phyla. Therefore, the phylogenetic tree distinguishes two main clades: a clade including a subclade where *N. crassa* DCL-1 could be found, containing a sub-clade solely formed by Basidiomycota proteins, and a clade including *N. crassa* DCL-2.

3.3.2. Argonaute protein evolution

The number of AGO proteins is highly variable in both Ascomycota and Basidiomycota phyla (Table 3.3). However, the number of AGO proteins in basidiomycetes is higher, as in the case of *Heterobasidion annosum*, where there are seven different homologs. In contrast, the number of AGO proteins in Ascomycota species ranges between one and three. The phylogenetic analysis suggests that an ancestral fungus most likely only had a single gene encoding an AGO protein. Duplication events and functional divergence of AGO proteins seem to have taken place before Ascomycota and Basidiomycota diversification. Accordingly, the phylogenetic tree reveals two main clades of AGO proteins.

3.3.3. RNA-dependent RNA polymerase evolution

RdRP proteins are the most diversified proteins from the core RNAi machinery, in both Ascomycota and Basidiomycota phyla (Table 3.3). In Ascomycota species, the number of RdRPs ranges from one to five proteins, being three RdRP proteins the most common number. In contrast, for Basidiomycota, the number of proteins ranges from three to eleven and the number is highly variable. After the phylogenetic analysis of RdRP protein family, six sub-clades can be distinguished, included in two main clades. Protein diversification appears to have initiated by one duplication, followed by divergence events taken place before Ascomycota and Basidiomycota diversification.

This chapter revealed that *B. mediterranea* and *D. corticola* hold all the machinery necessary to uptake dsRNA and for a functional RNAi silencing. When compared to *Neurospora crassa*, the filamentous fungus model for RNAi silencing, the encoding genes of DCL, AGO and RdRP in both pathogens have an identity of about 95%. Furthermore, the proteins present in both cork oak pathogens follow the same evolutive diversification as *Neurospora crassa* proteins. These results sustain the hypothesis that both pathogens can be possible targets for SIGS biocontrol strategy.

4. Chapter IV: Evidences of dsRNA uptake and RNAi silencing in cork oak pathogens

Before proceeding with the design and production of targeted dsRNA to pathogens, the function of the quelling mechanism in both fungi should be confirmed. A SIGS strategy will only works if pathogens are able to uptake RNA and display a functional RNAi silencing pathway (quelling). For these reasons, a proof-of-concept efficacy of RNA uptake and silencing is needed. In the last years, the use of GFP and labelling dyes offered an easy way to visualize certain cellular mechanisms. By labelling dsRNA with fluorescent probes, it is possible to identify if the cork oak pathogens are able to uptake these molecules. Additionally, through transformation of *Biscogniauxia mediterranea* and *Diplodia corticola* with an expression construct comprising a GFP gene, the fungi will gain the capacity to produce this fluorescent protein. By targeting this exogene with a specific GFP-dsRNA, a reduction in the fluorescence levels will indicate a functional RNAi pathway.

4.1. Pathogens ability to uptake dsRNA

For ensuring that *B. mediterranea* and *D. corticola* are able to uptake dsRNA, a fluorescent-labelled dsRNA assay was used for following the possible internalization of dsRNA within the cells. For this, a sGFP-dsRNA molecule was labelled with a fluorescein, being applied immediately before microscopic observation. The obtained images suggest that both fungi are indeed able to uptake exogenous dsRNA. In *D. corticola*, the fluorescent signal was detected within the hyphae, while in *B. mediterranea* the fluorescent labelling appears to be stronger at hyphal tip (Figure 4.1). This last result agrees with the hypothesis of Wytnick and co-authors (2020) that suggests that dsRNA uptake is more pronounced at hyphal tips. According to this hypothesis, *D. corticola* uptake could be more efficient when compared to *B. mediterranea*. After the same period upon labelled dsRNA application, the fluorescent signal is still on the tip of *B. mediterranea* hyphae, while is more ubiquitous within *D. corticola* hyphae.

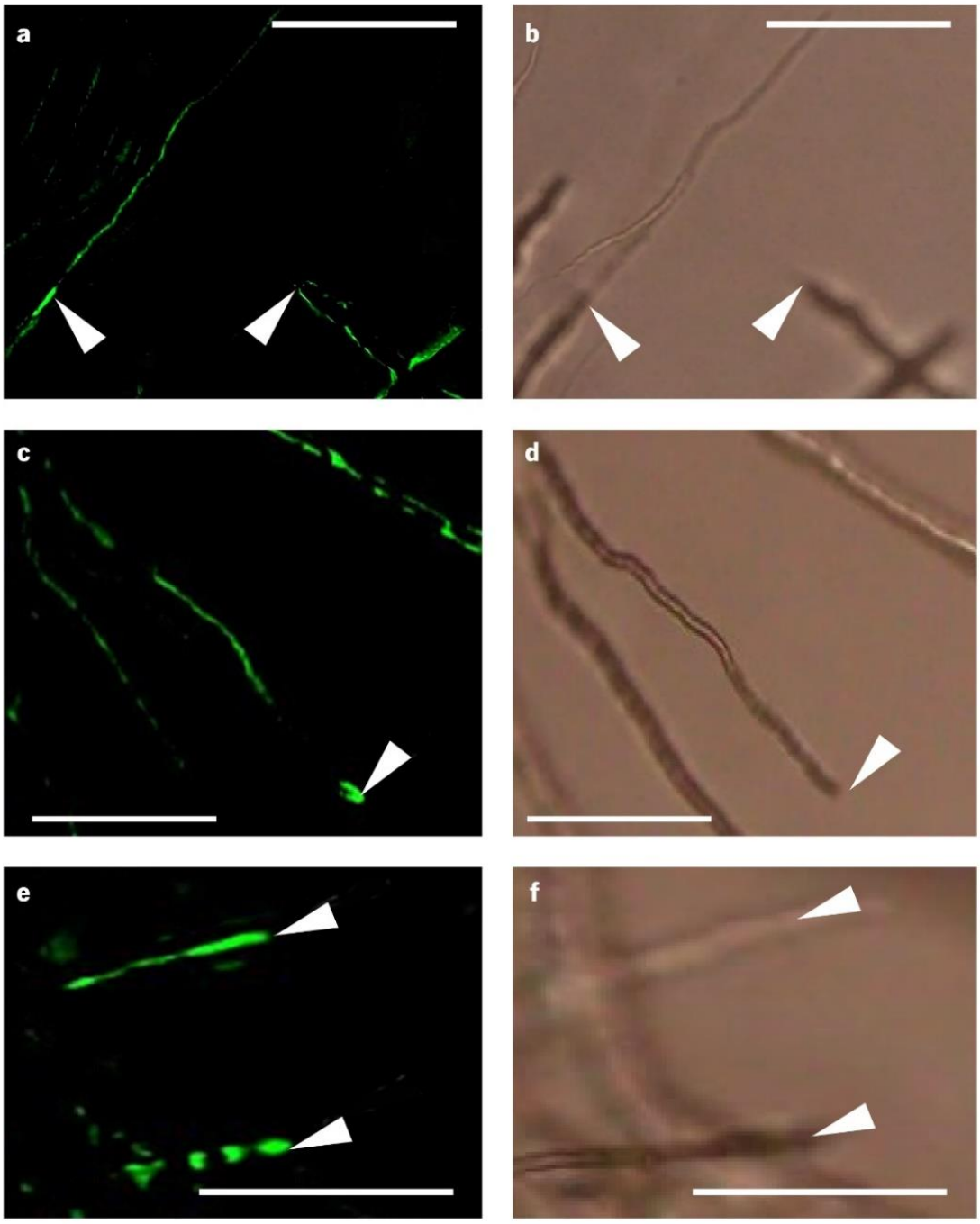

Figure 4. 1: Uptake of dsRNA by *D. corticola* (a, b) and *B. mediterranea* (c-f). The assay for detecting dsRNA uptake was based on the detection of fluorescein-tagged sGFP-dsRNA in newly germinated hyphae from conidia. h after dsRNA application). After 8h of inoculation, hyphae were visualized under a fluorescence microscope. Fluorescent images (left) were compared to the corresponding images obtained under Photographs were taken under fluorescent (left) and bright light settings (right). A stronger signal of the labelled sGFP-dsRNA molecule (arrows) is observed inside hyphae or at hyphae tips. (Bars indicate 100 μm).

4.2. Pathogens ability to silence targeting genes

Fungal transformation is a crucial step for *in vitro* RNAi silencing assays, as allows the introduction in the fungal cells of a transgene coding a protein easily detected (sGFP). Although in the transformation protocol a selection medium was used, some fungal isolates could have skipped the selection made by antibiotics. For this reason, validation of both cork oak pathogens transformation by measuring GFP production is mandatory. When observed under a fluorescence microscope, transformants from both cork oak pathogens produced a fluorescent signal (Figure 4.2), contrasting with non-transformed fungi, revealing the success of transformation process. Additionally, transformation was validated by the amplification of the transgene (*sGFP*) from transformants and non-transformants fungi (*B. mediterranea* and *D. corticola*). Only DNA extracted from transformed isolates produced an amplicon about 550 bp (Figure 4.3), which was the expected size for the amplicon (552 bp). Moreover, DNA extracted from non-transformed *B. mediterranea* and *D. corticola* did not result in any amplicon.

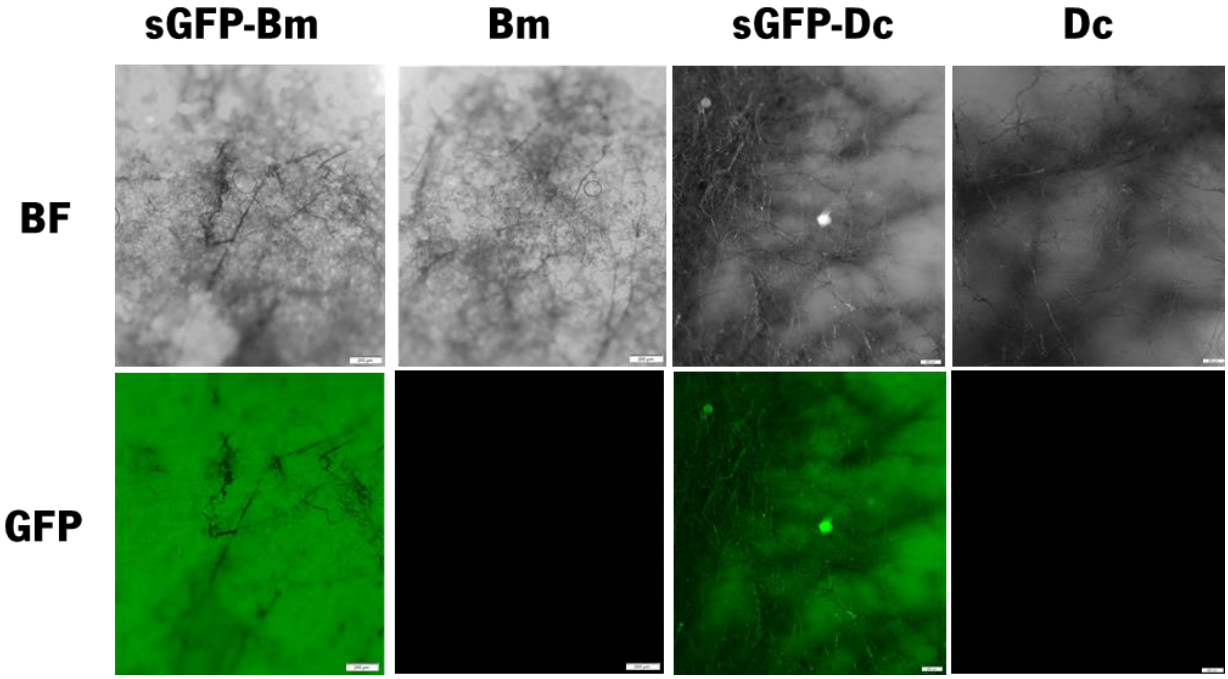

Figure 4. 2: Validation of fungal transformation by detection of green fluorescence as result of GFP synthesis. Transformants of *B. mediterranea* and *D. corticola* overexpressing sGFP (sGFP-Bm and sGFP-Dc, respectively) and corresponding non-transformed controls (Bm and Dc) were visualized under a fluorescence microscope. Fluorescent images (lefts) were compared to the corresponding images obtained under Photographs were taken bright field (BF) or UV light (GFP). (Bar indicates 200 µm).

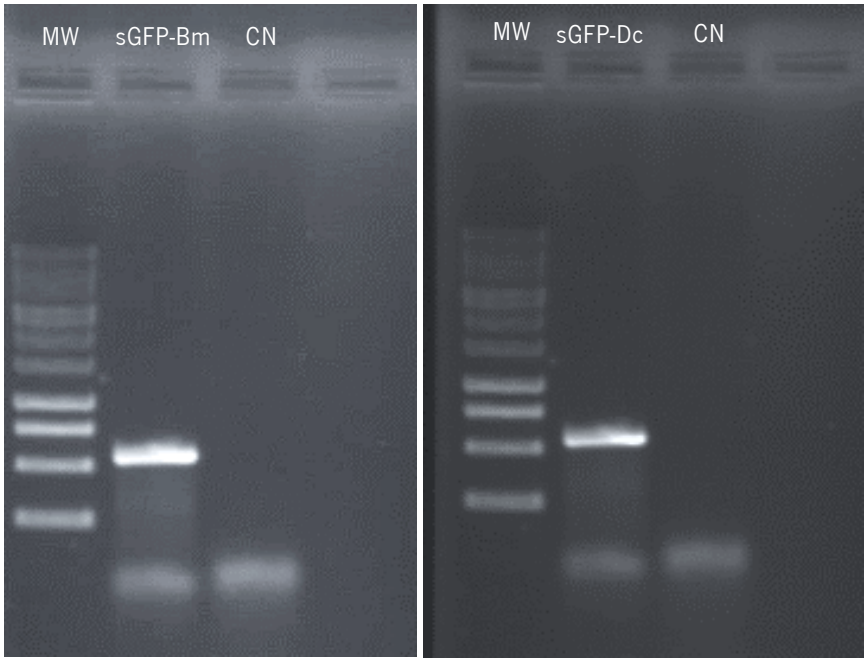

Figure 4. 3: Validation of fungal transformation by detection of *sGFP* amplicon. DNA from transformed *B. mediterranea* (sGFP-Bm) and *D. corticola* (sGFP-Dc), as well as DNA from the corresponding non-transformed isolates (Bm and Dc, respectively), were tested by the presence of *sGFP* transgene through amplification. An amplicon of about 550 bp was detected in both transformed cork oak pathogens, but not in non-transformed isolates. (MW – 100 bp ladder).

To test if *B. mediterranea* and *D. corticola* have their RNAi machinery in place and is able to silence targeting genes, an *in vitro* assay was performed by applying sGFP dsRNA to transformed conidia (*B. mediterranea* and *D. corticola*) expressing *sGFP*. In case germinated conidia were able to uptake and silence *sGFP* gene, the resulting fluorescence (measured as RFU) will decrease with time. The results revealed that *B. mediterranea sGFP* expression levels were reduced in about 40%, during the first 24 hours post dsRNA application, decreasing only to 30% after 48 hours (Figure 4.4). A similar result was observed for *D. corticola*, a 40% reduction of RTU values (24 h) and 30% (48h). These results suggest, not only that both fungi have the capacity for silencing genes through RNAi pathway, but also corroborate the ability of cork oak pathogens to uptake dsRNA.

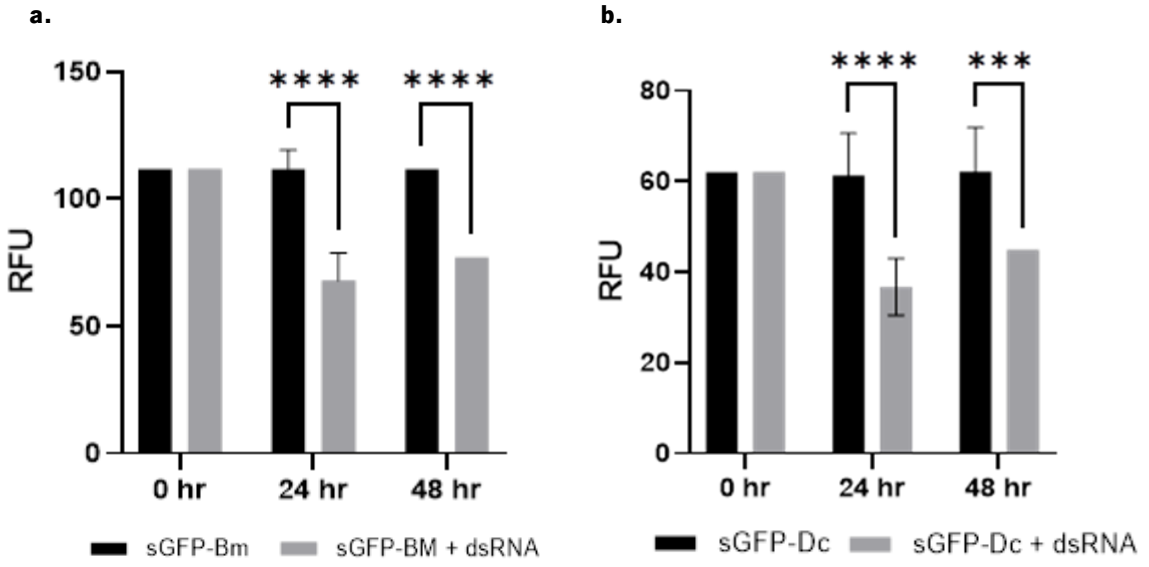

Figure 4. 4: *In vitro* RNAi silencing of *sGFP* transgene in *B. mediterranea* (a) and *D. corticola*. (b). Suspension of *sGFP* transgenic conidia were treated or not with sGFP-dsRNA and relative fluorescence unit (RFU) was determined along time. Asterisks represent statistical significance among samples ** ($p \leq 0.05$), ** ($p \leq 0.01$) and *** ($p \leq 0.001$)*

Altogether, the results suggest that both *B. mediterranea* and *D. corticola* are capable of uptaking exogenous dsRNA and silencing genes, contrasting with other fungi that have lost this ability (Qiao *et al.*, 2021). Noteworthy, the silencing effects appear to decrease after the first 24 hours, as no further decrease in RTU was observed. This effect may suggest that RdRP proteins are not functional, being unable to amplify the initial dsRNA signal. The same pattern was recognized in *Fusarium solani*, in which 48 hours after dsRNA application a reduction of the silencing effect was detected (Dalakouras *et al.*, 2022). Additionally, in *Fusarium asiaticum* the lost of gene silencing was reported nine hours after dsRNA application (Song *et al.*, 2018). Using this biological model, gene silencing lasted for seven days with constant supply of dsRNA. In any case, even if fungal RdRPs are not working properly, the use of a SIGS approach for controlling cork oak pathogens would not be invalidated, as plant cells could also uptake dsRNA and produce siRNA. Such siRNAs can be continually used by the plant during the plant-pathogen interaction (Filho *et al.*, 2021).

5. Chapter V: Target genes characterization, off-target prediction and dsRNA production

After checking the capacity of uptaking and processing dsRNA (chapter IV), target genes selection, characterization and dsRNA design was performed. In this chapter, a list of possible target genes was created and five genes were selected for dsRNA molecules design. For ensuring dsRNA specificity, off-target predictions were additionally performed.

5.1. Selection of target genes and design of dsRNA molecules

Several RNAi based strategies already proved to work in some plant pathogens (Nerva *et al.*, 2020; Spada *et al.*, 2021; Tetorya and Rajam, 2021). Part of their success is related with the choice of an ideal target gene from the pathogen, although there is not a clear justification for the choice of specific target genes (Lata *et al.*, 2022). Chosen genes are often associated to pathogen essential functions, as is the case of *cytochrome P450 lanosterol C-14* α*-demethylase* (Koch *et al.*, 2018) or *elongation factor 2* (Nerva *et al.*, 2020). In the present work, the selection of pathogen target genes was based on the biological processes their encoding proteins are involved in. Specifically, silencing of genes associated with cell wall development, protein modification, transcription, and sexual development, are expected to result in visible phenotypes. The functional redundant or genes with multiple paralogs were avoided.

From the 25 possible target genes identified, five genes were selected to proceed with further testing (Table 5.1). This selection was based in two criteria: cellular function and gene deletion effect. The genes *Sc1* and *Sc2* are both essential for a typical cellular structure. While deletion of *Sc1* gene results into an inviable phenotype, the deletion of *Sc2* gene produces abnormal cellular morphogenesis. When deleting *Ptm1* and *Ps1* genes, inviable phenotypes are also originated. While Ps1 protein function is related to protein synthesis, Ptm1 protein is associated to post transcriptional modifications. Finally, *St1* encodes a protein with a function related with signal transduction. *St1* mutants produce an abnormal morphogenesis.

Table 5. 1: List of the five selected target genes. The corresponding cellular function and gene deletion effect is revealed. The used genes were named after their cellular function.

Gene code	Cellular function	Deletion effect
Sc1	Structural components	Inviable phenotype
Sc2	Structural components	Abnormal cellular morphogenesis
Ptm1	Post Transcriptional modifications	Inviable phenotype
Ps1	Protein synthesis	Inviable phenotype
St1	Signal transduction	Abnormal cellular morphogenesis

Design of dsRNAs is still one of the main challenges in any RNAi silencing strategy. The influence of dsRNA design on the subsequent processing and target gene silencing efficiency is still scarcely known. However, dsRNA size has been considered a relevant factor in RNAi efficiency (Höfle *et al.*, 2020). An example of this could be observed when trying to silence genes from the two-spotted spider mite, *Tetranychus urticae* (Bensoussan *et al.*, 2020). Lower size dsRNA (100-200 bp) is less efficient for gene silencing, when compared with 400 bp to 600 bp molecules. The same result was observed when considering fungi. When using a SIGS approach, *Fusarium graminearum* presents no problem in uptaking molecules from different sizes (200-1500 bp) (Höfle *et al.*, 2020). However, the silencing efficiency is higher when dsRNA molecules range from 200 bp to 550 bp. Taking into consideration these results, the designed dsRNA from *B. mediterranea* and *D. corticola* never exceeded 550 bp, for anticipating maximum efficiency for the tested molecules.

Different methods to design dsRNA for the target genes were used (Table 5.2). Five dsRNA molecules for each pathogen were synthesized using the non-conserved protein domain method. In contrast, only two from the five selected genes were randomly chosen for using the fragmented method, as regions used for non-conserved protein domain method were avoided. Both methods were used as exploratory protocols, in order to understand differences in dsRNA based on the targeted area.

Each designed dsRNA molecules could produce *in vivo* several effective siRNA molecules, which are able to interact and silence mRNA homologues. The number of these produced siRNAs was estimated for each dsRNA molecule, using a specific software (for an example of data output, see Figure S.1). The results reveal that the number of possibly efficient siRNAs produced depends on the designed dsRNA and was not always correlated with the dsRNA length (Table 5.2). For example, *Ptm1_2* from *B. mediterranea* is the shortest dsRNA, but produces the greatest number of possibly efficient siRNAs for *B. mediterranea.* In this cork oak pathogen, dsRNA molecules that can produce a higher number of siRNA and thus display a higher chance to silence their homologous mRNAs, are not only *Ptm1_2*, but also *Ptm1_1*, *St1* and *Ptm1*. As for, *D. corticola* the *Sc1* and *Sc2* are the molecules with higher number of possible efficient siRNAs.

Table 5. 2: Length of designed dsRNAs, produced by different methods from *B. mediterranea and D. corticola* sequences, and corresponding number of estimated efficient siRNA molecules.

Designed method	Gene code	*B. mediterranea*		*D. corticola*	
		dsRNA length (bp)	number of siRNA	dsRNA length (bp)	number of siRNA
Non-conserved domain method	*Sc1*	483	222	540	267
	Sc2	483	214	548	295
	Ptm1	543	253	499	163
	St1	503	261	543	167
	Ps1	473	248	514	235
Fragmented gene method	*Ptm1_1*	503	251	534	225
	Ptm1_2	441	267	425	180
	St1_1	529	195	463	204
	St1_2	542	195	540	239

5.2. Prediction of off-targets

A RNAi silencing process is recognized by the ability to silence target genes, in a highly specific manner (Das and Sherif, 2020). However, siRNAs could target non-specific genes, possibly creating an off-target gene silencing (Senthil-Kumar and Mysore, 2011). This is more likely to occur when using the fragmented method for creating dsRNAs, as conserved domains could be additionally targeted. For this reason, an initial *in silico* screening was performed to all designed dsRNA molecules in the target genome, in order to detect possible off-targets. For further testing the specificity of dsRNA molecules, the same off-target effect was studied in the host plant (*Q. suber*) and in other *Q. suber* fungal endophytes (Costa *et al.*, 2020). For this screening, all endophytes with an available transcriptome data (12) were used. Results revealed that none of the tested species appears to hold a possible off-target for the designed dsRNA molecules (Figure 4.3). Indeed, the possible dsRNA target was only recognized in the fungal species from which the dsRNA was designed. This result reveals that the designed dsRNAs will possibly not silence genes, either in the host plant or in most of their fungal endophytes, which could indicate a high specificity of designed dsRNA if used in a SIGS strategy.

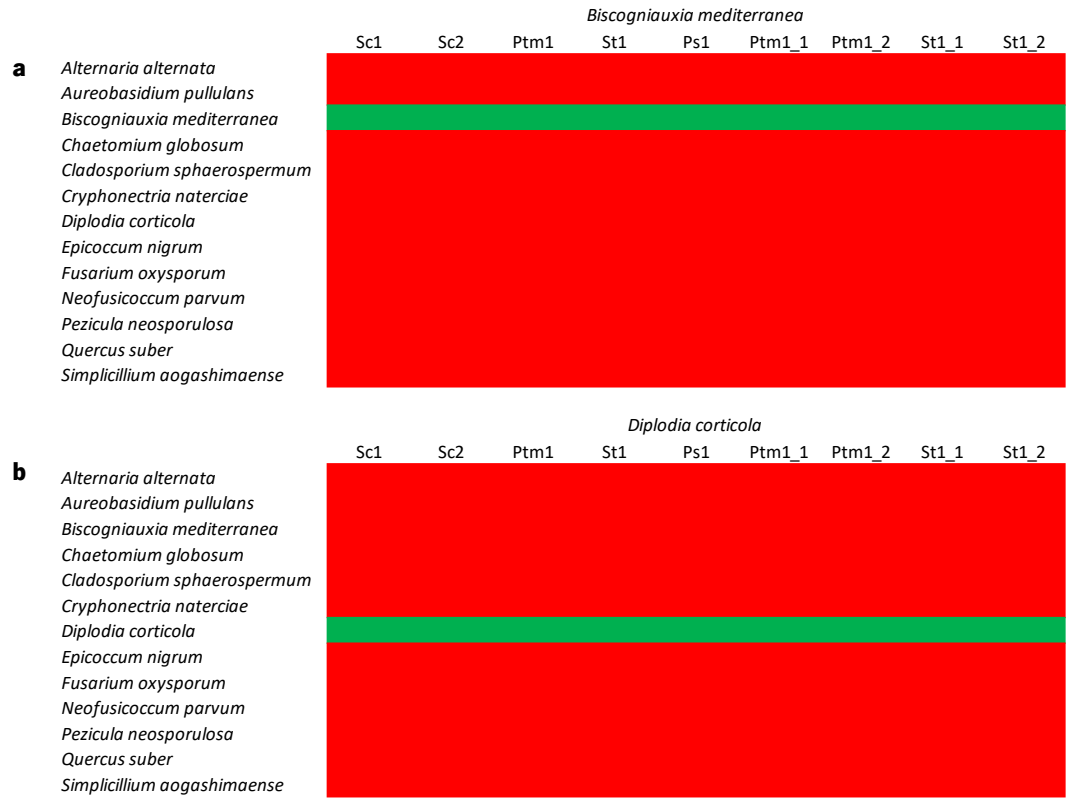

Figure 5. 1: Detection of possible off-targets for *B. mediterranea* (a) and *D. corticola* (b) dsRNAs. Eleven cork oak fungal endophytic species and cork oak transcriptomes were searched for possible off-targets, using *si-Fi v21* software (default parameters). Whenever a target was recognized in the tested transcriptome a green colour is used, otherwise a red colour was used.

5.3. *In vitro* production of dsRNA

Two main approaches are commonly used for producing dsRNA molecules (Ongvarrasopone et al., 2007). The first includes the *in vitro* transcription of RNA by using *Escherichia coli* HT115(DE_3). This specific strain lacks the dsRNA-specific RNase type III, which results into a higher level of dsRNA production. When transformed with expression plasmids containing T7 promoter sequences, *E. coli* HT115(DE_3) can produce large quantities of sequence-specific dsRNAs. A second approach corresponds to the *in vitro* synthesis of dsRNA, by using commercially available kits based on the activity of RNA-dependent RNA polymerases. The *MEGAscript™ RNAi* kit (Ambion) allows the *in vitro* transcription from PCR generated templates. However, this last method is increasingly expensive when large amounts of dsRNA are needed (Ongvarrasopone *et al.*, 2007). However, as this approach offers an easier process for screening different genes, the use of *in vitro* transcription was the method of choice for this work.

The dsRNA designed sequences were successfully amplified using *D. corticola* and *B. mediterranea* genomic DNA. The produced amplicons were used for dsRNA synthesis, yielding the expected values (40-50 µg) provided by manufacturer of RNA synthesis kit. Moreover, the produced dsRNAs quality was evaluated for understanding if the purification process (included in the kit) was successful (Figure 5.2). All synthesized dsRNAs originated a single fluorescent band, revealing a successful purification process. Noteworthy, as dsRNA mobility in a agarose gel is slower when compared to DNA (Livshits *et al.*, 1990), the expected molecular weight of each dsRNA do not fully corresponds with the molecular marker (100 bp).

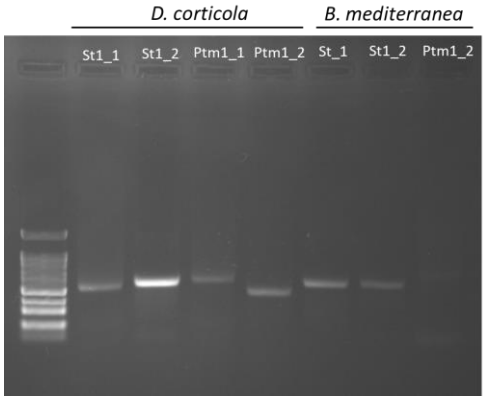

Figure 5. 2: Evaluation of produced dsRNA molecules by gel electrophoresis. The quality of purified *in vitro* transcribed dsRNA was confirmed by agarose gel electrophoresis (1%, w/v) and expected molecule size was verified (representative gel).

At the end, nine dsRNA molecules were designed and synthesized for each cork oak pathogen, in order to follow with a SIGS strategy for impair their growth. The designed dsRNAs do not seem to have off-targets effects and are predicted to produce over than 150 possible effective siRNA. The most promising are able to produce more than 250 siRNAs. Their application for effectively impairing the growth of cork oak pathogens needs to be further confirmed.

6. Chapter VI: Ability of designed dsRNA on silencing cork oak pathogen genes

The search for new sustainable strategies for the control of pathogen/pests are a true requirement in a world of climate change and world population rising (Nishimoto, 2019). State-of-the-art approaches like *host induced gene silencing* (HIGS) and *spray induced gene silencing* (SIGS), which are based on the eukaryotic RNA interference pathways, have been an enormous breakthrough. When using a SIGS strategy, one of the major challenges is the ability to design functional dsRNA molecules. Despite *in silico* studies could be performed to understand the potential of dsRNA molecules, *in vivo* assays are essential to truly test their capacity and effect produced on pathogen development.

D. corticola and *B. mediterranea*, as bark pathogens (Campanile *et al.*, 2007; Henriques, 2015), make *in planta* dsRNA assays difficult to follow and to identify possible plant symptoms. Furthermore, the use of other plant hosts to perform such assays is frequently discarded, due to the fact that plant-pathogen interactions are very specific and pathogen behaviour could change in a different host (Blumenstein *et al.*, 2022). In this situation, application of cork oak pathogen targeted dsRNA could result in a different response from the pathogen or from the host. For these reasons, the effect of dsRNA designed molecules on both cork oak pathogens was performed using *in vitro* assays. In this chapter, all the designed and produced dsRNAs are tested to understand their effect in the cork oak pathogens growth and hyphae morphology, aspects that could impair the infection process.

6.1. Results and discussion

After the evidences that *D. corticola* and *B. mediterranea* have the appropriate components for uptaking dsRNA and silencing genes (chapter III), together with the proof-of-concept that hyphae can indeed uptake dsRNA and silence genes (chapter IV), the designed dsRNAs (chapter V) were used for silencing cork oak pathogens. For understanding which dsRNA amount would produce the most effective results, an initial *in vitro* assay was performed where hyphae were challenged with dsRNA molecules (either designed by the non-conserved protein domain method or by fragmented gene method).

6.1.1. *In vitro* assays for determining the impairment of *D. corticola* growth

The results related to *D. corticola* reveal that from the five tested dsRNAs, produced by the non-conserved domain method, *Sc1*, *St1* and *Ps1* affected significantly the normal development of the targeted fungus, mainly during the first days after dsRNA treatment (Figure 6.1). In both *Sc1* and *Ps1*, a significant difference was detected in the first three days, when compared with no-dsRNA control, suggesting that dsRNAs are indeed affecting fungal growth. In contrast, *Ps1* results revealed a statistical difference, but with the water control, thus masking the real effect of *Ps1*-dsRNA. Therefore, for this dsRNA molecule, the effect on fungal growth still remains inconclusive. Whatever the case, a higher amount of dsRNA molecule appears to induce a stronger growth inhibition. For both effective dsRNAs (*Sc1* and *St1*), an amount of 1000 ng of dsRNA reveals a constant stronger effect over the first three days. However, using 200 ng of *St1* dsRNA also affected *D. corticola* development, even though this effect was not as strong as for 1000 ng The effective dsRNA amounts that produce a noticeable effect in these assays were higher than expected, as only above 200 ng a significant growth decrease was registered. The most common value is 20 ng/µl of dsRNA applied as a spray (Koch *et al.*, 2018; Höfle *et al.*, 2020; Duanis-Assaf *et al.*, 2022). However, when spraying plants, both plant and pathogen will absorb the dsRNA and produce siRNA based on it (Filho *et al.*, 2021). This process can amplify the initial dsRNA signal.

Due to the large amounts of dsRNA molecules required for testing such a large range of dsRNA concentration, a single concentration was subsequently used for testing dsRNA molecules produced by the gene fragmentation method. The results revealed a general trend for fungal growth reduction, but only *St1_2* dsRNA application resulted in a statistical significant growth impairment, registered only 24 hours after dsRNA treatment (Figure 6.2).

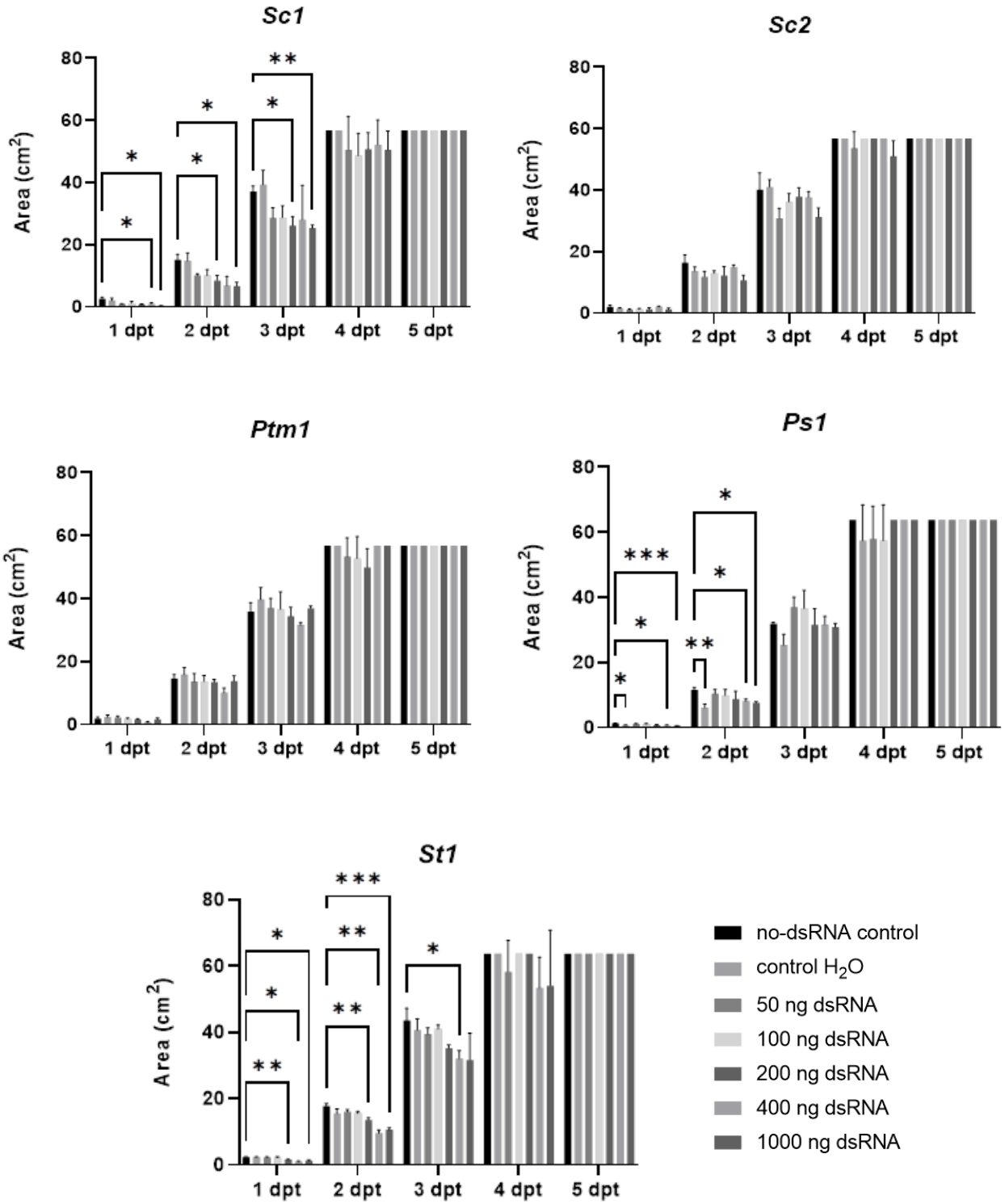

Figure 6. 1: Effects of dsRNAs prepared using non-conserved domain method in *D. corticola* growth. After challenging a *D. corticola* plug (5 mm) with 10 µl of *Sc1*, *Sc2*, *Ptm1*, *St1*, and *Ps1* dsRNAs (50 – 1000 ng), the fungal growth area (cm^2) was measured during five days post treatment (dpt). Different dsRNA amounts were tested, as described in the legend. Controls without dsRNA treatment (no-dsRNA control) and with application of 10 µl of water (control H_2O) were performed. Asterisks represent statistical significances * ($p \leq 0.05$), ** ($p \leq 0.01$) and *** ($p \leq 0.001$).

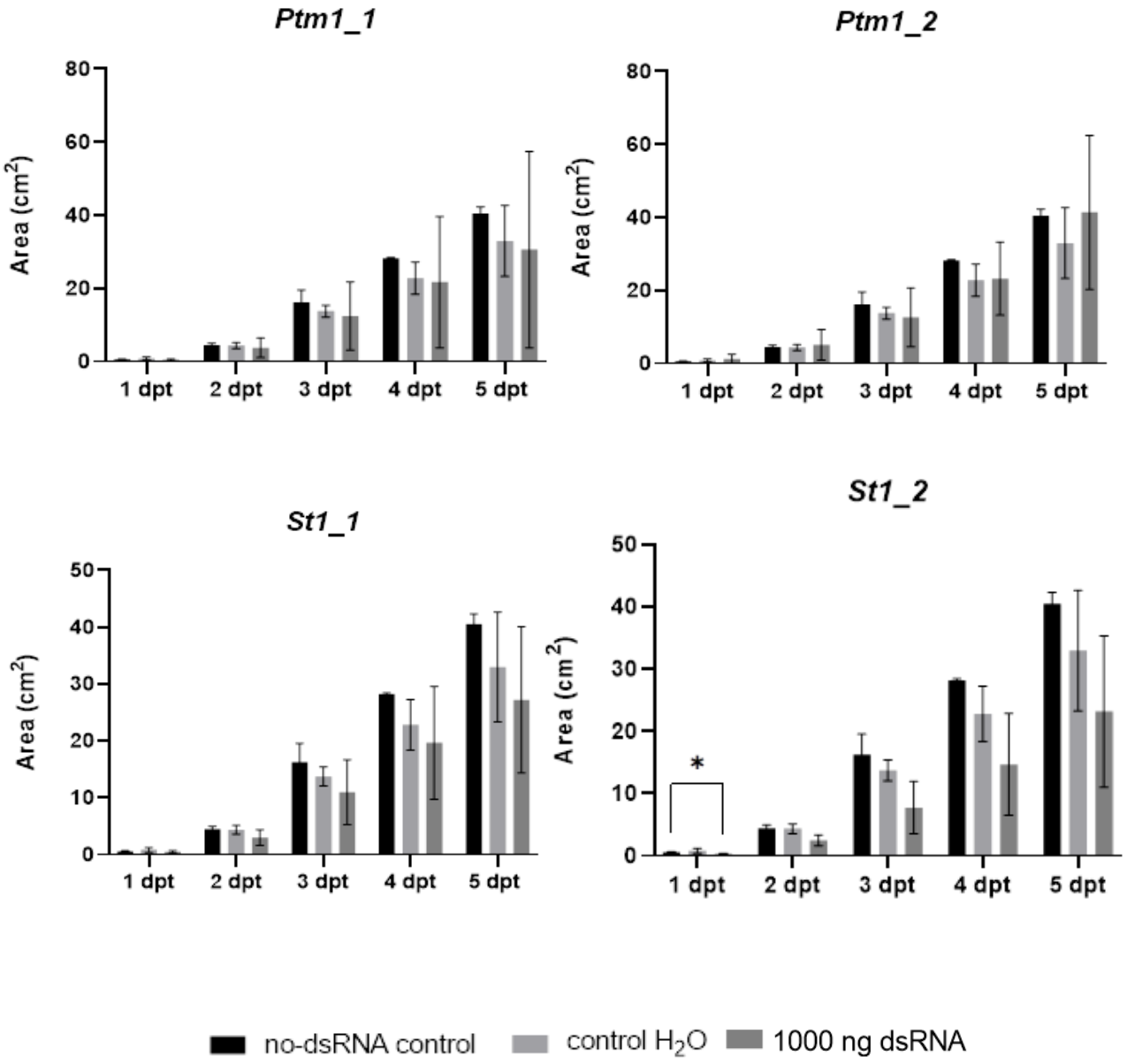

Figure 6. 2: Effects of dsRNAs prepared using gene fragmentation method in *D. corticola*. After challenging a *D. corticola* plug (5 mm) with 10 µl of *Ptm1_1*, *Ptm1_2*, *St1_1*, *St1_2* dsRNAs (1000 ngl), the fungal growth area (cm^2) was measured during five days post treatment (dpt). Controls without dsRNA treatment (no-dsRNA control) and with application of 10 µl of water (control H_2O) were performed. Asterisks represent statistical significances * ($p \leq 0.05$), ** ($p \leq 0.01$) and *** ($p \leq 0.001$).

6.1.2. *In vitro* assays for determining the impairment of *B. mediterranea* growth

In contrast with *D. corticola*, when considering the assays for the silencing of *B. mediterranea* genes, dsRNA molecules designed by the non-conserved protein domain method did not result into a significant impairment on fungal growth (Figure 6.3). Even *Sc2* dsRNA seems to promote fungal growth after three days, when compared to the control without dsRNA. For saving dsRNA molecules, and based on *D. corticola* assays, the subsequent assays for further testing *B. mediterranea* were only performed with 1000 ng of dsRNA. When using dsRNAs designed by the gene fragmentation method, a significant reduction of *B. mediterranea* growth was detected in the first 24 hours (for *St1_1*, *St1_2* and *Ptm1_2* dsRNAs) (Figure 6.4). However, this growth inhibition was rapidly surpassed after.

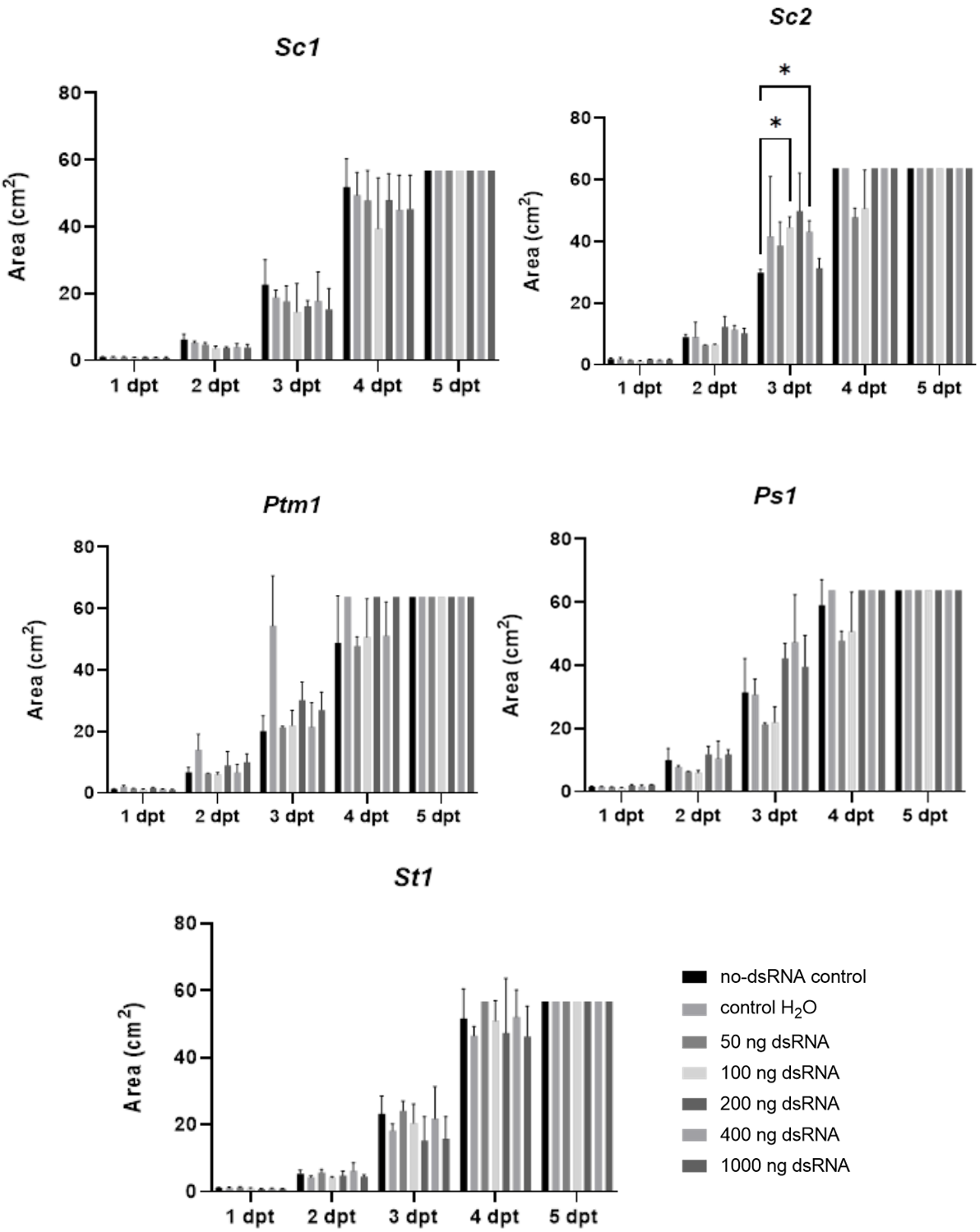

Figure 6. 3: Effects of dsRNAs prepared using non-conserved domain method in *B. mediterranea* growth. After challenging a *B. mediterranea* plug (5 mm) with 10 µl of *Sc1*, *Sc2*, *Ptm1*, *St1*, and *Ps1* dsRNAs (50 – 1000 ng), the fungal growth area (cm^2) was measured during five days post treatment (dpt). Different dsRNA amounts were tested, as described in the legend. Controls without dsRNA treatment (no-dsRNA control) and with application of 10 µl of water (control H_2O) were performed. Asterisks represent statistical significances * ($p \leq 0.05$), ** ($p \leq 0.01$) and *** ($p \leq 0.001$).

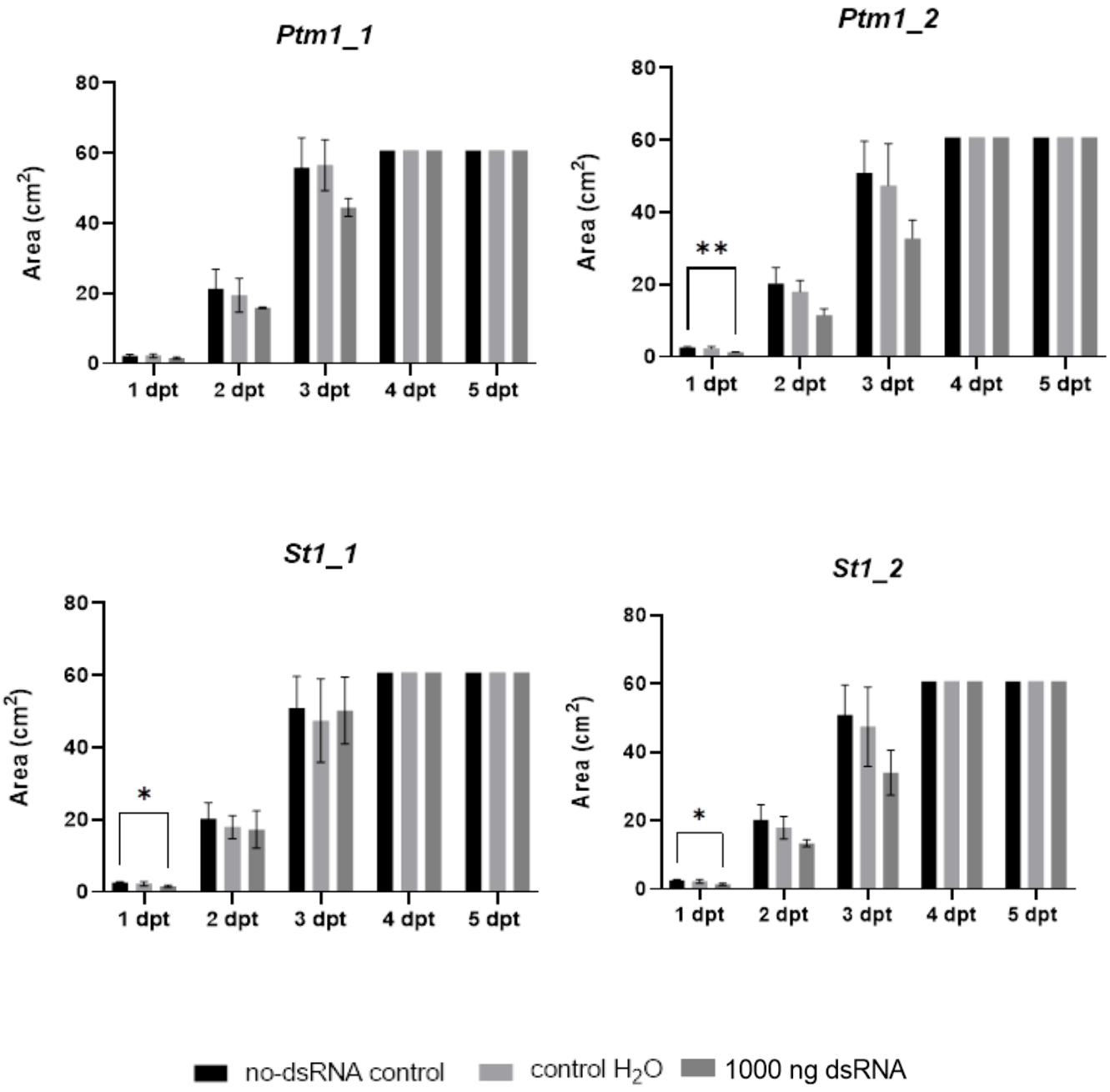

Figure 6. 4: Effects of dsRNAs prepared using gene fragmentation method in *B. mediterranea*. After challenging a *D. corticola* plug (5 mm) with 10 µl of *Ptm1_1*, *Ptm1_2*, *St1_1*, *St1_2* dsRNAs (1000 ng), prepared using gene fragmentation method, the fungal growth area (cm^2) was measured during five days post treatment (dpt). Controls without dsRNA treatment (no-dsRNA control) and with application of 10 µl of water (control H_2O) were performed. Asterisks represent statistical significances * ($p \leq 0.05$), ** ($p \leq 0.01$) and *** ($p \leq 0.001$).

6.1.3. Effect of permanent contact of dsRNA for the inhibition of fungal growth

During a plant-pathogen interaction, the cross-kingdom RNA trafficking has been recognized (Cai *et al.*, 2018). When applying a SIGS approach, not only the targeted pathogen will uptake dsRNA, but also the plant would be able to do so and produce siRNAs based on the applied dsRNA (Filho *et al.*, 2021). For this reason, pathogens will be continuously in the presence of challenging siRNAs. In order to mimic this effect, the PDA medium was supplemented with designed RNAs for promoting the constant contact of growing hyphae with dsRNA molecules. The idea is to allow the fungus to continually uptake dsRNA. Due to their availability, only dsRNAs produced by gene fragmentation were used for this assay.

In the presence of a continuous source of dsRNA, the developing hyphae seem to have their growth more compromised. This was particularly evident for *D. corticola*, in which all of the four tested dsRNA molecules significantly reduced fungal growth (*Ptm1_1, Ptm1_2, St1_1, and St1_2*) (Figure 6.5). In contrast, there were no significant differences in the growth of *B. mediterranea* after dsRNA application (Figure 6.5). The results revealed that, at least for *D. corticola,* the continuous supply of dsRNA enhance the silencing effect. When dsRNA was applied in the inoculation region, only *St1_2* revealed a significant inhibitory effect, but when in permanent contact with dsRNA all tested molecules impaired *D. corticola* growth.

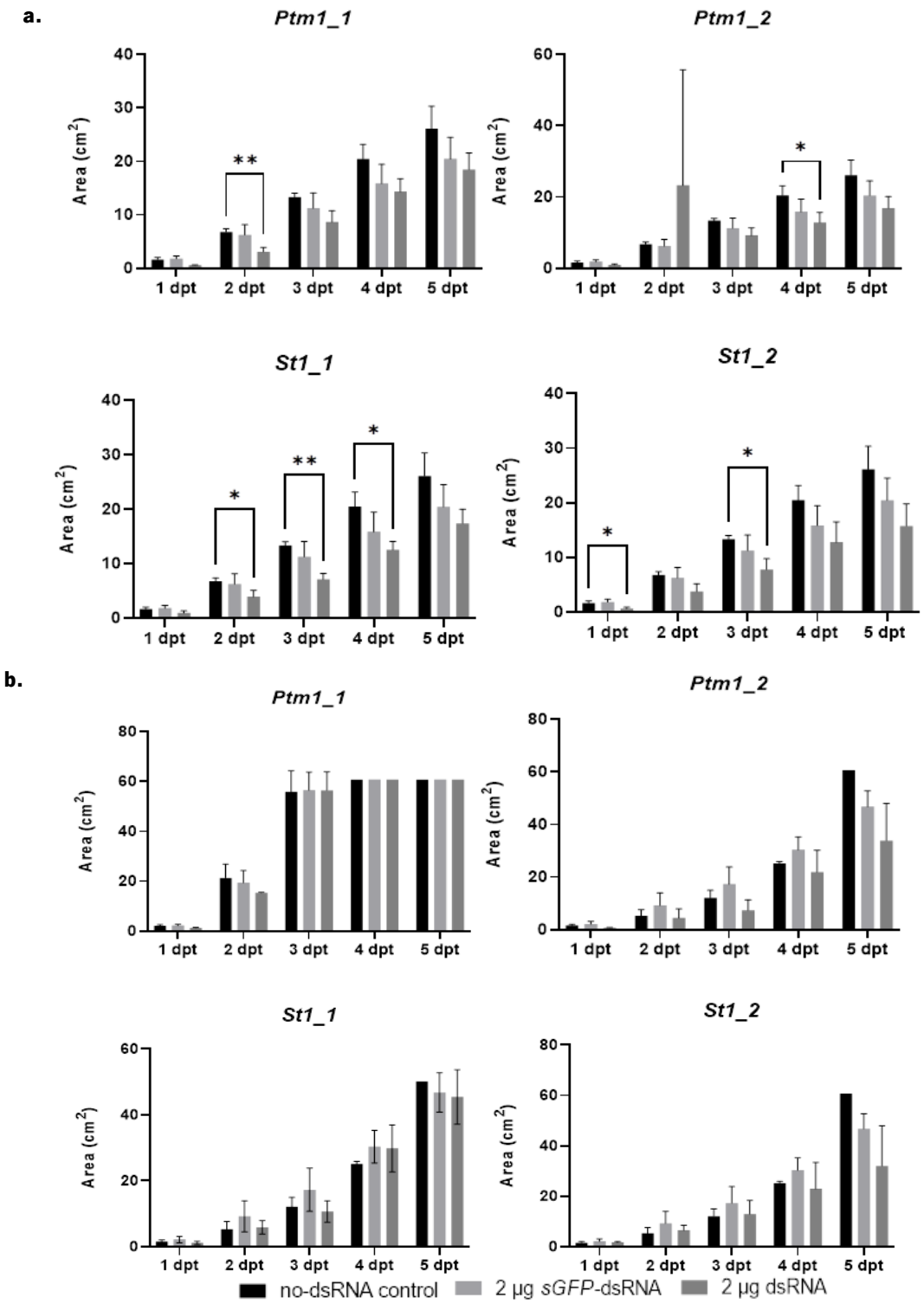

Figure 6. 5: Effects of constant presence of dsRNA prepared using the gene fragmentation method in *D. corticola* (a) and *B. mediterranea* (b) growth. A plug (5 mm) was placed to growth on PDA medium, supplemented to a final concentration of 2 µg/10 ml of ds RNA (*Ptm1_1*, *Ptm1_2*, *St1_1* and *St1_2*). The fungal growth area (cm^2) was measured during five days post treatment (dpt). Controls without dsRNA treatment (no-dsRNA control) and PDA supplemented with 2 µg/10 ml non target gene *sGFP* (2 µg s*GFP*-dsRNA) were performed. Asterisks represent statistical significances ** ($p \leq 0.05$), ** ($p \leq 0.01$) and *** ($p \leq 0.001$).*

6.1.4. Effect of stress conditions for inhibition of fungal growth by dsRNA

In response to a pathogen attack, plants have developed sophisticate pathways for the recognition of pathogen-associated molecular patterns (PAMPS) through their pattern recognition receptors (PRR) and activate a defence response (Peng *et al.*, 2018). One of those defences is a biphasic ROS burst, composed by hydrogen peroxide (H_2O_2), being the first burst fast and transient and the second stronger and sustained (Yuan *et al.*, 2021). For mimicking an oxidative stress environment, the assay for determining the growth reduction promoted by *Ptm1_1*, *Ptm1_2*, *St1_1* and *St1_2* dsRNA was repeated as described, but using a PDA medium supplemented with hydrogen peroxide (H_2O_2) up to a final concentration of 3 mM. This assay was performed for both cork oak pathogens. In every tested condition, there were no significant differences in fungal growth in the presence or absence of a dsRNA molecule (Figure S.2 and S.3). These results suggest that oxidative stress do not enhance gene silencing and could even reduce any existent effect of dsRNA. For example, while both *St1* dsRNAs significantly affected the growth of *D. corticola* (Figure 6.1) *or St1_1 of B. mediterranea* (Figure 6.4), the same molecules did not produce any fungal growth inhibition under oxidative stress conditions (Figure S.2 and S.3). This effect could be due to dsRNA instability due to the presence of H_2O_2. Although the double stranded structure confers more stability to dsRNA molecule, when compared to mRNA, degradation and hydrolysis processes are still possible (Zhang *et al.*, 2021). The direct contact of dsRNA molecule with H_2O_2 could promote oxidative damages to dsRNA.

In the presence of osmotic stress, the previously effective dsRNA molecules in *D. corticola* did not affect the fungal growth. Only *Ptm1_2*-dsRNA was still able to restrict fungal growth, suggesting that this molecule is more stable than the others. The specific nucleotide sequence of dsRNA could render the molecules more or stable under different osmotic pressures. In contrast, osmotic stress appears to promote the silencing effect on *B. mediterranea*, as the previously ineffective dsRNA molecules, promoted fungal growth inhibition under osmotic stress (*Ptm1_2* and *St1_2*). Therefore, a different fungal response may result from the specific physiological aspects of the targeted fungi.

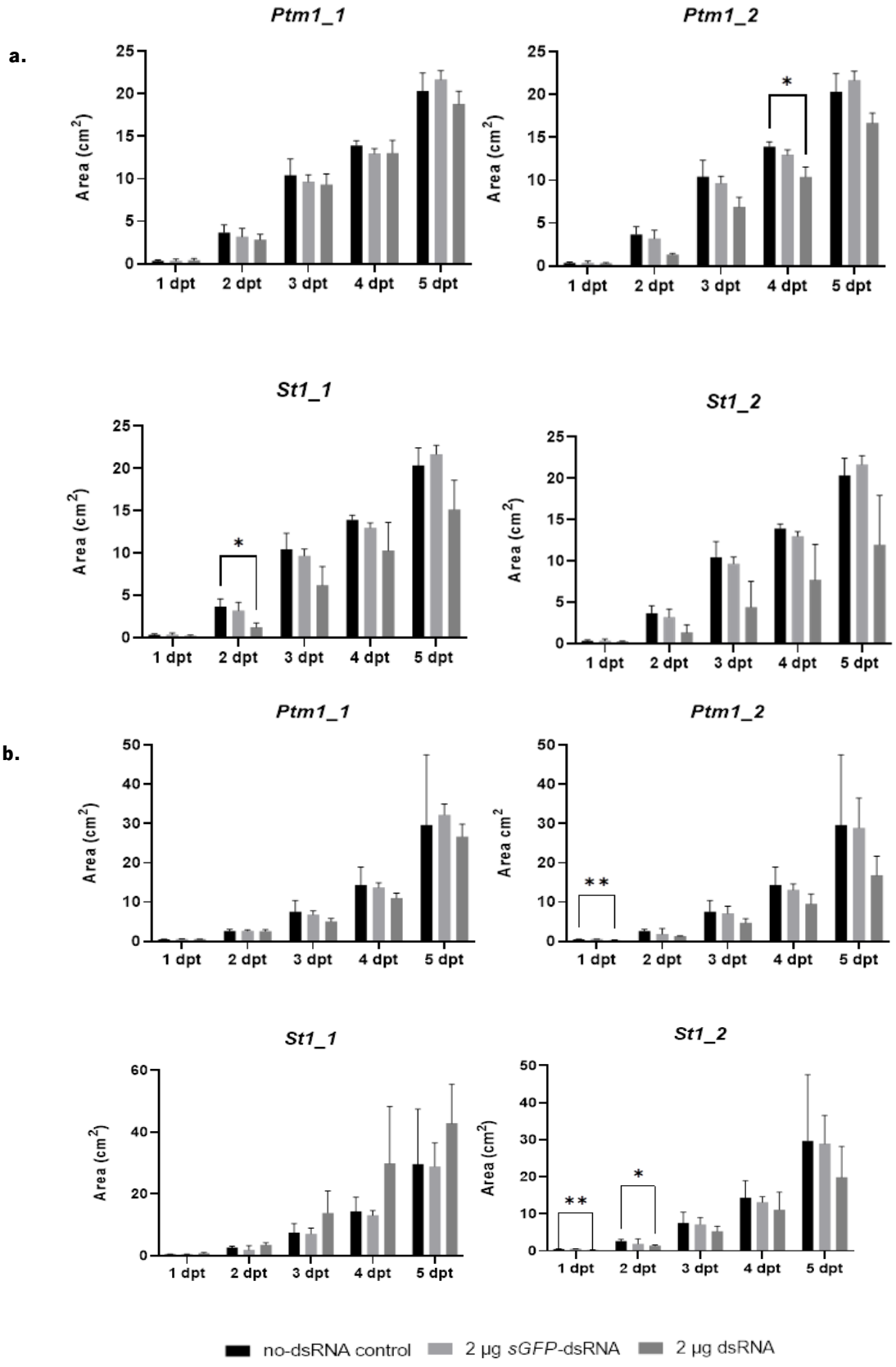

Figure 6. 6: Effects of constant presence of dsRNA prepared using the gene fragmentation method in *D. corticola* (a) and *B. mediterranea* (b) growth, under osmotic stress. A plug (5 mm) was placed to growth on a PDA supplemented sorbitol up to a final concentration of 1.2 M and 2 µg/10 ml *Ptm1_1* (a), *Ptm1_2* (b), *St1_1* (c) and *St1_2* (d) dsRNAs the fungal growth area (cm^2) was measured during five days post treatment (dpt). Controls without dsRNA treatment (no-dsRNA control) and PDA supplemented with 2 µg/10 ml non target gene *sGFP* (2 µg s*GFP*-dsRNA) were performed. Asterisks represent statistical significances ** ($p \leq 0.05$), ** ($p \leq 0.01$) and *** ($p \leq 0.001$).*

In summary, previous results revealed that *B. mediterranea* display RNAi silencing capacity (chapter IV). However, *in vivo* assays suggest that the control of this fungus by gene silencing would be not so efficient as in *D. corticola*. This result corroborates with the fact that not all organisms are equally sensible to RNAi. Some insects from the order Lepidoptera have been recognized to be generally less sensible to gene silencing approaches than others (Sharath Chandra *et al.*, 2019). For example, *Trichoderma virens* has been recognized as unable to use RNAi silencing (Qiao *et al.*, 2021). This could be related with the stability of dsRNA molecules on insect guts, which could present differences on pH (Vylkova, 2017; Kunte *et al.*, 2020). The dsRNA stability could also be important for the results observed in the assays. *D. corticola Ptm1_2* revealed similar results in both optimal and stress conditions, while *D. corticola St1_1* had a reduction in the impairing effect under stress, revealing a possible lesser stable molecule than *Ptm1_2*.

7. Chapter VII – Concluding remarks and future perspectives

Climate changes are related to increases in temperature and fluctuations in rainfall patterns, such as long and more severe drought periods. These conditions will be particularly severe for Mediterranean ecosystems, as recent climate predictions considered that in Mediterranean basin the warming is 20% faster than the global average, turning this region a climate change hotspot (Lionello and Scarascia, 2018). These new environmental conditions have been severally affecting the cork oak populations (Moricca *et al.*, 2011). Indeed, by weakening plant fitness, opportunistic pathogens can change their lifestyle and cause host diseases. Among cork oak pathogens, the severity of two opportunistic fungi have been rising in the last decade: the causing agent of charcoal disease (*Biscogniauxia mediterranea*) and one of the causing agents of bot canker (*Diplodia corticola*). As no treatment is available for these pathogens, disease control is mainly performed through good phytosanitary measures. Taking this into account, new solutions to control such pathogens are in urgent need.

In the last years, new solutions based in RNAi silencing are emerging. The activation of a common eukaryotic defence mechanism is promoted through the presence of a double stranded RNA (dsRNA), which will be processed and used as a template for post-transcriptional silencing. In this field, two state-of-the-art biotechnological approaches have been gaining relevance, the *Host-inducing gene silencing* (HIGS) and *Spray-induced gene silencing* (SIGS). Although based on the same biological principle, both techniques are quite distinct. In HIGS, plants are transformed and produce a dsRNA molecule that targets a fungal essential gene. In SIGS, dsRNA molecules that target pathogen essential genes are exogenously applied to the host plant, being uptaken by the pathogen. This last technique presents some advantages, including the exemption of developing a transformation protocol for a specific host species. Furthermore, dsRNA application could be done in any life stage of the host and for being a GMO-free approach, the public acceptance will be higher than with HIGS strategies. For all these reasons, SIGS was the chosen approach to develop a solution for controlling both cork oak pathogens.

For an effective SIGS strategy, two conditions must be met, the pathogens need to uptake the exogenous dsRNA and the RNAi silencing pathway should be functional. For this reason, in **chapter III**, an *in silico* analysis was performed to understand if both *B. mediterranea* and *D. corticola* comprise the necessary machinery for a successful SIGS approach. The main pathway for dsRNA uptake by cells has been considered the clathrin-meditated endocytosis (CME), which was fully described in the fungal model *Sclerotinia sclerotiorum* (Wytinck, *et al.*, 2020). All the seven proteins considered as essential for the dsRNA uptake were found in both cork oak pathogens

and did not reveal significant differences in their structure, apart from the presence of additional domains in the AP2-α subunit and amphiphysin. In addition, the core proteins used in RNAi silencing pathways, which have been thoroughly studied in *Neurospora crassa*, were also found in both pathogens. In this case, major differences in protein structure were found in both pathogens, comprising the lack of certain domains in Dicer and Argonaute proteins, which could be related with their function in different RNAi silencing pathways. Indeed, a phylogenetic analysis of RNAi silencing proteins (DCL, AGO and RdRP) revealed the diversification of these proteins with evolution, suggesting a distinction of proteins related to MSUD and quelling pathways.

The recognition of essential proteins for dsRNA uptake and processing in both cork oak pathogens suggests that a successful SIGS application could be possible for controlling them. However, not all fungi are able to uptake or process exogenous RNA molecules, as is the case of *Trichoderma virens* (Qiao *et al.*, 2021). For this reason, in **chapter IV**, *in vitro* assays were performed to test the dsRNA uptake by cork oak pathogens, as well as the ability of RNAi silencing. To test dsRNA uptake, fluorescent dsRNA was applied to pathogen hyphae and fluorescence signal was followed through live cell imaging. This experimental approach confirmed that both pathogens have the capacity to uptake dsRNA. For testing gene silencing ability, both *B. mediterranea* and *D. corticola* were previously transformed, in order to produce a sGFP protein, and a *sGFP*-dsRNA was applied to the transformant for silencing *sGFP* transgene. The results revealed that after 24 hours the fluorescence emitted by sGFP was reduced in about 40%, but after 48 hours the fluorescence levels raised again. This result suggests that RdRP proteins may not be functional for keeping the dsRNA signal in the growing hyphae. The capacity to amplify the initial dsRNA appears to be lacking. Still, the function of both CME and RNAi silencing was proved, corroborating *in silico* results (chapter III). Noteworthy, the lack of RdRP function in the studied fungi could still be compensated after *in planta* SIGS application, as the host is also able to uptake the dsRNA and produce siRNA (Filho *et al.*, 2021)..

To proceed with a gene silencing approach that could be used in a future SIGS strategy for controlling *B. mediterranea* and *D. corticola* pathogens, a pipeline was created to design target dsRNAs for essential genes (**chapter V**). Gene selection was based on the possible effects for fungal viability after silencing those genes. An aspect that has been recognized as important for a successful SIGS strategy is dsRNA size, which could compromise an efficient uptake. Based on the work of Bensoussan and co-authors (2020), the designed dsRNA molecules were within range 400-600 bp range. All designed dsRNA molecules revealed not to be complementary to *Q. suber* nor to

cork oak endophytes transcripts and were able to produce more than 150 possible effective siRNAs, revealing their feasibility to act as silencing dsRNA targets. Nevertheless, the dsRNAs that result in more possible efficient siRNAs were *B. mediterranea Ptm1_1*, *Ptm1_2*, *St1* and *Ptm1* and *D. corticola Sc1*, *Sc2*. Accordingly, when the capacity of synthesized molecules was tested for the impairment of cork oak pathogens growth (**chapter VI**), the most effective dsRNA molecules were those targeting *St1* gene, which encodes a protein related to a signal transduction pathway. Indeed, dsRNAs prepared for silencing the *St1* gene were the most efficient in impairing fungal growth (*St1*-dsRNA in *D. corticola*; *St1_1*-dsRNA and *St1_2*-dsRNA in *B. mediterranea*). Furthermore, *St1* dsRNA was the only dsRNA molecule able to impair fungal growth and caused hyphal anomalies in both cork oak pathogens.

All tested dsRNA molecules are predicted to produce a high number of possible effective siRNAs, but this number do not translate in a better performance. For example, one of the most effective silencing effects was detected in *D. corticola*, after the application of *St1*-dsRNA, which corresponds to the designed dsRNA with the lowest number of predicted effective siRNAs. Moreover, the results do not allow concluding about the efficiency of dsRNA designed method with different methods, as no distinct pattern emerged. The most effective dsRNAs for silencing *B. mediterranea* genes were designed based on the gene fragmented method, while in *D. corticola* both methods resulted in dsRNAs able to impair fungal growth.

Comparing both cork oak pathogens, the results suggest that *B. mediterranea* is less sensible to the designed dsRNAs than *D. corticola*, which is probably related with species-specific effects, including differences in uptaking dsRNA. This hypothesis is corroborated with the suggestion that *D. corticola* uptake is efficient when compared to *B. mediterranea* (chapter IV).

The main focus of this thesis was to understand if *B. mediterranea* and *D. corticola* could be controlled by RNA based biofungicides was possible. The results presented are promising and opens new possibilities for new research.

Results from *in silico* suggest that some CME and RNAi core proteins from both cork oak pathogens have lost some domains, described as essential for proteins function. However, both revealed a functional uptake and RNAi silencing machinery. The comparation of these proteins with others homologues from the same genus would be interesting to understand if these differences are a recent evolutionary adaptation of this species.

Results revealed that *St1* dsRNAs is able to impair fungal growth and promote hyphal anomalies in both cork oak pathogens. The quantification of *St1* gene expression (qRT-PCR) could build a strong correlation between the effects observed and transcript silencing.

Validation of silencing ability should be performed by using *in planta* assays, which are essential to understand if the produced effects are preserved in a plant-pathogen interaction.

As a concluding remark, the results of this thesis provided valuable information about a possible pipeline to apply when a SIGS application is considered to new fungal species.

8. References

A.Carapeto, P.V.Araújo, F.Clamote, M.Porto, S.Malveiro, J.Lourenço, P.Beja, D. T. H. (2022). *Floraon*. https://flora-on.pt/#/1sobreiro

Agrawal, N., Dasaradhi, P. V. N., Mohmmed, A., Malhotra, P., Bhatnagar, R. K., & Mukherjee, S. K. (2003). RNA Interference: Biology, Mechanism, and Applications. *Microbiology and Molecular Biology Reviews*, *67*(4), 657–685. https://doi.org/10.1128/mmbr.67.4.657-685.2003

APCOR. (2022). *APCOR 2022*. https://www.apcor.pt/media-center/estatisticas/

Aryal, C. M., Bui, N. N., Song, L., & Pan, J. (2022). The N-terminal helices of amphiphysin and endophilin have different capabilities of membrane remodeling. *Biochimica et Biophysica Acta (BBA) - Biomembranes*, *1864*(7), 183907. https://doi.org/10.1016/J.BBAMEM.2022.183907

Beacham, G. M., Partlow, E. A., & Hollopeter, G. (2019). Conformational regulation of AP1 and AP2 clathrin adaptor complexes. *Traffic*, *20*(10), 741–751. https://doi.org/10.1111/tra.12677

Bensoussan, N., Dixit, S., Tabara, M., Letwin, D., Milojevic, M., Antonacci, M., Jin, P., Arai, Y., Bruinsma, K., Suzuki, T., Fukuhara, T., Zhurov, V., Geibel, S., Nauen, R., Grbic, M., & Grbic, V. (2020). Environmental RNA interference in two-spotted spider mite, Tetranychus urticae, reveals dsRNA processing requirements for efficient RNAi response. *Scientific Reports*, *10*(1), 1–16. https://doi.org/10.1038/s41598-020-75682-6

Bhattacharjee, S., Roche, B., & Martienssen, R. A. (2019). RNA-induced initiation of transcriptional silencing (RITS) complex structure and function. *RNA Biology*, *16*(9), 1133–1146. https://doi.org/10.1080/15476286.2019.1621624

Bitsikas, V., Corrêa, I. R., & Nichols, B. J. (2014). Clathrin-independent pathways do not contribute significantly to endocytic flux. *ELife*, *2014*(3), 1–26. https://doi.org/10.7554/eLife.03970

Brodsky, F. M. (2012). Diversity of clathrin function: New tricks for an old protein. *Annual Review of Cell and Developmental Biology*, *28*, 309–336. https://doi.org/10.1146/annurev-cellbio-101011-155716

Cai, Q., He, B., Kogel, K. H., & Jin, H. (2018). Cross-kingdom RNA trafficking and environmental RNAi — nature's blueprint for modern crop protection strategies. *Current Opinion in Microbiology*, *46*, 58–64. https://doi.org/10.1016/j.mib.2018.02.003

Campanile, G., Ruscelli, A., & Luisi, N. (2007). Antagonistic activity of endophytic fungi towards Diplodia corticola assessed by in vitro and in planta tests. *European Journal of Plant Pathology*, *117*(3), 237–246. https://doi.org/10.1007/s10658-006-9089-1

Cappelle, K., De Oliveira, C. F. R., Van Eynde, B., Christiaens, O., & Smagghe, G. (2016). The involvement of clathrin-mediated endocytosis and two Sid-1-like transmembrane proteins in double-stranded RNA uptake in the Colorado potato beetle midgut. *Insect Molecular Biology*, *25*(3), 315–323. https://doi.org/10.1111/imb.12222

Cerutti, H., & Casas-Mollano, J. A. (2006). On the origin and functions of RNA-mediated silencing: From protists to man. *Current Genetics*, *50*(2), 81–99. https://doi.org/10.1007/s00294-006-0078-x

Chang, S. S., Zhang, Z., & Liu, Y. (2012). RNA interference pathways in fungi: Mechanisms and functions. *Annual Review of Microbiology*, *66*(June), 305–323.

https://doi.org/10.1146/annurev-micro-092611-150138

Chen, J., Peng, Y., Zhang, H., Wang, K., Zhao, C., Zhu, G., Reddy Palli, S., & Han, Z. (2021). Off-target effects of RNAi correlate with the mismatch rate between dsRNA and non-target mRNA. *RNA Biology*, *18*(11), 1747–1759. https://doi.org/10.1080/15476286.2020.1868680

Collins, B. M., McCoy, A. J., Kent, H. M., Evans, P. R., & Owen, D. J. (2002). Molecular architecture and functional model of the endocytic AP2 complex. *Cell*, *109*(4), 523–535. https://doi.org/10.1016/S0092-8674(02)00735-3

Cooper, A. M. W., Silver, K., Zhang, J., Park, Y., & Zhu, K. Y. (2019). Molecular mechanisms influencing efficiency of RNA interference in insects. *Pest Management Science*, *75*(1), 18–28. https://doi.org/10.1002/ps.5126

Costa, A., & Pereira, H. (2007). Montados e sobreirais: uma espécie, duas perspectivas. *Os Montados – Muito Para Além Das Árvores*, *October*, 17–37.

Costa, A., Pereira, H., & Madeira, M. (2009). Landscape dynamics in endangered cork oak woodlands in Southwestern Portugal (1958-2005). *Agroforestry Systems*, *77*(2), 83–96. https://doi.org/10.1007/s10457-009-9212-3

Costa, A., Pereira, H., & Madeira, M. (2010). Analysis of spatial patterns of oak decline in cork oak woodlands in Mediterranean conditions. *Annals of Forest Science*, *67*(2), 204–204. https://doi.org/10.1051/forest/2009097

Costa, D. F. F. (2021). Cork oak endophyte community as a way to control diseases in a climate changing world. *Doctoral Thesis*, 8–20.

Costa, D., Tavares, R. M., Baptista, P., & Lino-Neto, T. (2020). Cork Oak Endophytic Fungi as Potential Biocontrol Agents against Biscogniauxia mediterranea and Diplodia corticola. *Journal of Fungi*, *6*(4), 287. https://doi.org/10.3390/jof6040287

Court, D. L., Gan, J., Liang, Y.-H., Shaw, G. X., Tropea, J. E., Costantino, N., Waugh, D. S., & Ji, X. (2013). RNase III: Genetics and Function; Structure and Mechanism. *Annual Review of Genetics*, *47*(1), 405–431. https://doi.org/10.1146/annurev-genet-110711-155618

Dalakouras, Athanasios and Vlachostergios, D. (2021). Epigenetic approaches for crop breeding: current status and perspectives. *Oxford University Press on Behalf of the Society for Experimental Biology*, 1–32.

Dalakouras, A., Katsaouni, A., Avramidou, M., Dadami, E., Tsiouri, O., Vasileiadis, S., Makris, A., Georgopoulou, M. E., & Papadopoulou, K. K. (2022). Systemic silencing and DNA methylation of a host reporter gene induced by a beneficial fungal root endophyte. *BioRxiv*, 2022.06.19.496700. https://www.biorxiv.org/content/10.1101/2022.06.19.496700v1%0Ahttps://www.biorxiv.org/content/10.1101/2022.06.19.496700v1.abstract

Dalakouras, A., Wassenegger, M., Dadami, E., Ganopoulos, I., Pappas, M. L., & Papadopoulou, K. (2020). Genetically modified organism-free RNA interference: Exogenous application of RNA molecules in plants1[open]. *Plant Physiology*, *182*(1), 38–50. https://doi.org/10.1104/pp.19.00570

Dang, Y., Yang, Q., Xue, Z., & Liu, Y. (2011). RNA interference in fungi: Pathways, functions, and applications. *Eukaryotic Cell*, *10*(9), 1148–1155. https://doi.org/10.1128/EC.05109-11

Das, P. R., & Sherif, S. M. (2020). Application of Exogenous dsRNAs-induced RNAi in Agriculture: Challenges and Triumphs. *Frontiers in Plant Science*, *11*(June). https://doi.org/10.3389/fpls.2020.00946

de Oliveira Filho, J. G., Silva, G. da C., Cipriano, L., Gomes, M., & Egea, M. B. (2021). Control of postharvest fungal diseases in fruits using external application of RNAi. *Journal of Food Science*, *86*(8), 3341–3348. https://doi.org/10.1111/1750-3841.15816

Duanis-Assaf, D., Galsurker, O., Davydov, O., Maurer, D., Feygenberg, O., Sagi, M., Poverenov, E., Fluhr, R., & Alkan, N. (2022). Double-stranded RNA targeting fungal ergosterol biosynthesis pathway controls Botrytis cinerea and postharvest grey mould. *Plant Biotechnology Journal*, *20*(1), 226–237. https://doi.org/10.1111/pbi.13708

Espino, J., González, M., González, C., & Brito, N. (2014). Efficiency of different strategies for gene silencing in Botrytis cinerea. *Applied Microbiology and Biotechnology*, *98*(22), 9413–9424. https://doi.org/10.1007/s00253-014-6087-7

Fletcher, S. J., Reeves, P. T., Hoang, B. T., & Mitter, N. (2020). A Perspective on RNAi-Based Biopesticides. *Frontiers in Plant Science*, *11*(February), 1–10. https://doi.org/10.3389/fpls.2020.00051

Gaffar, F. Y., Imani, J., Karlovsky, P., Koch, A., & Kogel, K.-H. (2019). Different Components of the RNA Interference Machinery Are Required for Conidiation, Ascosporogenesis, Virulence, Deoxynivalenol Production, and Fungal Inhibition by Exogenous Double-Stranded RNA in the Head Blight Pathogen Fusarium graminearum. *Frontiers in Microbiology*, *10*(August). https://doi.org/10.3389/fmicb.2019.01662

Geley, S., & Müller, C. (2004). RNAi: Ancient mechanism with a promising future. *Experimental Gerontology*, *39*(7), 985–998. https://doi.org/10.1016/j.exger.2004.03.040

Gil L, V. M. (2008). Technical guidelines for genetic conservation and use of cork oak (quercus suber). *News.Ge*, *Bioversity International*, 6.

Goubanova, K., & Li, L. (2007). Extremes in temperature and precipitation around the Mediterranean basin in an ensemble of future climate scenario simulations. *Global and Planetary Change*, *57*(1–2), 27–42. https://doi.org/10.1016/j.gloplacha.2006.11.012

Haar, Ernst; Musacchio, Andrea; C. Harrison, Stephen; Kirchhauseen, T. (1998). Atomic Structure of Clathrin: A β Propeller Terminal Domain Joins an α Zigzag Linker Ernst. *Physiology & Behavior*, *176*(1), 139–148.

Hagiwara, D., Takahashi-Nakaguchi, A., Toyotome, T., Yoshimi, A., Abe, K., Kamei, K., Gonoi, T., & Kawamoto, S. (2013). NikA/TcsC histidine kinase is involved in conidiation, hyphal morphology, and responses to osmotic stress and antifungal chemicals in Aspergillus fumigatus. *PLoS ONE*, *8*(12). https://doi.org/10.1371/journal.pone.0080881

Hammond, S. M. (2005). Dicing and slicing: The core machinery of the RNA interference pathway. *FEBS Letters*, *579*(26), 5822–5829. https://doi.org/10.1016/j.febslet.2005.08.079

Hammond, T. M. (2017). Sixteen Years of Meiotic Silencing by Unpaired DNA. In *Advances in Genetics* (Vol. 97). Elsevier Ltd. https://doi.org/10.1016/bs.adgen.2016.11.001

Hannon, G. J. (2002). RNA interference. *Nature*, *418*(6894), 244–251. https://doi.org/10.1038/418244a

Hardham, A. R., & Blackman, L. M. (2018). Phytophthora cinnamomi. *Molecular Plant Pathology*, *19*(2), 260–285. https://doi.org/10.1111/mpp.12568

Henriques, J. M. C. (2015). Charcoal Canker (Biscogniauxia Mediterranea) in Cork Oak Decline in Portugal. *Ph.D. Dissertation*.

Höfle, L., Biedenkopf, D., Werner, B. T., Shrestha, A., Jelonek, L., & Koch, A. (2020). Study on the efficiency of dsRNAs with increasing length in RNA-based silencing of the Fusarium CYP51 genes. *RNA Biology*, *17*(4), 463–473. https://doi.org/10.1080/15476286.2019.1700033

Homet, P., González, M., Matías, L., Godoy, O., Pérez-Ramos, I. M., García, L. V., & Gómez-Aparicio, L. (2019). Exploring interactive effects of climate change and exotic pathogens on Quercus suber performance: Damage caused by Phytophthora cinnamomi varies across contrasting scenarios of soil moisture. *Agricultural and Forest Meteorology*, *276–277*(June), 107605. https://doi.org/10.1016/j.agrformet.2019.06.004

Hu, Y., Stenlid, J., Elfstrand, M., & Olson, A. (2013). Evolution of RNA interference proteins dicer and argonaute in Basidiomycota. *Mycologia*, *105*(6), 1489–1498. https://doi.org/10.3852/13-171

Hung, Y. H., & Slotkin, R. K. (2021). The initiation of RNA interference (RNAi) in plants. *Current Opinion in Plant Biology*, *61*, 102014. https://doi.org/10.1016/j.pbi.2021.102014

Hutvagner, G., & Simard, M. J. (2008). Argonaute proteins: Key players in RNA silencing. *Nature Reviews Molecular Cell Biology*, *9*(1), 22–32. https://doi.org/10.1038/nrm2321

J. M. LORANG, R. P. TUORI, J. P. MARTINEZ, 1 T. L. SAWYER, R. S. R., ROLLINS, J. A., WOLPERT, T. J., K. B. JOHNSON, R. J. RODRIGUEZ, M. B. D., & CIUFFETTI, A. L. M. (2001). Green Fluorescent Protein Is Lighting Up Fungal Biology. *APPLIED AND ENVIRONMENTAL MICROBIOLOGY*, *67*(5), 1987–1994. https://doi.org/10.1128/AEM.67.5.1987

Kaksonen, M., & Roux, A. (2018). Mechanisms of clathrin-mediated endocytosis. *Nature Reviews Molecular Cell Biology*, *19*(5), 313–326. https://doi.org/10.1038/nrm.2017.132

Kim, H. N., Jin, H. Y., Kwak, M. J., Khaine, I., You, H. N., Lee, T. Y., Ahn, T. H., & Woo, S. Y. (2017). Why does Quercus suber species decline in Mediterranean areas? *Journal of Asia-Pacific Biodiversity*, *10*(3), 337–341. https://doi.org/10.1016/j.japb.2017.05.004

Koch, A., Biedenkopf, D., Furch, A., Weber, L., Rossbach, O., Abdellatef, E., Linicus, L., Johannsmeier, J., Jelonek, L., Goesmann, A., Cardoza, V., McMillan, J., Mentzel, T., & Kogel, K. H. (2016a). An RNAi-Based Control of Fusarium graminearum Infections Through Spraying of Long dsRNAs Involves a Plant Passage and Is Controlled by the Fungal Silencing Machinery. *PLoS Pathogens*, *12*(10), 1–22. https://doi.org/10.1371/journal.ppat.1005901

Koch, A., Biedenkopf, D., Furch, A., Weber, L., Rossbach, O., Abdellatef, E., Linicus, L., Johannsmeier, J., Jelonek, L., Goesmann, A., Cardoza, V., McMillan, J., Mentzel, T., & Kogel, K. H. (2016b). An RNAi-Based Control of Fusarium graminearum Infections Through Spraying of Long dsRNAs Involves a Plant Passage and Is Controlled by the Fungal Silencing Machinery. *PLoS Pathogens*, *12*(10). https://doi.org/10.1371/journal.ppat.1005901

Koch, A., Stein, E., & Kogel, K. H. (2018). RNA-based disease control as a complementary measure to fight Fusarium fungi through silencing of the azole target Cytochrome P450

Lanosterol C-14 α-Demethylase. *European Journal of Plant Pathology*, *152*(4), 1003–1010. https://doi.org/10.1007/s10658-018-1518-4

Kuhn, C. D., & Joshua-Tor, L. (2013). Eukaryotic Argonautes come into focus. *Trends in Biochemical Sciences*, *38*(5), 263–271. https://doi.org/10.1016/j.tibs.2013.02.008

Kunte, N., McGraw, E., Bell, S., Held, D., & Avila, L. A. (2020). Prospects, challenges and current status of RNAi through insect feeding. *Pest Management Science*, *76*(1), 26–41. https://doi.org/10.1002/ps.5588

Lata, H., Sharma, A., Chadha, S., Kaur, M., & Kumar, P. (2022). RNA interference (RNAi) mechanism and application in vegetable crops. *Journal of Horticultural Science and Biotechnology*, *97*(2), 160–170. https://doi.org/10.1080/14620316.2021.1988729

Lax, C., Tahiri, G., Patiño-Medina, J. A., Cánovas-Márquez, J. T., Pérez-Ruiz, J. A., Osorio-Concepción, M., Navarro, E., & Calo, S. (2020). The evolutionary significance of rnai in the fungal kingdom. *International Journal of Molecular Sciences*, *21*(24), 1–22. https://doi.org/10.3390/ijms21249348

Leite, C., & Pereira, H. (2017). Cork-containing barks—a review. *Frontiers in Materials*, *3*(January), 1–19. https://doi.org/10.3389/fmats.2016.00063

Li, L., Chang, S. S., & Liu, Y. (2010). RNA interference pathways in filamentous fungi. *Cellular and Molecular Life Sciences*, *67*(22), 3849–3863. https://doi.org/10.1007/s00018-010-0471-y

Lionello, P., Abrantes, F., Gacic, M., Planton, S., Trigo, R., & Ulbrich, U. (2014). The climate of the Mediterranean region: research progress and climate change impacts. *Regional Environmental Change*, *14*(5), 1679–1684. https://doi.org/10.1007/s10113-014-0666-0

Lionello, P., & Scarascia, L. (2018). The relation between climate change in the Mediterranean region and global warming. *Regional Environmental Change*, *18*(5), 1481–1493. https://doi.org/10.1007/s10113-018-1290-1

Livshits, M. A., Amosova, O. A., & Lyubchenko, Y. L. (1990). Flexibility difference between double-stranded RNA and DNA as revealed by gel electrophoresis. *Journal of Biomolecular Structure and Dynamics*, *7*(6), 1237–1249. https://doi.org/10.1080/07391102.1990.10508562

Lück, S., Kreszies, T., Strickert, M., Schweizer, P., Kuhlmann, M., & Douchkov, D. (2019). siRNA-Finder (si-Fi) Software for RNAi-Target Design and Off-Target Prediction. *Frontiers in Plant Science*, *10*(August), 1–12. https://doi.org/10.3389/fpls.2019.01023

Luque, J., Pera, J., & Parladé, J. (2008). Evaluation of fungicides for the control of Botryosphaeria corticola on cork oak in Catalonia (NE Spain). *Forest Pathology*, *38*(3), 147–155. https://doi.org/10.1111/j.1439-0329.2007.00526.x

Mandal, K. (2020). Review of PIP2 in cellular signaling, functions and diseases. *International Journal of Molecular Sciences*, *21*(21), 1–20. https://doi.org/10.3390/ijms21218342

Margis, R., Fusaro, A. F., Smith, N. A., Curtin, S. J., Watson, J. M., Finnegan, E. J., & Waterhouse, P. M. (2006). The evolution and diversification of Dicers in plants. *FEBS Letters*, *580*(10), 2442–2450. https://doi.org/10.1016/j.febslet.2006.03.072

MARY K. MONTGOMERY, SIQUN XU, A. F. (1998). RNA as a target of double-stranded RNA-mediated genetic interference in Caenorhabditis elegans. *Proceedings of the National*

Academy of Sciences of the United States of America, *95*(26), 15502–15507. https://doi.org/10.1073/pnas.95.26.15502

Mazhab-Jafari, M. T., & Rubinstein, J. L. (2016). Cryo-EM studies of the structure and dynamics of vacuolar-type ATPases. *Science Advances*, *2*(7), 1–10. https://doi.org/10.1126/sciadv.1600725

Mazzaglia, A., Anselmi, N., Gasbarri, A., & Vannini, A. (2001). Development of a Polymerase Chain Reaction (PCR) assay for the specific detection of Biscogniauxia mediterranea living as an endophyte in oak tissues. *Mycological Research*, *105*(8), 952–956. https://doi.org/10.1016/S0953-7562(08)61951-6

Medley, J. C., Panzade, G., & Zinovyeva, A. Y. (2021). microRNA strand selection: Unwinding the rules. *Wiley Interdisciplinary Reviews: RNA*, *12*(3), 1–22. https://doi.org/10.1002/wrna.1627

Michielse, C. B., Hooykaas, P. J. J., van den Hondel, C. A. M. J. J., & Ram, A. F. J. (2008). Agrobacterium-mediated transformation of the filamentous fungus Aspergillus awamori. *Nature Protocols*, *3*(10), 1671–1678. https://doi.org/10.1038/nprot.2008.154

Moar, W., Khajuria, C., Pleau, M., Ilagan, O., Chen, M., Jiang, C., Price, P., McNulty, B., Clark, T., & Head, G. (2017). Cry3Bb1-Resistant western corn rootworm, diabrotica virgifera virgifera (LeConte) does not exhibit cross-resistance to DvSnf7 dsRNA. *PLoS ONE*, *12*(1), 1–15. https://doi.org/10.1371/journal.pone.0169175

Moricca, S., Linaldeddu, B., & Ginetti, B. (2011). Stem , Branch , and Twig Pathogens. *The American Phytopathological Society*, *100*(11), 2184–2193.

Mukherjee, K., Campos, H., & Kolaczkowski, B. (2013). Evolution of animal and plant dicers: Early parallel duplications and recurrent adaptation of antiviral RNA binding in plants. *Molecular Biology and Evolution*, *30*(3), 627–641. https://doi.org/10.1093/molbev/mss263

Nakayashiki, H., Kadotani, N., & Mayama, S. (2006). Evolution and diversification of RNA silencing proteins in fungi. *Journal of Molecular Evolution*, *63*(1), 127–135. https://doi.org/10.1007/s00239-005-0257-2

Napoli, C., Lemieux, C., & Jorgensen, R. (1990). Introduction of a chimeric chalcone synthase gene into petunia results in reversible co-suppression of homologous genes in trans. *Plant Cell*, *2*(4), 279–289. https://doi.org/10.2307/3869076

Nerva, L., Sandrini, M., Gambino, G., & Chitarra, W. (2020). Double-stranded rnas (Dsrnas) as a sustainable tool against gray mold (botrytis cinerea) in grapevine: Effectiveness of different application methods in an open-air environment. *Biomolecules*, *10*(2). https://doi.org/10.3390/biom10020200

Nishimoto, R. (2019). Global trends in the crop protection industry. *Journal of Pesticide Science*, *44*(3), 141–147. https://doi.org/10.1584/jpestics.D19-101

Niu, D., Hamby, R., Sanchez, J. N., Cai, Q., Yan, Q., & Jin, H. (2021). RNAs — a new frontier in crop protection. *Current Opinion in Biotechnology*, *70*, 204–212. https://doi.org/10.1016/j.copbio.2021.06.005

Nugent, L. K., Sihanonth, P., Thienhirun, S., & Whalley, A. J. S. (2005). Biscogniauxia: A genus of latent invaders. *Mycologist*, *19*(1), 40–43. https://doi.org/10.1017/S0269915X05001060

Oliveira, G., & Costa, A. (2012). How resilient is Quercus suber L. to cork harvesting? A review and identification of knowledge gaps. *Forest Ecology and Management*, *270*, 257–272. https://doi.org/10.1016/j.foreco.2012.01.025

Ongvarrasopone, C., Roshorm, Y., & Panyim, S. (2007). A simple and cost effective method to generate dsRNA for RNAi studies in invertebrates. *ScienceAsia*, *33*(1), 35–39. https://doi.org/10.2306/scienceasia1513-1874.2007.33.035

Ozturk, T., Ceber, Z. P., Türkeş, M., & Kurnaz, M. L. (2015). Projections of climate change in the Mediterranean Basin by using downscaled global climate model outputs. *International Journal of Climatology*, *35*(14), 4276–4292. https://doi.org/10.1002/joc.4285

Paturi, S., & Deshmukh, M. V. (2021). A Glimpse of "Dicer Biology" Through the Structural and Functional Perspective. *Frontiers in Molecular Biosciences*, *8*(May). https://doi.org/10.3389/fmolb.2021.643657

Peng, Y., Van Wersch, R., & Zhang, Y. (2018). Convergent and divergent signaling in PAMP-triggered immunity and effector-triggered immunity. *Molecular Plant-Microbe Interactions*, *31*(4), 403–409. https://doi.org/10.1094/MPMI-06-17-0145-CR

Pujol-Carrion, N., Petkova, M. I., Serrano, L., & de la Torre-Ruiz, M. A. (2013). The MAP kinase Slt2 is involved in vacuolar function and actin remodeling in Saccharomyces cerevisiae mutants affected by endogenous oxidative stress. *Applied and Environmental Microbiology*, *79*(20), 6459–6471. https://doi.org/10.1128/AEM.01692-13

Qiao, L., Lan, C., Capriotti, L., Ah-Fong, A., Nino Sanchez, J., Hamby, R., Heller, J., Zhao, H., Glass, N. L., Judelson, H. S., Mezzetti, B., Niu, D., & Jin, H. (2021). Spray-induced gene silencing for disease control is dependent on the efficiency of pathogen RNA uptake. *Plant Biotechnology Journal*, *19*(9), 1756–1768. https://doi.org/10.1111/pbi.13589

Rosa, C., Kuo, Y. W., Wuriyanghan, H., & Falk, B. W. (2018). RNA interference mechanisms and applications in plant pathology. *Annual Review of Phytopathology*, *56*, 581–610. https://doi.org/10.1146/annurev-phyto-080417-050044

Saleh, M. C., van Rij, R. P., Hekele, A., Gillis, A., Foley, E., O'Farrell, P. H., & Andino, R. (2006). The endocytic pathway mediates cell entry of dsRNA to induce RNAi silencing. *Nature Cell Biology*, *8*(8), 793–802. https://doi.org/10.1038/ncb1439

San-Epifanio, L. E. (2022). *79 . Challenges faced by the EU regulatory framework on GMOs after the ECJ ruling on mutagenesis*. 507–512. https://doi.org/https://doi.org/10.3920/978-90-8686-939-8

Sang, H., & Kim, J. II. (2020). Advanced strategies to control plant pathogenic fungi by host-induced gene silencing (HIGS) and spray-induced gene silencing (SIGS). *Plant Biotechnology Reports*, *14*(1), 1–8. https://doi.org/10.1007/s11816-019-00588-3

Sauguet, L. (2019). The Extended "Two-Barrel" Polymerases Superfamily: Structure, Function and Evolution. *Journal of Molecular Biology*, *431*(20), 4167–4183. https://doi.org/10.1016/J.JMB.2019.05.017

Schruefer, S., Böhmer, I., Dichtl, K., Spadinger, A., Kleinemeier, C., & Ebel, F. (2021). The response regulator Skn7 of Aspergillus fumigatus is essential for the antifungal effect of fludioxonil. *Scientific Reports*, *11*(1), 1–12. https://doi.org/10.1038/s41598-021-84740-6

Senthil-Kumar, M., & Mysore, K. S. (2011). Caveat of RNAi in plants: the off-target effect. In *Methods in molecular biology (Clifton, N.J.)* (Vol. 744, pp. 13–25).

https://doi.org/10.1007/978-1-61779-123-9_2

Shabalina, S. A., & Koonin, E. V. (2008). Origins and evolution of eukaryotic RNA interference. *Trends in Ecology and Evolution*, *23*(10), 578–587. https://doi.org/10.1016/j.tree.2008.06.005

Sharath Chandra, G., Asokan, R., Manamohan, M., & Krishna Kumar, N. (2019). Enhancing RNAi by using concatemerized double-stranded RNA. *Pest Management Science*, *75*(2), 506–514. https://doi.org/10.1002/ps.5149

Simonson, W. D., Allen, H. D., Parham, E., de Basto e Santos, E., & Hotham, P. (2018). Modelling biodiversity trends in the montado (wood pasture) landscapes of the Alentejo, Portugal. *Landscape Ecology*, *33*(5), 811–827. https://doi.org/10.1007/s10980-018-0627-y

Smahi, H., Belhoucine-Guezouli, L., Berraf-Tebbal, A., Chouih, S., Arkam, M., Franceschini, A., Linaldeddu, B. T., & Phillips, A. J. L. (2017). Molecular characterization and pathogenicity of Diplodia corticola and other Botryosphaeriaceae species associated with canker and dieback of Quercus suber in Algeria. *Mycosphere*, *8*(2), 1261–1272. https://doi.org/10.5943/mycosphere/8/2/10

Song, X. S., Gu, K. X., Duan, X. X., Xiao, X. M., Hou, Y. P., Duan, Y. B., Wang, J. X., Yu, N., & Zhou, M. G. (2018). Secondary amplification of siRNA machinery limits the application of spray-induced gene silencing. *Molecular Plant Pathology*, *19*(12), 2543–2560. https://doi.org/10.1111/mpp.12728

Spada, M., Pugliesi, C., Fambrini, M., & Pecchia, S. (2021). Silencing of the Slt2-Type MAP Kinase Bmp3 in Botrytiscinerea by Application of Exogenous dsRNA Affects Fungal Growth and Virulence on Lactuca sativa. *International Journal of Molecular Sciences*, *22*(10). https://doi.org/10.3390/ijms22105362

Swarts, D. C., Makarova, K., Wang, Y., Nakanishi, K., Ketting, R. F., Koonin, E. V., Patel, D. J., & Van Der Oost, J. (2014). The evolutionary journey of Argonaute proteins. *Nature Structural and Molecular Biology*, *21*(9), 743–753. https://doi.org/10.1038/nsmb.2879

Syed Ab Rahman, S. F., Singh, E., Pieterse, C. M. J., & Schenk, P. M. (2018). Emerging microbial biocontrol strategies for plant pathogens. *Plant Science*, *267*(June 2017), 102–111. https://doi.org/10.1016/j.plantsci.2017.11.012

Takeda, T., Kozai, T., Yang, H., Ishikuro, D., Seyama, K., Kumagai, Y., Abe, T., Yamada, H., Uchihashi, T., Ando, T., & Takei, K. (2018). Dynamic clustering of dynamin-amphiphysin helices regulates membrane constriction and fission coupled with GTP hydrolysis. *ELife*, *7*, 1–19. https://doi.org/10.7554/eLife.30246

Tetorya, M., & Rajam, M. V. (2021). RNAi-mediated silencing of PEX6 and GAS1 genes of Fusarium oxysporum f. sp. lycopersici confers resistance against Fusarium wilt in tomato. *3 Biotech*, *11*(10), 1–8. https://doi.org/10.1007/s13205-021-02973-8

Tiberi, R., Branco, M., Bracalini, M., Croci, F., & Panzavolta, T. (2016). Cork oak pests: a review of insect damage and management. *Annals of Forest Science*, *73*(2), 219–232. https://doi.org/10.1007/s13595-015-0534-1

Tiwari, R., & Rajam, M. V. (2022). RNA- and miRNA-interference to enhance abiotic stress tolerance in plants. *Journal of Plant Biochemistry and Biotechnology*, *9*. https://doi.org/10.1007/s13562-022-00770-9

Tsai, H. Y., Chen, C. C. G., Conte, D., Moresco, J. J., Chaves, D. A., Mitani, S., Yates, J. R., Tsai, M. D., & Mello, C. C. (2015). A ribonuclease coordinates siRNA amplification and mRNA Cleavage during NAi. *Cell*, *160*(3), 407–419. https://doi.org/10.1016/j.cell.2015.01.010

Ulvila, J., Parikka, M., Kleino, A., Sormunen, R., Ezekowitz, R. A., Kocks, C., & Rämet, M. (2006). Double-stranded RNA is internalized by scavenger receptor-mediated endocytosis in Drosophila S2 cells. *Journal of Biological Chemistry*, *281*(20), 14370–14375. https://doi.org/10.1074/jbc.M513868200

Vélez, A. M., & Fishilevich, E. (2018). The mysteries of insect RNAi: A focus on dsRNA uptake and transport. *Pesticide Biochemistry and Physiology*, *151*(July), 25–31. https://doi.org/10.1016/j.pestbp.2018.08.005

Vilà-Cabrera, A., Coll, L., Martínez-Vilalta, J., & Retana, J. (2018). Forest management for adaptation to climate change in the Mediterranean basin: A synthesis of evidence. *Forest Ecology and Management*, *407*(October 2017), 16–22. https://doi.org/10.1016/j.foreco.2017.10.021

Von Kleist, L., Stahlschmidt, W., Bulut, H., Gromova, K., Puchkov, D., Robertson, M. J., MacGregor, K. A., Tomlin, N., Pechstein, A., Chau, N., Chircop, M., Sakoff, J., Von Kries, J. P., Saenger, W., Kräusslich, H. G., Shupliakov, O., Robinson, P. J., McCluskey, A., & Haucke, V. (2011). Role of the clathrin terminal domain in regulating coated pit dynamics revealed by small molecule inhibition. *Cell*, *146*(3), 471–484. https://doi.org/10.1016/j.cell.2011.06.025

Vylkova, S. (2017). Environmental pH modulation by pathogenic fungi as a strategy to conquer the host. *PLoS Pathogens*, *13*(2), 1–6. https://doi.org/10.1371/journal.ppat.1006149

Wang, J., Wang, Y., & O'Halloran, T. J. (2006). Clathrin light chain: Importance of the conserved carboxy terminal domain to function in living cells. *Traffic*, *7*(7), 824–832. https://doi.org/10.1111/j.1600-0854.2006.00438.x

Wang, M., Weiberg, A., Lin, F. M., Thomma, B. P. H. J., Huang, H. Da, & Jin, H. (2016). Bidirectional cross-kingdom RNAi and fungal uptake of external RNAs confer plant protection. *Nature Plants*, *2*(10). https://doi.org/10.1038/nplants.2016.151

Wang, P., Zhou, Y., & Richards, A. M. (2021). Effective tools for RNA-derived therapeutics: siRNA interference or miRNA mimicry. *Theranostics*, *11*(18), 8771–8796. https://doi.org/10.7150/thno.62642

Wang, Z., Wang, Y., Liu, T., Wang, Y., & Zhang, W. (2019). Effects of the PIWI/MID domain of Argonaute protein on the association of miRNAi's seed base with the target. *Rna*, *25*(5), 620–629. https://doi.org/10.1261/rna.069328.118

Werner, B. T., Gaffar, F. Y., Schuemann, J., Biedenkopf, D., & Koch, A. M. (2020). RNA-Spray-Mediated Silencing of Fusarium graminearum AGO and DCL Genes Improve Barley Disease Resistance. *Frontiers in Plant Science*, *11*(April), 1–11. https://doi.org/10.3389/fpls.2020.00476

Wu, J., Yang, J., Cho, W. C., & Zheng, Y. (2020). Argonaute proteins: Structural features, functions and emerging roles. *Journal of Advanced Research*, *24*, 317–324. https://doi.org/10.1016/j.jare.2020.04.017

Wytinck, N., Manchur, C. L., Li, V. H., Whyard, S., & Belmonte, M. F. (2020). Dsrna uptake in plant pests and pathogens: Insights into RNAi-based insect and fungal control technology.

Plants, *9*(12), 1–17. https://doi.org/10.3390/plants9121780

Wytinck, N., Sullivan, D. S., Biggar, K. T., Crisostomo, L., Pelka, P., Belmonte, M. F., & Whyard, S. (2020). Clathrin mediated endocytosis is involved in the uptake of exogenous double-stranded RNA in the white mold phytopathogen Sclerotinia sclerotiorum. *Scientific Reports*, *10*(1), 1–12. https://doi.org/10.1038/s41598-020-69771-9

Xiao, D., Gao, X., Xu, J., Liang, X., Li, Q., Yao, J., & Zhu, K. Y. (2015a). Clathrin-dependent endocytosis plays a predominant role in cellular uptake of double-stranded RNA in the red flour beetle. *Insect Biochemistry and Molecular Biology*, *60*, 68–77. https://doi.org/10.1016/j.ibmb.2015.03.009

Xiao, D., Gao, X., Xu, J., Liang, X., Li, Q., Yao, J., & Zhu, K. Y. (2015b). Clathrin-dependent endocytosis plays a predominant role in cellular uptake of double-stranded RNA in the red flour beetle. *Insect Biochemistry and Molecular Biology*, *60*, 68–77. https://doi.org/10.1016/J.IBMB.2015.03.009

Yangui, I., Jamaa, B., Lahbib, M., Jamaa, H. Ben, Commission, A. E., & Vannini, A. (2020). *Trichoderma biocontrol of Biscogniauxia mediterranea : variation in responses among genetically diverse isolates*. *August*.

Yuan, M., Ngou, B. P. M., Ding, P., & Xin, X. F. (2021). PTI-ETI crosstalk: an integrative view of plant immunity. *Current Opinion in Plant Biology*, *62*, 102030. https://doi.org/10.1016/j.pbi.2021.102030

Zeno, W. F., Hochfelder, J. B., Thatte, A. S., Wang, L., Gadok, A. K., Hayden, C. C., Lafer, E. M., & Stachowiak, J. C. (2021). Clathrin senses membrane curvature. *Biophysical Journal*, *120*(5), 818–828. https://doi.org/10.1016/j.bpj.2020.12.035

Zhang, D. X., Spiering, M. J., & Nuss, D. L. (2014). Characterizing the roles of Cryphonectria parasitica RNA-dependent RNA polymerase-like genes in antiviral defense, viral recombination and transposon transcript accumulation. *PLoS ONE*, *9*(9). https://doi.org/10.1371/journal.pone.0108653

Zhang, H., Liu, K., Zhang, X., Song, W., Zhao, Q., Dong, Y., Guo, M., Zheng, X., & Zhang, Z. (2010). A two-component histidine kinase, MoSLN1, is required for cell wall integrity and pathogenicity of the rice blast fungus, Magnaporthe oryzae. *Current Genetics*, *56*(6), 517–528. https://doi.org/10.1007/s00294-010-0319-x

Zhang, K., Hodge, J., Chatterjee, A., Moon, T. S., & Parker, K. M. (2021). Duplex structure of double-stranded RNA provides stability against hydrolysis relative to single-stranded RNA. *Environmental Science and Technology*, *55*(12), 8045–8053. https://doi.org/10.1021/acs.est.1c01255

9. Supplementary material

Table S. 1: DCL proteins accession number and code used in phylogenetic analysis.

Species	code	Accession number
Alternaria alternata	AlaDCL1	OWY47687.1
	AlaDCL2	KAH6841800.1
Aspergillus flavus	AsfDCL1	KAB8242615.1
	AsfDCL2	KAB8243706.1
Aspergillus parasiticus	AspDCL1	KAB8202836.1
	AspDCL2	KAB8199093.1
Biscogniauxia mediterranea	BimDCL1	695335
	BimDCL2	673312
Bipolaris oryzae	BioDCL1	XP_007682742.1
	BioDCL2	XP_007685207.1
Bipolaris sorokiniana	BisDCL1	XP_007695017.1
	BisDCL2	KAF5853805.1
Blumeria graminis	BlgDCL1	EPQ62586.1
	BlgDCL2	EPQ67305.1
Botrytis cinerea	BocDCL1	XP_024552373.1
	BocDCL2	XP_024553022.1
Colletotrichum gloeosporioides	CogDCL1	XP_045265656.1
	CogDCL2	XP_045258642.1
Diplodia corticola	DicDCL1	XP_020132754.1
	DicDCL2	XP_020129607.1
Fusarium culmorum	FucDCL1	PTD02414.1
	FucDCL2	PTD08238.1
Fulvia fulva	FufDCL1	KAH3648029.1
	FufDCL2	KAH3656472.1
Fusarium graminearum	FugDCL1	EYB30504.1
	FugDCL2	CAF3516481.1
Fusarium oxysporum	FuoDCL1	XP_031036234.1
	FuoDCL2	XP_031033713.1
Fusarium solani	FusDCL1	XP_046131666.1
	FusDCL2	XP_046128399.1
Fusarium verticillioides	FuvDCL1	RBQ81062.1
	FuvDCL2	XP_018758712.1
Heterobasidion annosum	HeaDCL1	104842
	HeaDCL2	168380
	HeaDCL3	314326
Melampsora lini	MelDCL1	196667
Neurospora crassa	NecDCL1	XP_961898.1
	NecDCL2	XP_963538.3
Puccinia striiformis	PusDCL1	KAH9456137.1
	PusDCL2	7916

Table S.1 (*continuation)*

Species	code	Accession number
Puccinia triticina	PutDCL1	2748
	PutDCL2	9197
Pyricularia oryzae	PyoDCL1	XP_030984428.1
	PyoDCL2	XP_030981374.1
Sclerotinia sclerotiorum	ScsDCL1	APA13215.1
	ScsDCL2	XP_001588821.1
Schizosaccharomyces pombe	ShpDCL1	NP_588215.2
Stereum hirsutum	SthDCL1	155914
	SthDCL2	103751
	SthDCL3	93138
Verticillium dahliae	VedDCL1	XP_009650143.1
	VedDCL2	KAH6702336.1
Venturia inaequalis	VeiDCL1	RDI80688.1
	VeiDCL2	KAE9975081.1
Verticillium longisporum	VelDCL1	CRK17804.1
	VelDCL2	CRJ84667.1

Table S. 2: AGO proteins accession number and code used in phylogenetic analysis.

Species	Code	Accession number
Alternaria alternata	AlaAGO1	498656
	AlaAGO2	316269
	AlaAGO3	479826
Aspergillus flavus	AsfAGO1	29555
	AsfAGO2	34436
	AsfAGO3	27245
Aspergillus parasiticus	AspAGO1	237889
	AspAGO2	183538
Biscogniauxia mediterranea	BimAGO1	685257
	BimAGO2	674995
	BimAGO3	643717
Bipolaris oryzae	BioAGO1	48457
	BioAGO2	64335
Bipolaris sorokiniana	BipAGO1	XP_007696144.1
	BipAGO2	XP_007703532.1
Blumeria graminis	BlgAGO1	2922
	BlgAGO2	1873
	BlgAGO3	7807
Botrytis cinerea	BocAGO1	10590
	BocAGO2	4487
Colletotrichum gloeosporioides	CogAGO1	1747120
	CogAGO2	1719627

Table S.2 (*continuation*)

Species	Code	Accession number
Diplodia corticola	DicAGO1	XP_020131025.1
	DicAGO2	XP_020131586.1
	DicAGO3	XP_020135572.1
Fusarium culmorum	FucAGO1	373
	FucAGO2	4568
	FucAGO3	12081
Fulvia fulva	FufAGO1	195424
	FufAGO2	185632
	FufAGO3	184447
Fusarium graminearum	FugAGO1	1230192
	FugAGO2	1245450
Fusarium oxysporum	FuoAGO1	151694
	FuoAGO2	295188
Fusarium solani	FusAGO1	567428
	FusAGO2	544243
Fusarium verticillioides	FuvAGO1	1199
	FuvAGO2	9460
Heterobasidion annosum	HeaAGO1	426063
	HeaAGO2	444035
	HeaAGO3	314333
	HeaAGO4	480543
	HeaAGO5	382532
	HeaAGO6	309780
	HeaAGO7	37309
Melampsora lini	MelAGO1	199778
	MelAGO2	201636
Neurospora crassa	NecAGO1 (SMS-2)	XP_958586.1
	NecAGO2 (QDE-2)	XP_011394903.1
Puccinia striiformis	PusAGO1	502396
	PusAGO2	495237
	PusAGO3	504305
Puccinia triticina	PutAGO1	1494
	PutAGO2	4101
Pyricularia oryzae	PyoAGO1	8020
	PyoAGO2	3431
	PyoAGO3	8820
Sclerotinia sclerotiorum	ScsAGO1	6626
	ScsAGO2	334
Schizosaccharomyces pombe	ShpAGO1	4323

Table S.2 (*continuation*)

Species	Code	Accession number
Stereum hirsutum	SthAGO1	119245
	SthAGO2	171357
	SthAGO3	73335
	SthAGO4	155427
	SthAGO5	122781
	SthAGO6	78524
Verticillium dahliae	VedAGO1	513916
	VedAGO2	451547
Venturia inaequalis	VeiAGO1	KAE9965407.1
	VeiAGO2	KAE9975115.1
Verticillium longisporum	VelAgo1	19064
	VelAgo2	6574
	VelAgo3	7607

Table S. 3: RdRP proteins accession number and code used in phylogenetic analysis.

Species	Code	Accession number
Alternaria alternata	AlaRdRP1	111915
	AlaRdRP2	456187
	AlaRdRP3	435100
Aspergillus flavus	AsfRdRP1	2236243
	AsfRdRP2	2261486
	AsfRdRP3	2287556
Aspergillus parasiticus	AspRdRP1	144037
	AspRdRP2	227757
	AspRdRP3	191846
Biscogniauxia mediterranea	BimRdRP1	677448
	BimRdRP2	85611
	BimRdRP3	675676
Bipolaris oryzae	BioRdRP1	XP_007688003.1
	BioRdRP2	XP_007685740.1
	BioRdRP3	XP_007691637.1
Bipolaris sorokiniana	BisRdRP1	KAF5849236.1
	BisRdRP2	XP_007698643.1
	BisRdRP3	XP_007696101.1
Blumeria graminis	BlgRdRP1	331
	BlgRdRP2	330
Botrytis cinerea	BocRdRP1	5723
	BocRdRP2	6891
	BocRdRP3	6892
	BocRdRP4	15723

Table S.3 (*continuation*)

Species	Code	Accession number
Colletotrichum gloeosporioides	CogRdRP1	12025
	CogRdRP2	7988
	CogRdRP3	11961
Diplodia corticola	DicRdRP1	XP_020126451.1
	DicRdRP2	XP_020130197.1
	DicRdRP3	XP_020134021.1
Fusarium culmorum	FucRdRP1	9478
	FucRdRP2	4523
	FucRdRP3	11868
	FucRdRP4	12082
	FucRdRP5	1666
Fulvia fulva	FufRdRP1	196780
	FufRdRP2	194468
	FufRdRP3	197136
Fusarium graminearum	FugRdRP1	634003
	FugRdRP2	1204889
	FugRdRP3	1245609
	FugRdRP4	1254041
	FugRdRP5	1219033
Fusarium oxysporum	FuoRdRP1	12620
	FuoRdRP2	16927
	FuoRdRP3	16926
	FuoRdRP4	6974
	FuoRdRP5	19166
Fusarium solani	FusRdRP1	543677
	FusRdRP2	527526
	FusRdRP3	509670
	FusRdRP4	496541
Fusarium verticillioides	FuvRdRP1	17466
	FuvRdRP2	17585
	FuvRdRP3	9605
	FuvRdRP4	5211
Heterobasidion annosum	HeaRdRP1	431281
	HeaRdRP2	436863
	HeaRdRP3	475976
	HeaRdRP4	309978
	HeaRdRP5	443820
	HeaRdRP6	31769
	HeaRdRP7	318296

Table S.3 (*continuation*)

Species	Code	Accession number
Melampsora lini	MelRdRP1	197628
	MelRdRP2	212083
	MelRdRP3	209029
	MelRdRP4	202697
Neurospora crassa	NecRdRP1 (QDE-1)	XP_959047.1
	NecRdRP2 (SAD-1)	XP_964248.3
	NecRdRP3 (rrp-3)	XP_963405.1
Puccinia striiformis	PusRdRP1	504403
	PusRdRP2	493039
	PusRdRP3	488074
	PusRdRP4	487991
	PusRdRP5	503155
Puccinia triticina	PutRdRP1	4238
	PutRdRP2	12929
	PutRdRP3	7577
Pyricularia oryzae	PyoRdRP1	5555
	PyoRdRP2	12323
	PyoRdRP3	6024
Sclerotinia sclerotiorum	ScsRdRP1	10348
	ScsRdRP2	7738
	ScsRdRP3	3459
Schizosaccharomyces pombe	ShpRdRP1	547
Stereum hirsutum	SthRdRP1	101865
	SthRdRP2	124929
	SthRdRP3	161484
	SthRdRP4	119644
	SthRdRP5	170031
	SthRdRP6	101986
	SthRdRP7	137322
	SthRdRP8	73750
	SthRdRP9	117647
	SthRdRP10	96893
	SthRdRP11	139256
Verticillium dahliae	VedRdRP1	8489
	VedRdRP2	7686
	VedRdRP3	3147
Venturia inaequalis	VeiRdRP1	18749
	VeiRdRP2	15343
	VeiRdRP3	17861
	VeiRdRP4	21149
	VeiRdRP5	17862

Table S.3 (*continuation*)

Species	Code	Accession number
Verticillium longisporum	VelRdRP1	10188
	VelRdRP2	10190
	VelRdRP3	13360
	VelRdRP4	6231
	VelRdRP5	6124

Targets	Total siRNA hits	Efficient siRNA hits
Biscogniauxia	468	222

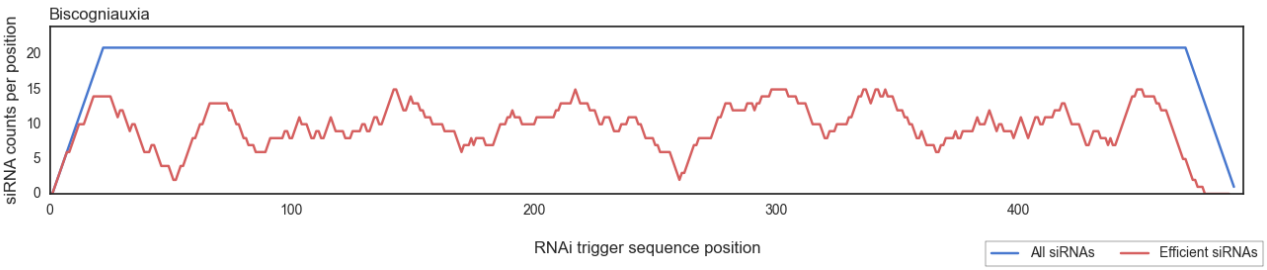

Figure S. 1: A representative *in silico* prediction of effective siRNA hits, using si-Fi v21 software. In the figure the prediction for *B. mediterranea* Sc1 is presented.

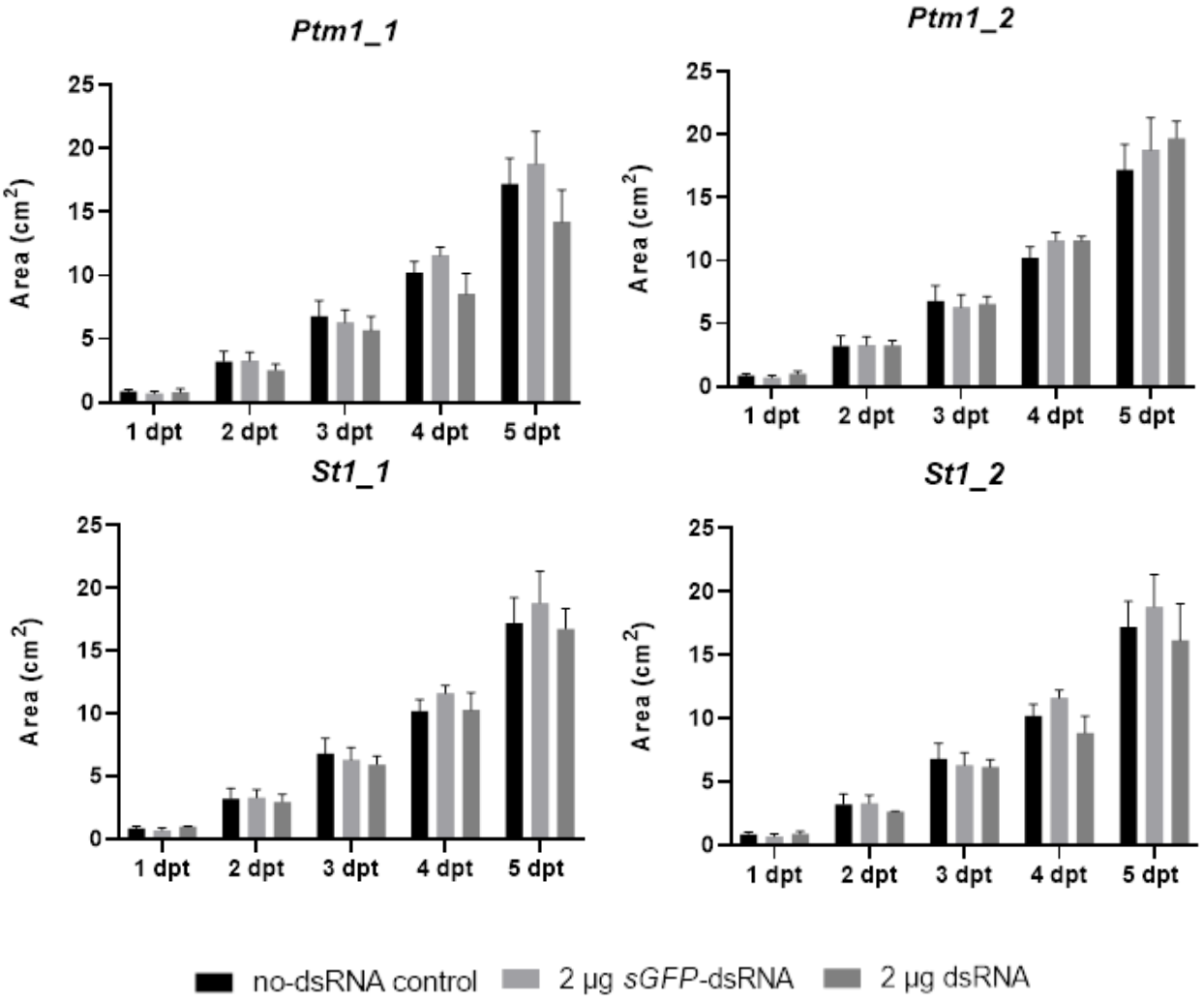

Figure S. 2: Effects of constant presence of dsRNA in *D. corticola* growth, under oxidative stress. A *D. corticola* plug (5 mm) was placed to growth on a PDA supplemented with hydrogen peroxide (H_2O_2) up to a final concentration of 3 mM and 2 µg/10ml *Ptm1_1*, *Ptm1_2*, *St1_1* and *St1_2* dsRNAs the fungal growth area (cm^2) was measured during five days post treatment (dpt). Controls without dsRNA treatment (no-dsRNA control) and PDA supplemented with 2 µg/10 ml non target gene *sGFP* (2 µg s*GFP*-dsRNA) were performed.

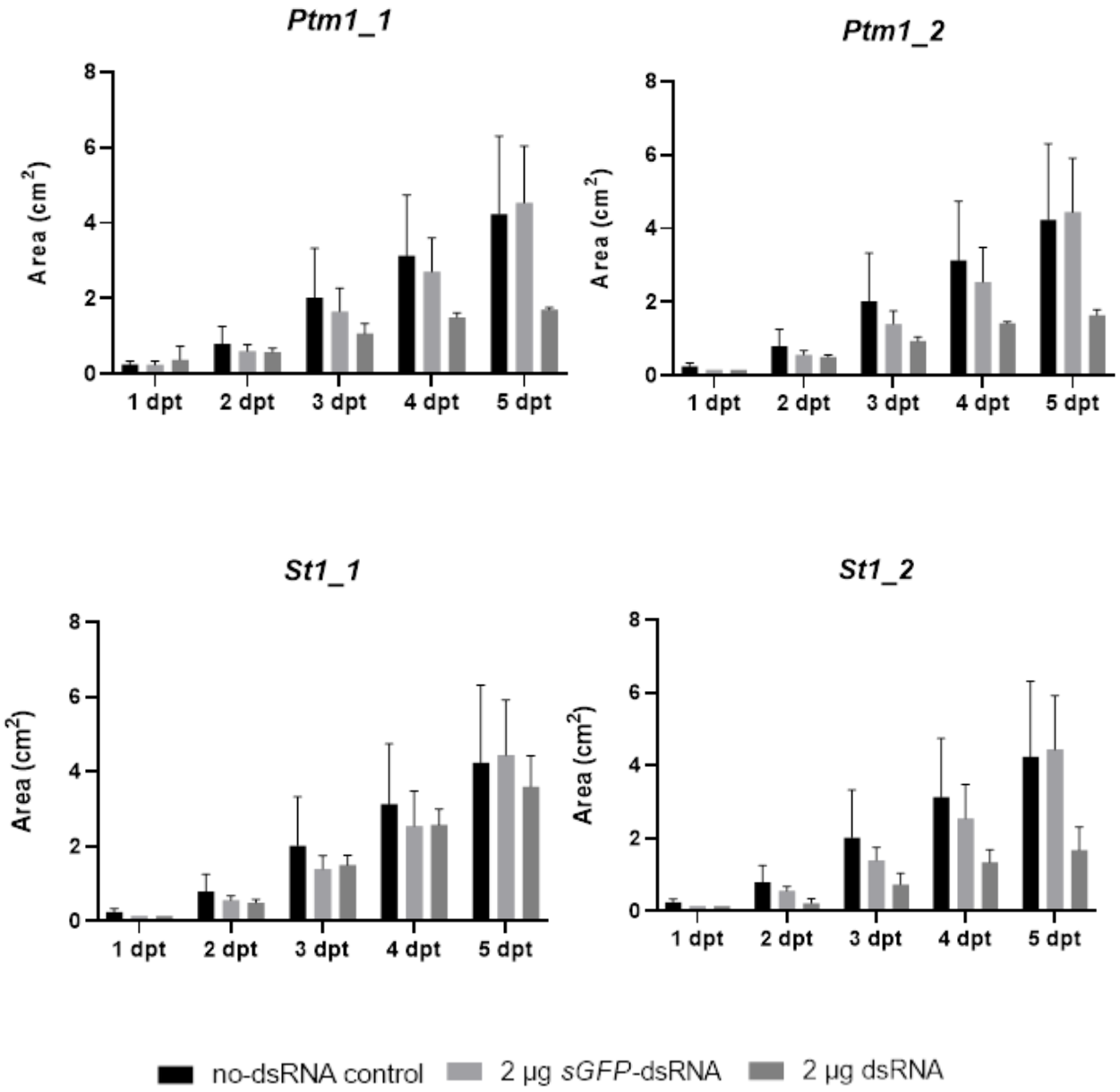

Figure S. 3: Effects of constant presence of dsRNA in *B. mediterranea* growth, under oxidative stress. A *B. mediterranea* plug (5 mm) was placed to growth on a PDA supplemented with hydrogen peroxide (H_2O_2) up to a final concentration of 3 mM and 2 µg *Ptm1_1*, *Ptm1_2*, *St1_1* and *St1_2* dsRNAs the fungal growth area (cm^2) was measured during five days post treatment (dpt). Controls without dsRNA treatment (no-dsRNA control) and PDA supplemented with 2 µg/10 ml non target gene *sGFP* (2 µg s*GFP*-dsRNA) were performed.